

NOTE TO USERS

This reproduction is the best copy available.

UMI[®]

University of Alberta

**Effects of Residual Bitumen Removal Techniques on the Separation
of Heavy Minerals from Athabasca Oil Sands Tailings**

By

Zhangming Cui



A thesis submitted to the Faculty of Graduate Studies and Research in partial fulfillment
of the requirements for the degree of Master of Science

In

Materials Engineering

Department of Chemical and Materials Engineering

Edmonton, Alberta

Spring, 2004



Library and
Archives Canada

Bibliothèque et
Archives Canada

Published Heritage
Branch

Direction du
Patrimoine de l'édition

395 Wellington Street
Ottawa ON K1A 0N4
Canada

395, rue Wellington
Ottawa ON K1A 0N4
Canada

Your file *Votre référence*
ISBN: 0-612-96462-0
Our file *Notre référence*
ISBN: 0-612-96462-0

The author has granted a non-exclusive license allowing the Library and Archives Canada to reproduce, loan, distribute or sell copies of this thesis in microform, paper or electronic formats.

L'auteur a accordé une licence non exclusive permettant à la Bibliothèque et Archives Canada de reproduire, prêter, distribuer ou vendre des copies de cette thèse sous la forme de microfiche/film, de reproduction sur papier ou sur format électronique.

The author retains ownership of the copyright in this thesis. Neither the thesis nor substantial extracts from it may be printed or otherwise reproduced without the author's permission.

L'auteur conserve la propriété du droit d'auteur qui protège cette thèse. Ni la thèse ni des extraits substantiels de celle-ci ne doivent être imprimés ou autrement reproduits sans son autorisation.

In compliance with the Canadian Privacy Act some supporting forms may have been removed from this thesis.

Conformément à la loi canadienne sur la protection de la vie privée, quelques formulaires secondaires ont été enlevés de cette thèse.

While these forms may be included in the document page count, their removal does not represent any loss of content from the thesis.

Bien que ces formulaires aient inclus dans la pagination, il n'y aura aucun contenu manquant.

Canada

ABSTRACT

In this study, the Alberta oil sands tailings were characterized and the effects of residual bitumen removal techniques on the separation of the heavy minerals from the oil sands tailings were studied. At the pretreatment stage, centrifugal separation can produce a rougher heavy mineral concentrate with acceptable heavy mineral recoveries and a very small proportion of the residual hydrocarbon. The effect of roasting, which was used to remove residual bitumen, on the magnetic properties of the minerals contained in the froth treatment tailings was investigated. Naphtha washing can reduce the residual bitumen content in the oil sands tailings to 0.8%. With the addition of NaOH or Na₂SiO₃, Attrition at 80°C also can remove residual bitumen as clean as naphtha washing does. Regardless of the bitumen-removal method, gravity concentration of bitumen-removed SB40 heavy product is effective. Flotation removal of pyrite from the bitumen-removed SB40 heavy product is possible. Due to the presence of trace residual bitumen, flotation separation of zircon from titanium minerals was more difficult for mechanically attritioned SB40 heavy product than for roasted SB40 heavy product.

ACKNOWLEDGEMENT

I would like to acknowledge the contributions of my supervisors, Dr. Qi Liu and Dr. Tom Etsell for their stance and explicit guidance and supervision throughout the project.

Financial support provided to this project by Alberta Energy Research Institute and Syncrude Canada Ltd is gratefully acknowledged.

During the course of this research project technicians in Chemical & Materials Engineering Department and my fellow students have helped me with the testwork. Tina Barker performed the SEM/EDX analyses, Adong Lu performed the XRD analyses, and Shiraz Merali provided help with day-to-day laboratory needs and operations.

I am also grateful to George Cymerman, my contact in Syncrude Research Center for his help and guidance.

TABLE OF CONTENTS

ABSTRACT

ACKNOWLEDGEMENT

TABLE OF CONTENTS

LIST OF TABLES

LIST OF FIGURES

1	INTRODUCTION.....	1
2	LITERATURE SURVEY.....	3
2.1	Heavy Minerals in Alberta Oil Sands.....	3
2.2	Titanium: Resources and Utilizations.....	12
2.3	Zirconium: Resources and Utilizations	27
2.4	Previous Studies to Recover Heavy Minerals from the Athabasca Oil Sands	32
3	OBJECTIVE	46
4	EXPERIMENTAL.....	47
4.1	Materials.....	47
4.2	Equipment	50
4.3	Experimental Procedures.....	51

5	CHARACTERIZATION AND PRE-TREATMENT OF OIL SANDS TAILINGS	61
5.1	Characterization of Oil Sand Tailings	61
5.2	Pre-treatment by Flotation	70
5.3	Pretreatment by Centrifugal Concentrator	72
5.4	Characterization of Separation Products.....	80
5.5	Summary	94
6	BITUMEN REMOVAL BY ROASTING.....	97
6.1	Effect of Roasting on the Magnetic Properties of Single Minerals	97
6.2	Effect of Roasting on the Magnetic Properties of Oil Sands Tailings.....	121
6.3	Low Temperature Roasting and Its Effect on Pyrite Flotation.....	128
6.4	Gravity Concentration of Roasted Oil Sand Tailings	138
6.5	Flotation Concentration of Roasted SB40 Heavy Product	138
6.6	Flotation Separation of Ti Minerals from Zircon.....	141
6.7	Summary	145
7	BITUMEN REMOVAL BY SOLVENT WASHING	147
7.1	Solvent Washing	147
7.2	Gravity Concentration	147
7.3	Flotation of Pyrite from the Bitumen-removed SB40 Heavy Products	150
7.4	Magnetic and Electrostatic Separation.....	155

7.5	Summary	156
8	BITUMEN REMOVAL BY MECHANICAL ATTRITION.....	158
8.1	Mechanical Attrition	158
8.2	Gravity Concentration	163
8.3	Flotation Concentration of Mechanically scrubbed SB40 Heavy Product ..	163
8.4	Flotation of Pyrite from the Bitumen-removed SB40 Heavy Products	164
8.5	Ti-Zr Separation of Mechanically Scrubbed SB40 Heavy Product.....	165
8.6	Magnetic and Electrostatic Separation.....	166
8.7	Mineral Electric Conductivity Measurement	168
8.8	Summary	169
9	CONCLUSIONS	170
10	RECOMMENDATIONS.....	175
11	REFERENCES.....	176

LIST OF TABLES

Table 1	Elemental analysis of Syncrude oil sands feed.....	4
Table 2	Elemental analysis of Syncrude centrifuge tailings.....	8
Table 3	Comparison of chemical analysis (Alberta Chamber of Resources, 1996).....	8
Table 4	Mineral speciation of Syncrude and Suncor process streams.....	9
Table 5	Heavy mineral assemblage of Syncrude scroll centrifuge tailings.....	10
Table 6	Titanium and zirconium balances in Syncrude bitumen extraction circuit.....	10
Table 7	Flow rates of heavy minerals from the oil sands in Alberta.....	11
Table 8	Production of titanium minerals by country (Gambogi, 2002).....	16
Table 9	Production of zirconium minerals by country (Hedrick, 2002).....	30
Table 10	Separation characteristics of heavy minerals.....	33
Table 11	Grades of rutile concentrates produced in previous studies.....	44
Table 12	Grades of ilmenite and leucoxene concentrates produced in previous studies.....	45
Table 13	Grades of zircon concentrates produced in previous studies.....	45
Table 14	Chemical analysis of mineral samples.....	47
Table 15	TLX of oil sand tailings and MCR of bitumen.....	49
Table 16	Reagents used in the test work.....	49
Table 17	Equipment used in this study.....	50
Table 18	Particle size distributions of froth treatment tailings samples.....	62
Table 19	Size assay (Ti, Zr) for samples No. 2 and No. 4.....	64
Table 20	Whole rock analysis of bitumen-removed oil sands tailings.....	64
Table 21	Approximate composition as determined from mineralogical analysis.....	65
Table 22	Approximate composition as determined from mineralogical analysis.....	70
Table 23	Flotation of residual bitumen and heavy minerals from froth treatment tailings	72
Table 24	Effect of back water temperature and centrifugal force on bitumen content in heavy product of sample No. 2 and No. 5 (Backwater pressure = 1psi).....	73
Table 25	Effect of centrifugal force (G) on the centrifugal separation.....	79
Table 26	Balance of the optimum centrifugal concentrator tests.....	80
Table 27	Heavy mineral distributions in heavy product of test G29 and G33.....	81

Table 28	Heavy mineral distribution in slime of tests G29 and G33.....	81
Table 29	Bitumen balance for SB40 tests.....	87
Table 30	Approximate composition as determined by mineralogical analysis	87
Table 31	Elemental analysis of centrifuge concentration products	91
Table 32	Magnetic Susceptibility of LR Rutile	117
Table 33	Summary of magnetic separation of roasted SB40 heavy products	125
Table 34	Sample sulfur assays under different roasting conditions.....	129
Table 35	Shaking table concentration of roasted (350°C, 60hrs) SB40 heavy product	138
Table 36	Suspension-cell flotation of roasted (600°C for 60') SB40 heavy product.	139
Table 37	Microflotation tube flotation of roasted (600°C for 60') SB40 heavy product	140
Table 38	Flotation balance for 1:1 mixture of LR Rutile and LR Zircon.....	141
Table 39	Suspension-cell flotation of roasted (600°C for 60) SB40 heavy product ..	144
Table 40	Microflotation tube flotation of roasted SB40 heavy product	144
Table 41	Heavy liquid (SG 3.3) separation of toluene-washed SB40 heavy product .	148
Table 42	Shaking table concentration of toluene-washed SB40 heavy product.....	150
Table 43	Flotation froth yield from naphtha-washed SB40 heavy product.....	151
Table 44	Pyrite flotation test results on naphtha-washed SB40 heavy product.....	151
Table 45	Microflotation tube flotation of pyrite from bitumen-removed SB40 heavy product	152
Table 46	Magnetic and electrostatic separation of heavy liquid concentrate	155
Table 47	Preliminary naphtha washing and attrition results.....	158
Table 48	Shaking table concentration of mechanically scrubbed SB40 heavy product	163
Table 49	Suspension-cell flotation of scrubbed SB40 heavy product (65°C)	164
Table 50	Microflotation tube flotation of scrubbed SB40 heavy product	164
Table 51	Microflotation tube flotation of pyrite from bitumen-removed SB40 heavy product	165
Table 52	Microflotation tube flotation of scrubbed SB40 heavy product	166

Table 53	Magnetic and electrostatic separation of tabled scrubbed SB40 heavy product	167
Table 54	Electric resistance of minerals	168

LIST OF FIGURES

Figure 1	Overall flow sheet of bitumen extraction from oil sands (Oxenford et al.,.....	7
Figure 2	Generalized process flow sheet for recovery of ilmenite, rutile leucoxene, zircon, monazite and Sillimanite from beach sands (Padmanabhan, etc., 1990).....	17
Figure 3	QIT Process Schematic (QIT, www.qit.com,2001).....	20
Figure 4	Synthetic Rutile Processes (Padmanabhan et al., 1990).....	22
Figure 5	Production of TiO ₂ from different feedstocks (Kogler and Engelhardt, 1997)	25
Figure 6	Schematic flow sheet of bitumen and slime removal (Trevoy et al., 1978; Trevoy and Schutte, 1981).....	37
Figure 7	Removal of residual bitumen/slimes/gangue by hydrocyclone, flotation and burn off (Owen and Tipman, 1999).....	38
Figure 8	Schematic flow sheet of bulk flotation and burn-off (Bulatovic, 1999 and 2000).....	39
Figure 9	Falcon SB40 Centrifugal Concentrator	52
Figure 10	Magnetic separation flow sheet of roasted SB40 heavy products.....	55
Figure 11	Modified Microflotation Tube.....	57
Figure 12	Mechanical attrition equipment (including Isotherm 3028H Circulating Water Bath, Suspension Frame, and Plexiglass Attrition Cell)	59
Figure 13	Bitumen content in solids of scroll tailings as a function of weight yield of - 38 µm material	63
Figure 14	Sample No. 2 head under plane-polarized transmitted light	66
Figure 15	Same field as in Figure 14 but under cross-polarized transmitted light.....	67
Figure 16	Same field as in Figure 14 but under reflected light.....	68
Figure 17	Same field as in Figure 14 but under cross-polarized reflected light	69
Figure 18	Recovery of heavy minerals and bitumen as a function of the weight yield of heavy products of sample No. 2 and No. 5 from SB40 tests	76
Figure 19	Bitumen content in heavy minerals as a function of back water pressure.....	77

Figure 20	Bitumen and heavy mineral distributions in heavy product as a function of back water pressure.....	78
Figure 21	Settling curves of SB40 sample No.5 and the SB40 sample No. 5 light.....	83
Figure 22	Optical absorbance of the clarified water from SB40 sample No.5 and the SB40 sample No.5 light product.....	84
Figure 23	Sample No.2 Falcon SB40 heavy product under plane-polarized transmitted light	89
Figure 24	SEM/EDX analysis of bitumen-removed SB40 heavy product	90
Figure 25	Particle size distribution of flotation concentrate and centrifugal concentration heavy product	93
Figure 26	Oxidation roasting of ilmenite – magnetic susceptibility of ilmenite as a function of roasting time	98
Figure 27	Oxidation roasting of ilmenite – magnetic susceptibility of ilmenite as a function of roasting temperature	100
Figure 28	Magnetic susceptibility of ilmenite as a function of roasting temperature..	101
Figure 29	Magnetic susceptibility of oxidation roasted ilmenite as a function of the.	102
Figure 30	Yield of ilmenite into the magnetic product as a function of roasting time	105
Figure 31	Yield of ilmenite into the magnetic product as a function of roasting temperature	106
Figure 32	Yield of ilmenite into the magnetic product as a function of roasting time	107
Figure 33	Yield of ilmenite into the magnetic product as a function of roasting temperature	108
Figure 34	Magnetic susceptibility of hematite as a function of roasting time.....	111
Figure 35	Magnetic susceptibility of hematite as a function of roasting time.....	112
Figure 36	Comparison of reduction roasting of hematite at different charcoal dosage	113
Figure 37	Magnetic susceptibility of hematite as a function of roasting temperature.	114
Figure 38	Magnetic susceptibility of hematite as a function of roasting temperature.	115
Figure 39	Magnetic susceptibility of reduction roasted hematite as a function of peak intensity ratio between maghemite and hematite.....	116
Figure 40	Fe ₂ O ₃ and TiO ₂ content in the non-magnetic product as a function of magnetic field intensity.....	119

Figure 41	Fe ₂ O ₃ content in the non-magnetic product after different pretreatment of the LR Rutile.....	120
Figure 42	Magnetic susceptibility of roasted SB40 heavy products as a function of roasting temperature.....	123
Figure 43	Magnetic susceptibility of roasted SB40 heavy product as a function of roasting time.....	124
Figure 45	Stereomicroscopic image of roasted (800°C 30 minutes) SB40 heavy product under transmitted light (Magnification = 60).....	126
Figure 46	Stereomicroscopic image of roasted (900°C 30') SB40 heavy product under transmitted light (Magnification = 60).....	126
Figure 47	Stereomicroscopic image of roasted (600°C 30') SB40 heavy product under transmitted light (Magnification = 60).....	127
Figure 48	Stereomicroscopic image of roasted (500°C 30') SB40 heavy product under transmitted light (Magnification = 60).....	127
Figure 49	Stereomicroscopic image of roasted (1000°C 30') SB40 heavy product under transmitted light (Magnification = 60).....	128
Figure 50	Weight losses of roasted SB40 heavy products as a function of roasting time	130
Figure 51	The yield of froth in the single mineral flotation of fresh pyrite and aged pyrite as a function of xanthate dosage.....	132
Figure 52	The yield of froth in the single mineral flotation of roasted fresh pyrite as a function of roasting temperature	133
Figure 53	The yield of froth in the single mineral flotation of roasted aged pyrite as a function of roasting temperature	134
Figure 54	The yield of froth in the single mineral flotation of roasted aged pyrite as a function of exposure time	135
Figure 55	The yield of froth of aged pyrite as a function of Na ₂ S dosage.....	136
Figure 56	The yield of froth in the single mineral flotation of roasted fresh pyrite as a function of cornstarch dosage	137
Figure 57	Yield of froth in the single mineral flotation of LR Rutile and LR Zircon as a function of cornstarch dosage	142

Figure 58	Yield of froth in the single mineral flotation tests of LR Rutile and LR.....	143
Figure 59	SEM/EDX analysis of bitumen-removed SB40 heavy product	149
Figure 60	SEM/EDX analysis of bitumen-removed SB40 heavy product	153
Figure 61	SEM/EDX analysis of bitumen-removed SB40 heavy product	154
Figure 62	Magnetic and electrostatic separation flowsheet of heavy liquid heavy	156
Figure 63	Residual bitumen content as a function of attrition temperature.....	160
Figure 64	Residual bitumen content as a function of attrition time.....	161
Figure 65	Residual bitumen content as a function of stirring intensity	162
Figure 66	Magnetic and electrostatic separation flowsheet of tabled scrubbed SB40 heavy product.....	167

1 INTRODUCTION

The extraction of bitumen from the Athabasca oil sands in Alberta represents one of the largest mining operations in the world. More than half a million tonnes of oil sands are processed daily by Syncrude Canada Ltd and Suncor Energy Inc using the Clark hot water extraction process (Kasperski, 1985, Helper et al., 1989, Oxenford et al., 2001). During this process, a froth treatment tailing that typically contains 8% titanium and 4% zirconium is produced (Oxenford et al., 2001), although the original oil sands feeds contain only about 0.21% titanium and 0.024% zirconium. Typically, the froth treatment tailings recover about 50% of the titanium minerals and 85% of the zircon (Owen and Tipman, 1999). At the current production rates at Syncrude and Suncor, the quantity of heavy minerals (titanium and zirconium minerals) contained in the tailings is equivalent to about 6% of the world's production of titanium and about 9% of the world's production of zirconium (Oxenford et al., 2001).

Since the 1970s, there have been several metallurgical studies that attempted to recover the heavy minerals from the oil sands tailings and to produce saleable titanium and zirconium mineral concentrates. Based on these early studies, a mineral development agreement (MDA) project was carried out from 1994 to 1996 by the Federal and Alberta Provincial governments to exam the by-product mineral potential of oil sands operations. This study showed that it would not be profitable if a mixed titanium mineral concentrate was produced from the froth treatment tailings. However, if the titanium minerals could be fractionated into a high grade and a low grade concentrate, an initial capital investment of \$51 million would yield a return of investment of 19% and a net present value of \$40 million at a discount rate of 11% (Alberta Chamber of Resources, 1996). Unfortunately, up until now, none of the studies achieved the objective of producing saleable heavy mineral concentrates from the tailings, although some came very close. This situation has reinforced the widely-held suspicion that there must be some major metallurgical challenges to recover the heavy minerals from the Athabasca oil sands tailings.

While the previous metallurgical studies mainly focused on the process development work, we intend to examine the fundamental separation characteristics of the residual bitumen and the individual minerals contained in the oil sands tailings, and to study the effects of techniques used to remove the residual bitumen on the separation characteristics of the minerals. It is anticipated that this fundamental study will result in a better understanding of the properties of the different constituents in the oil sands tailings, as well as their association and separation characteristics, which will provide the bases for any further process development testwork.

2 LITERATURE SURVEY

2.1 Heavy Minerals in Alberta Oil Sands

2.1.1 *Scope of Alberta Oil Sands Operations*

The oil sands in northern Alberta region are a tremendous petroleum resource. These oil sands deposits are Cretaceous in age and cover an area in Alberta of over 6 million hectares (60,000 square kilometers). The McMurray Formation is mainly oil bearing quartz sand containing up to 18% by weight of extra heavy oil or bitumen. These deposits are the largest hydrocarbon accumulations in the world with an estimated 400 billion cubic meters of bitumen, 12 percent of which (or some 49 billion cubic meters) is ultimately recoverable (National Energy Board, 2000). At present, Syncrude Canada Ltd., Suncor Energy Inc., and Albian Sands Energy Inc. are the three large scale oil sands mining operators in the Athabasca region. A fourth operator, True North Energy L.P., is going to enter the oil sands industry in 2004. Syncrude Canada Ltd has been operating since 1978. In 2001, Syncrude produced 81.4 million barrels of Syncrude Sweet Blend (www.syncrude.com, 2001). Suncor Energy Inc has been operating since 1967. In 2001, Suncor's annual production rate is 82.1 million barrels of upgraded product (www.suncor.com, 2002). Albian Sands Energy Inc entered the oil sands industry in 2003 (www.albiansands.com, 2003) with a nominal capacity of 60 million barrels per year.

With proposed expansions, by 2008 total annual production from Syncrude is expected to be 170 million barrel of Syncrude Sweet Blend, and by 2012 total annual production from Suncor will be 200 million barrels. Oil sands plant of Albian Sands Energy Inc has a capacity of producing almost 60 million barrels per year of upgraded product, while True North Energy L.P. is constructing a plant to produce 70 million barrels per year of bitumen by 2008 (Oxenford et al, 2001). Therefore, in about ten years, the total annual oil production from the Alberta oil sands will reach 500 million barrels. The total annual discharge of froth treatment tailings will reach 10 million tonnes, containing about 1 million tonnes of titanium oxide and 280,000 tonnes of zirconium oxide and representing

a much larger share of world's titanium and zirconium market (over 20% and 28%, respectively).

2.1.2 Elemental Analysis of Oil Sands Feed

Although elemental analyses of oil sands feed and froth treatment tailings were reported since the 1960s (Blair, 1950; Scotland and Benthin, 1954; Mellon and Wall, 1956; Carrigy, 1963 and 1966; Kramers and Brown, 1976), the study by McCosh in the Mineral Development Agreement (MDA) program was the most comprehensive (McCosh, 1996). McCosh examined core samples from virtually all the geological faces within the leases of all oil sands operators. In general, the heavy mineral concentration in most of the Athabasca McMurray Formation was found to be consistently low: averaging about 0.35% TiO₂ (0.21% titanium) and 0.032% ZrO₂ (0.024% zirconium) in the feed grade oil sands. TiO₂ content varied from 0.08% to 1.6%, and ZrO₂ content ranged from about 0.0012% to 0.13%. Other valuable elements that were identified in the oil sands included rare earths and trace amount of palladium, platinum and gold, none of which occurred in high enough grades to warrant economic extraction. Table 1 shows a typical elemental assay of oil sands feed of Syncrude lease from the MDA study.

Table 1 Elemental analysis of Syncrude oil sands feed
(Alberta Chamber of Resources, 1996)

Element	Al	Ca	Fe	Mg	Si	Ti	Zr
Wt %	0.83	0.05	0.27	0.02	43.52	0.18	0.04

2.1.3 Oil Sands and Bitumen Characteristics

The oil sands deposits are composed primarily of quartz sand, silt and clay, water and bitumen, along with minor amounts of other minerals, including titanium, zirconium, tourmaline and pyrite. Although there can be considerable variations, a typical composition is:

- 75% to 80% inorganic material, 90% of which is quartz sand;
- 3% to 5% water; and 10% to 12% bitumen, with bitumen content varying between zero and 18% by weight.

The oil sands are generally unconsolidated, and are therefore friable and crumble easily.

A key aspect of the oil sands is the presence of bound formation water, which surrounds the individual sand grains as a thin film. The sand is said to be “water-wet” because of this thin film which is about 10 nm thick. The presence of the water film around the grains enables the bitumen to be recovered more easily since the bonding forces between the bitumen and water are much weaker than those between the water and the sand grains.

The bitumen contained in the oil sands is characterized by high densities, very high viscosities, high metal concentrations and a high carbon to hydrogen molecular ratio in comparison to conventional crude oil. The average composition of Alberta’s bitumen is 83.2% carbon, 10.4% hydrogen, 0.94% oxygen, 0.36% nitrogen and 4.8% sulfur, along with trace amounts of heavy metals such as vanadium, nickel and iron (National Energy Board, 2000).

2.1.4 Bitumen Extraction from Oil Sands - Clark Hot Water Process

The bitumen extraction processes initially used by Suncor and Syncrude were based on the Hot Water Extraction Method developed by Dr. Karl Clark and colleagues at the Alberta Research Council in the 1930s. According to this process, oil sands ore is mined from the base mine dump pocket by conveyor and enters large rotating tumblers where the ore is slurred by steam, water and caustic soda to condition it for bitumen liberation at 85°C. The conditioned slurry from the tumblers discharges onto vibrating screens where coarse particles such as rocks and lumps of clays are rejected. The slurry is diluted in pump boxes and pumped to Primary Separation Vessels (PSV), where bitumen rises to the surface as froth and is skimmed off, while the sands settle to the bottom. Naphtha is

added to the froth product as a diluent and the mixture enters high speed centrifuges to separate the bitumen from entrapped sands and water. The bitumen is then sent to Upgraders while the sand and other material that settles during the centrifuging processes are removed as froth treatment tailings.

The Clark hot water process has been modified in many ways and among the major improvements are:

- The addition of Tailings Oil Recovery (TOR) vessels – a technology developed by Syncrude Canada Ltd. These deep cone vessels recover most of the remaining bitumen that was discharged from the PSV as tailings;
- A second flotation unit to receive froth from the TOR;
- Inclined Plate Settlers (IPS) developed by Suncor Energy Inc, and the use of disc centrifuges, to provide better separation between bitumen and sand/clay in froth treatment stage;
- A Diluent Recovery Unit (DRU) developed by Syncrude Canada Ltd to recover naphtha from froth treatment tailings;
- A low energy extraction process, developed by Syncrude Canada Ltd. to operate the extraction processes at 25°C to 35°C, which consumes 40% less energy than the 80°C operation.
- Hydrotransport of oil sands slurries which replaces the traditional tumblers.

The present extraction processes are able to extract about 91% of the bitumen contained in the oil sands, compared to about 84% in 1975.

The Athabasca Oil Sands Project, planned by Shell and its partners for startup in 2002, includes a major innovative feature, i.e., the “multi-stage counter-current decantation” process, which provides partial upgrading of bitumen in the field. In this process, the extracted bitumen is blended with a paraffinic solvent which promotes the precipitation of asphaltenes, and thereby removes most of the carbon-laden or coke-producing components in the bitumen.

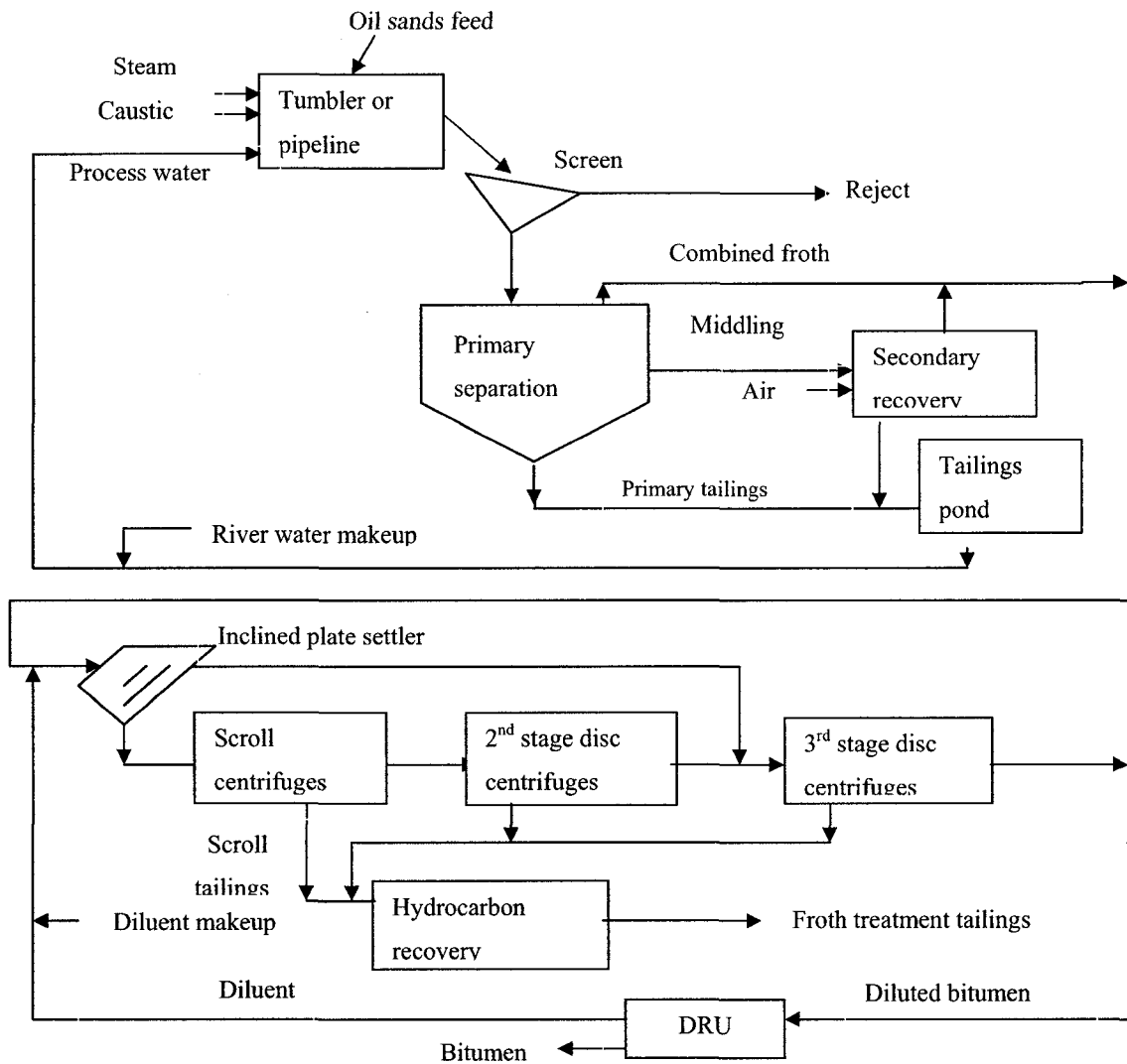


Figure 1 Overall flow sheet of bitumen extraction from oil sands (Oxenford et al., 2001, Trevoy et al., 1978)

An overall flow sheet of bitumen extraction from oil sands is shown in Figure 1. As can be seen, two tailings streams are produced from the oil sands operations: the Primary Tailings and the Froth Treatment Tailings (also called Centrifuge Tailings). While generally both tailings contain mineral solids, water, silt and residual bitumen, the Primary Tailings contain mostly clays, fine solids and water, and the Froth Treatment Tailings contain primarily coarse sands, fine mineral sands and residual bitumen. The

TiO₂ content in the Froth Treatment Tailings is 11.5%, which makes them the second richest titanium mineral resources in the world.

2.1.5 Heavy Minerals in Froth Treatment Tailings

Titanium and zirconium minerals are concentrated in the froth treatment tailings. Chemical analyses indicated that Suncor froth treatment tailings contained between 10.9% and 12.9% TiO₂, and between 1.1% and 3.6% ZrO₂; and the corresponding Syncrude samples contained between 8.5% and 14% TiO₂, and about 3.6% ZrO₂. A typical elemental analysis of Syncrude centrifuge tailings is shown in Table 2.

Table 2 Elemental analysis of Syncrude centrifuge tailings
(Alberta Chamber of Resources, 1996)

Element	Al	Ca	Fe	Mg	Si	Ti	Zr
Wt %	5.83	0.75	6.07	0.74	24.99	6.54	2.7

Compared with Table 1, there are significant enrichments of every element shown except for Si. Table 3 shows a comparison of chemical analysis between froth treatment tailings and typical head grades of some commercial titanium resources. As can be seen, the centrifuge tailings are the second richest titanium resource in the world. Only the grade of a hard rock ilmenite deposit in Quebec is higher than the tailings samples from Suncor and Syncrude.

Table 3 Comparison of chemical analysis (Alberta Chamber of Resources, 1996)

Deposit	TiO ₂ %	ZrO ₂ %
Suncor	10.9 – 12.9	1.5 -4.9
Syncrude	8.5 – 14.0	0.5 -3.6
Plant Design Basis	11.5	3.4
Queensland	1.8	
Florida	1.4	
Sierra Leone	1.5	
South Africa	2.5	
Western Australia	2.5	
Norway	9.7	
Quebec	22.2	

2.1.5.1 Mineral assemblage in the oil sands tailings

Generally, the elemental analyses conducted by different researchers on the oil sands agreed with each other. However, the speciation of minerals in the oil sands showed significant variations. Table 4 presents the mineral assemblage in some process streams of Syncrude and Suncor. These results were reported by the MDA study using image analysis techniques (Alberta Chamber of Resources, 1996). Apparently, the Suncor oil sands feed was reported to contain higher concentrations of rutile but lower concentrations of zircon and monazite than the Syncrude feed. After bitumen extraction, the oil sands tailings (Suncor Pond 1 beach sand and Syncrude Froth) were reported to have similar mineral content.

Table 4 Mineral speciation of Syncrude and Suncor process streams

(compiled from data in Alberta Chamber of Resources, 1996)

Stream	Rutile	Ilmenite	Leucoxene	Zircon	Monazite	Pyrite	Magnetite
Syncrude oil sands feed	22.9	0	47.9	10.4	10.4	6.3	2.1
Suncor oil sands feed	42.3	0	45.1	5.6	2.8	1.4	2.8
Syncrude froth	23.9	0.69	52.2	14.0	2.1	5.8	1.3
Suncor Pond 1 beach sand	26.2	0.40	52.0	12.1	1.4	6.9	1.0

A more recent mineral assemblage analysis was conducted by Lakefield Research Ltd on the Syncrude scroll centrifuge tailing, and the results are presented in Table 5. As can be seen, while the reported concentrations of other titanium and zirconium minerals were similar to those shown in Table 4, there was a sharp drop in the estimated concentrations of rutile, from about 23 - 26% down to only 4%. Also, a significant amount of the material was attributed to tourmaline, which did not appear in the MDA study (Table 4).

Table 5 Heavy mineral assemblage of Syncrude scroll centrifuge tailings

(Oxenford et al., 2001)

	Mineral	Wt %
Opaque:	Altered Ilmenite	23.0
	Leucoxene	16.6
	Pyrite	4.0
	Rutile	4.0
	Ilmenite	2.8
	Goethite	1.6
Non-Opaque:	Tourmaline	16.7
	Zircon	15.2
	Garnet	6.0
	Staurolite	4.8
	Siderite	3.0
	Calcite	0.6
	Kyanite	0.6
Apatite	0.6	
Others:	Monazite, feldspars and micas	0.5
Total		100.0

2.1.5.2 Heavy mineral department in the commercial extraction processes

As already mentioned, there is selective enrichment of the heavy minerals in the bitumen extraction processes, and the titanium and zirconium minerals are concentrated in the bitumen froths. As the froths are treated to remove the mineral solids and water, these heavy minerals are concentrated in the froth treatment tailings. This is clearly demonstrated by Table 6, which shows the heavy mineral department.

Table 6 Titanium and zirconium balances in Syncrude bitumen extraction circuit

(Alberta Chamber of Resources, 1996)

Stream	Wt. %	Ti Assay, %	Zr Assay, %	Ti Dist. %	Zr Dist. %
Oil sands feed	100.0	0.18	0.04	100.0	100.0
Primary tailings	98.5	0.08	0.01	46.3	11.3
Plant 5 froth	1.5	6.51	2.67	53.8	88.7
Centrifuge tailings	1.4	6.54	2.70	53.1	88.1
Scroll tailings	1.3	6.95	2.91	51.8	87.7

2.1.5.3 Grain size and mineral liberation in froth treatment tailings

The MDA study completed a basic feed analysis of the froth treatment tailings by image analysis (Owen, 1996). It showed that the mineral grains were essentially liberated. Rutile was reported to be 75.3% liberated with 73.4% in the optimal size range for flotation (10 to 100 μm). Leucoxene was 89% liberated with 91.9% in the optimal size range for flotation. Zircon was 95.5% liberated with 94.5% in the optimal size range for flotation (Owen, 1996).

2.1.5.4 Production rate of heavy minerals from froth treatment tailings

The tremendous scales of the oil sands operations in Alberta, and the enrichment of heavy minerals in the froth treatment tailings, make the extraction of heavy minerals from the oil sands tailings a very attractive venture. In fact, based on the current production rates at Syncrude and Suncor, the Ti and Zr contained in the froth treatment tailings represent about 6% and 9%, respectively, of the world's production of titanium and zirconium. Both Syncrude and Suncor are expanding productions, and two new producers will get on stream very soon, so that the amount of contained TiO_2 and ZrO_2 will quadruple in about 8 years (Table 7), occupying a higher potential share of Ti and Zr in the world markets.

Table 7 Flow rates of heavy minerals from the oil sands in Alberta

(Oxenford et al., 2001, Alberta Chamber of Resources, 1996)

Year	1995	2000	2005	2010
Total centrifuge tailings, t/y	2.5×10^6	2.9×10^6	7.0×10^6	10.0×10^6
Contained TiO_2 , t/y	250,000	290,000	700,000	1,000,000
Contained ZrO_2 , t/y	75,000	90,000	200,000	280,000

Furthermore, the production of titanium and zirconium minerals will add new commodities to Alberta. This not only means more jobs, it will also create more

economic opportunities, and help to diversify Alberta's economy. It is also to be noted that there is currently no zirconium mineral production in Canada.

The extraction of heavy minerals from the oil sands tailings should be a low-cost operation as well. Although the metallurgical flow sheet may be more complex than is normal in the industry, the operating cost of mineral recovery is extremely favorable due to the high grade of TiO_2 in the scroll centrifuge tailings streams, and due to the elimination of mining, tailing disposal and environmental remediation charges. In fact, in the 1996 MDA study, it was assumed that 288,000 tonnes of titanium mineral concentrates and 62,000 tonnes of zircon concentrates could be produced annually from the froth treatment tailings by a two-stage mineral processing plant. The capital investment would be \$51 million. A sales revenue of \$60 million was estimated at an annual operating expenses of \$13.7 million. The projected return of investment was 19% (Alberta Chamber of Resources, 1996).

2.2 Titanium: Resources and Utilizations

2.2.1 Titanium Minerals

Titanium is the ninth most abundant element on the Earth, comprising an estimated 0.62% of the Earth's crust. There are only a few minerals in which it occurs in major amounts: rutile, anatase, and brookite (which are polymorphs of TiO_2), ilmenite, and its alteration products, including leucoxene, perovskite (CaTiO_3), and sphene (CaTiSiO_5) (Lefond, 1983). The following mineral definitions were referenced from Lefond (1983) unless otherwise indicated.

Ilmenite

The chemical formula of theoretically pure ilmenite is $\text{FeO} \cdot \text{TiO}_2$. It was shown that up to 6% Fe_2O_3 may be dissolved as solid solution, and at 1050°C a continuous solid solution series exists between ilmenite and hematite. Hematite may, and often does, occur with ilmenite as minute exsolution lamellae. Magnesium and manganese may substitute for the

ferrous iron in ilmenite, which produces the rare end-member MgTiO_3 (geikelite) and MnTiO_3 (pyrophanite), but usually these two elements are present as minor impurities. Magnetite is a common associate of ilmenite in igneous and metamorphic rocks, and in such coexisting pairs chromium, nickel, and vanadium tend to concentrate in magnetite while manganese concentrate in ilmenite (Lefond, 1983).

In basic igneous rocks, notably anorthosites, gabbros, and basic lavas, ilmenite frequently occurs in intimate intergrowths with magnetite. The ilmenite forms lenses following octahedral parting planes in the magnetite host, and magnetite may, in turn, form crystallographically oriented inclusions within the ilmenite lenses.

Altered Ilmenite and Leucoxene

In sand deposits ilmenite frequently exhibits a degree of alteration caused by oxidation and removal of iron. The end product is essentially TiO_2 . The process was described by Temple (1966) as follows: "Alteration is initiated along grain boundaries and structural discontinuities within the grain. After going through an amorphous stage, oxidation and partial removal of iron from the ilmenite lattice results in an intermediate iron titanate of definite structure for which the name pseudorutile has been proposed. The alteration product at the stage of complete oxidation of the original iron in the ilmenite analyses 65~70% TiO_2 as compared with the 52% TiO_2 of ilmenite. Complete removal of iron from the pseudorutile lattice results in a grain composed of crystallites of the mineral rutile. Only the three mineral phases: ilmenite, pseudorutile and rutile have been identified in the commercial titanium mineral concentrates studied. Natural occurrence, in sand deposits, indicates that in weathering final removal of iron from pseudorutile to give the rutile end product takes place only either above or in the zone of the fluctuation water table."

The alteration products of the mineral ilmenite are herein termed "altered ilmenite." Many commercial ilmenite concentrates actually consist of altered ilmenite. However, the term "leucoxene" is also applied to high- TiO_2 products of alteration. Commercial justification for distinguishing between the high and low-iron products of alteration lies

in the fact that the former are used in the sulfate process by pigment manufacturers whereas the latter are not economically soluble in sulfuric acid but are used, as is rutile, for the production of titanium tetrachloride used for pigment and titanium metal manufacture.

Alteration is an extremely slow process that is aided by elevated temperature, so that older sand deposits in temperate and tropical regions of the world generally contain high TiO_2 ilmenite. Younger deposits, for example, those found on modern beaches, and those in the higher latitudes usually contain unaltered ilmenite with a TiO_2 content around 50%, near the theoretical level for pure ilmenite.

Rutile

Rutile, the high pressure, high temperature polymorph of TiO_2 , is the most common form of titanium in nature and is a widespread accessory mineral in high-grade metamorphic gneisses and schists and in igneous rocks. It is also a common detrital mineral.

Commercial rutile concentrates contain 95% TiO_2 or more, with SiO_2 , Cr_2O_3 , V_2O_3 , Al_2O_3 , and iron oxides comprising the remainder. Analyses of rutile from other occurrences may show major amounts of tantalum and columbium, which can enter titanium minerals because of the close similarity in ionic radius between Ti^{4+} and both Cb^{5+} and Ta^{5+} . There is also a high iron variety termed ferroan rutile.

Rutile may form by alteration from ilmenite or anatase, and while it is very stable over a broad range of geologic conditions, occasionally processes may be reversed so that rutile alters to sphene, possibly ilmenite, and more rarely anatase. The characteristic color of rutile is reddish brown, but it may be black, violet, yellow, or green as well.

2.2.2 Concentration Methods for Titanium Minerals

In alluvial deposits, ilmenite, rutile, and leucoxene normally occur along with other valuable minerals such as zircon, monazite, garnet, and sillimanite. These are the so-

called “heavy minerals” since their specific gravity is above 2.9. Quartz is the major gangue mineral. Mining of these deposits is usually carried out by dredging, shoveling, or drag-lines. These minerals occur in relatively coarse size and in fully liberated form, therefore no size reduction is needed. Pre-concentration is usually carried out at the mining site in order to reduce the bulk quantity to be treated in the subsequent separation stages. Gravity separation using Humphrey spirals and/or Reichert cones is universally used for pre-concentration.

Separation of individual heavy minerals is usually a complex multi-stage operation including magnetic and high-tension separation, air-tabling, flotation, etc. Ilmenite, garnet, and monazite are paramagnetic minerals and their magnetic susceptibility decreases in that order. Low intensity magnetic separation can produce an ilmenite concentrate, while a high intensity magnetic separation can separate garnet and monazite. Rutile, zircon, and sillimanite are non-magnetic while the magnetic susceptibility of leucoxene is variable depending upon the extent of its oxidation so that careful processing control for its optimum recovery is required. Ilmenite, altered ilmenite and rutile are electrical conductors, while all other heavy minerals are non-conducting. Sillimanite and monazite have good flotation properties. In addition to these differences in the physical properties of the different heavy minerals, particle sizes also play a significant role in the separation, necessitating multi-stage operations.

2.2.3 *World Titanium Resources and Demand*

Table 8 shows the world titanium mineral production (Gambogi, 2002). Ilmenite, its altered products and rutile are the only current commercial sources for titanium dioxide. Ilmenite, leucoxene, rutile, slag and synthetic rutile are feedstock sources for the production of TiO_2 pigment, titanium metal and welding rod coatings. Ilmenite contributes about 90% of the world's demand for titanium minerals (Gambogi, 2002). In Canada, mine production is mainly used to produce titaniferous slag from ilmenite. The world ilmenite resources total about 1 billion tons of titanium dioxide. Identified world resources of rutile (including anatase) total about 230 million tons of contained TiO_2 .

Table 8 Production of titanium minerals by country (Gambogi, 2002)

Unit: Kilo Tones of TiO₂

	Mine Production		Reserves	Reserve Base
Ilmenite:	2000	2001		
United States	300 ^a	300 ^a	13000	59000
Australia	1230	1190	110000	130000
Canada	760	720	31000	36000
India	205	200	30000	38000
Norway	275	270	40000	40000
South Africa	935	1000	63000	63000
Ukraine	242	240	5900	13000
Other Countries	331	320	49000	84000
World Total	4300	4200	340000	470000
Rutile:				
United States	(^a)	(^a)	750	1800
Australia	225	220	21000	32000
India	16	15	6600	7700
South Africa	94	90	8300	8300
Ukraine	56	55	2500	2500
Other Countries	4	4	8000	17000
World Total	4700	4600	38000	540000

^a : Included with ilmenite

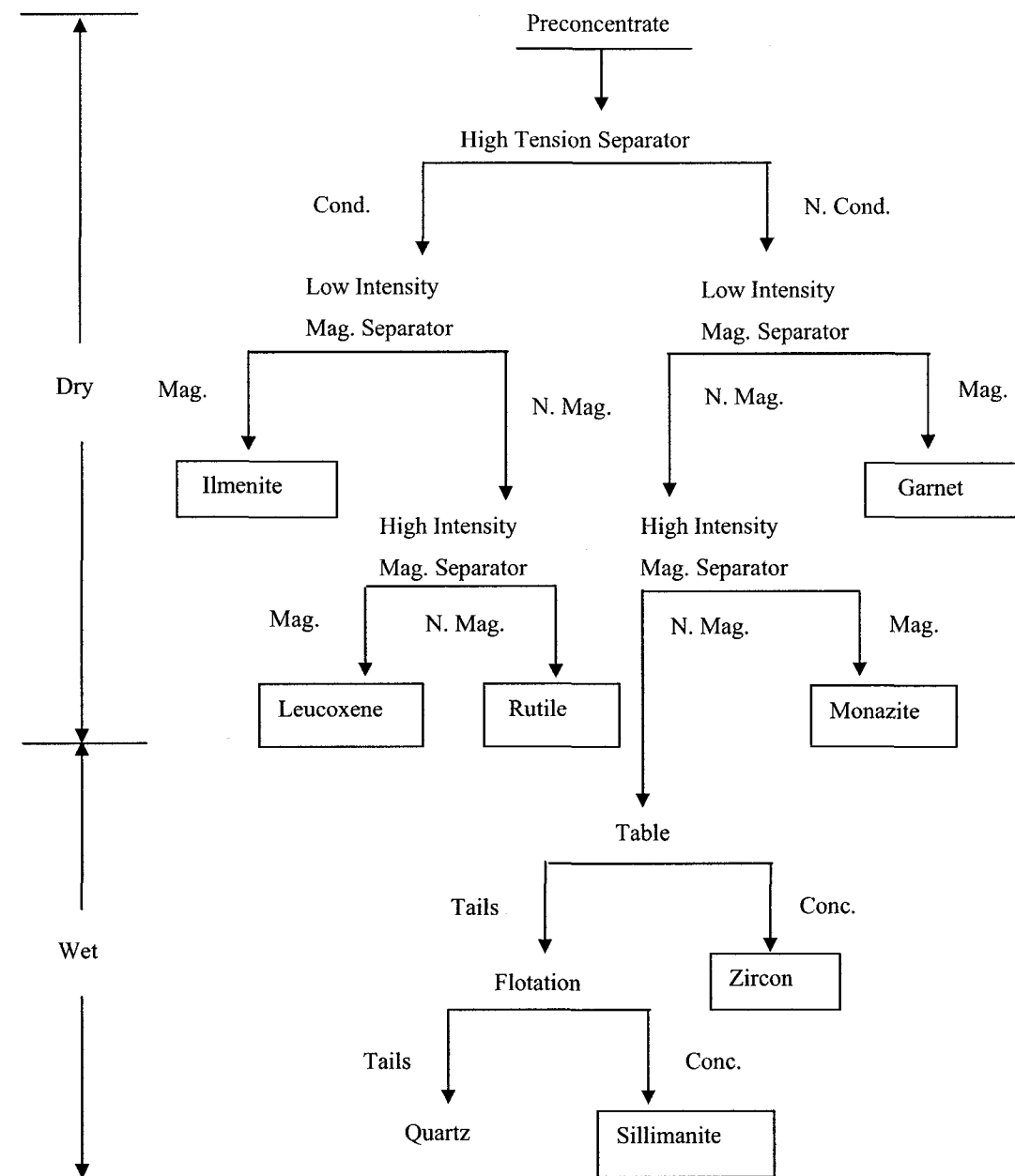


Figure 2 Generalized process flow sheet for recovery of ilmenite, rutile leucoxene, zircon, monazite and Sillimanite from beach sands (Padmanabhan, etc., 1990)

2.2.4 Use of Titanium Minerals

Titanium dioxide (TiO₂) pigment is the primary consumer of titanium minerals. Over 95% of rutile and ilmenite production is used to manufacture titanium dioxide pigment for use as white pigment in paint, rubber, plastics, paper, ink, textiles, cosmetics, leather and ceramics (Mineral Sands, www.minerals.org.au). The remaining 4 to 5% is mostly used for making titanium metal.

More specific uses of titanium products are as follows (Consolidated Rutile limited, www.consrutile.com.au/text/ac-minuse.htm):

Rutile

Rutile is processed to titanium dioxide to form the basis for a high quality, white pigment used in paints, paper, plastics, and cosmetics. Rutile and synthetic rutile are also processed to produce titanium metal for aerospace industries and for the manufacture of surgical equipment, such as hip replacements and pacemakers.

Ilmenite

As a mixture of iron and titanium oxides, ilmenite is used in steel making industry for furnace linings and for sand blasting. By removing the iron, ilmenite can also be upgraded to produce synthetic rutile, which can also be used to make titanium dioxide.

Titanium Dioxide

Titanium dioxide is a non-toxic pigment and has the ability to reflect and scatter all colours of light while absorbing ultra violet light. It has replaced lead based pigments in paints. When mixed with plastic and paper it gives them a white glossy sheen. It can also be added to foodstuffs such as flour, icing sugar and sweets as well as cosmetics and toothpaste to improve their brightness. Titanium dioxide is also used in the manufacture of many sunscreens because of its non-toxicity and UV absorption properties.

Titanium Metal

Titanium metal is an incredibly light and strong metal with a high melting point and is used in rockets, jet aircraft and sporting equipment. An Olympic standard bicycle frame made of titanium weighs only 1.7kg (approximately half the normal weight).

Titanium's lightness, strength and inertness (bio-compatibility) make it ideal for use in heart pacemakers, artificial limbs/joints, spectacle frames and watches.

When mixed with other metals such as iron, manganese and aluminium, it forms alloys, which are temperature and corrosion resistant. These alloys are used in power stations, paper mills, oil refineries and desalination plants.

2.2.5 Processing of Titanium Minerals and Products Derived from Titanium Minerals

The purposes of processing titanium minerals include: upgrading the titanium mineral concentrate to contain as high a TiO_2 content as possible; removing the impurity content in the concentrate so that the processed concentrate is suitable for the production of titanium dioxide pigments and titanium metal. Products derived from titanium minerals include: synthetic rutile, titanium dioxide pigment and titanium metal.

2.2.5.1 Upgrading of titanium mineral concentrates

One large upgrading process of titanium mineral concentrate is the slag process operated in Quebec Iron Titanium (QIT). At its Sorel smelter, concentrated ore of about 36.8% TiO_2 is mixed with 0 - 10% lime and 8 - 14% low ash coal, and heated to 1500 - 1700°C in electric arc smelter furnaces. During the smelting process a lighter titanium slag (80% TiO_2) and pig iron are produced (QIT, www.qit.com, 2001). Since impurities in the Sorel slag were detrimental to the chloride process, only sulfate process pigments producer used the slag. In the 1990s, QIT improved its process to satisfy the requirement of the chloride process by producing higher grade slag. In 1997, the UGSTM process was used to produce a UGSTM slag which contained 94.5% titanium dioxide. This slag of low impurities is suitable as a direct

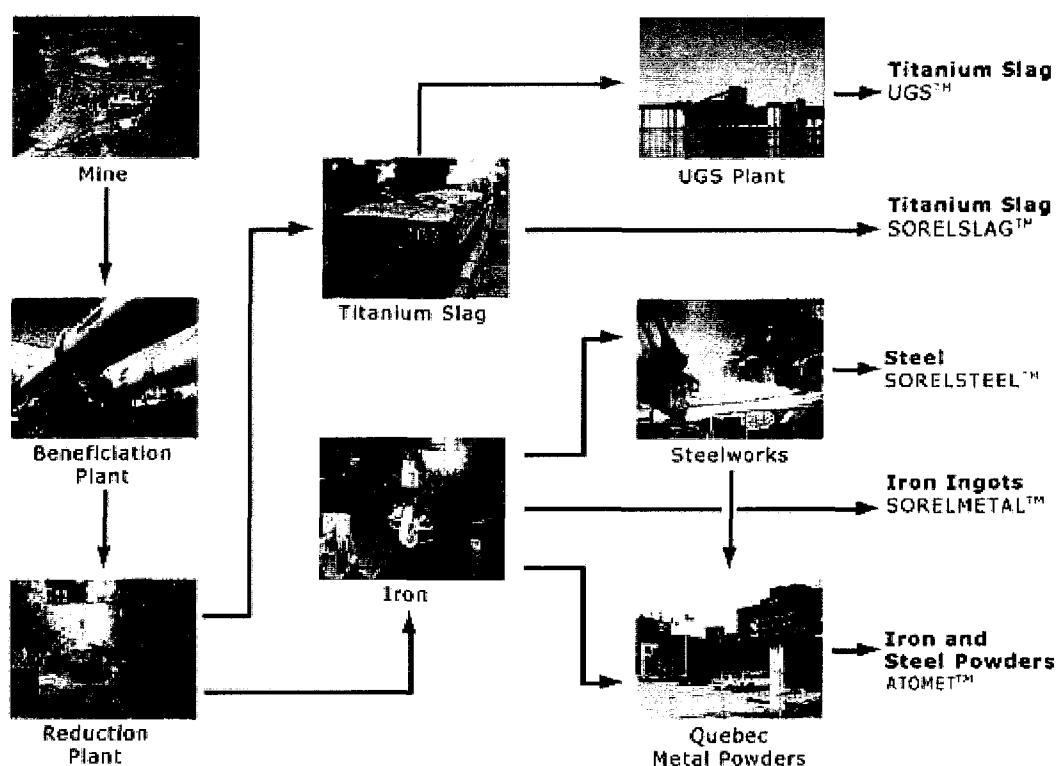


Figure 3 QIT Process Schematic (QIT, www.qit.com, 2001)

feed for the chloride titanium pigment process (QIT, www.qit.com, 2001). A graphical representation of the QIT process components is shown in Figure 3.

In South Africa, Richards Bay Minerals operates a similar slagging operation using the QIT technology. The difference is that its smelter feedstock is about 48% TiO_2 and is very low in impurities. Its slag contains 80 - 85% TiO_2 and can be used in both chloride and sulfate pigments manufacture (Garnar and Stanaway, 1994).

Another typical process, developed by the Norwegians, is reduction roasting of titanium mineral concentrate with coal. After removing the coal ash and fines by magnetic separation, the reduced pellets are smelted in an electric furnace. The resulting TiO_2 slag is then crushed and loaded for shipment (Garnar and Stanaway, 1994).

Leucoxene sample from oil sands tailings was subjected to reduction roasting, followed by leaching with ammonium chloride. The iron content dropped from 16.4% in the feed to 2.2% in the leaching residue, and TiO_2 content increased from 61.2% in the feed to 81.6% in the residue. However, the residue had relatively high silica content (8.8%). Pressure leaching with caustic soda at 200°C reduced the silica content from 8.8% to 1.6% (Alberta Chamber of Resources, 1996).

Other chemical processes such as those described in U.S. patents 5,885,536 (Hollit, 1999) and 5,085,837 (Chao and Senkler, 1992) could remove impurity elements by leaching with mineral acid and alkali metal salts. These impurities include iron, alkali metal, alkaline earth metal, rare earth metal, aluminum, phosphorus, thorium, uranium, chromium, manganese, silicon, vanadium and yttrium.

2.2.5.2 Production of synthetic rutile

Rutile can be directly treated by chlorination (chloride process) to yield titanium tetrachloride, an intermediate product which can be further processed to obtain the metal or titanium dioxide pigment. For ilmenite and altered ilmenite, the presence of iron oxide in the crystal lattice makes direct processing difficult, synthetic rutile is then produced when the iron in ilmenite, altered ilmenite or leucoxene is removed from the lattice structure leaving a relatively pure titanium dioxide as the final product. There are a number of processes available for the production of synthetic rutile from ilmenite series feed. Some of the different processes are schematically shown in Figure 4. More detailed process descriptions are as follows:

Benilite Process, in this process ilmenite is subjected to reduction roasting with coke, and is then leached by hydrochloric acid. The iron goes into solution, while filter cake contains synthetic rutile, with $>93 \text{ TiO}_2$ (Padmanabhan, 1990).

Ishihara Process, in this process, ilmenite (or leucoxene) is mixed with coke and reduced in an oil-fired rotary kiln for about 1 hour at about 900°C, converting over 95%

of the iron in the ilmenite to the ferrous state. After cooling, the residual coke is removed and the reduced ore is leached with waste acid from a sulfate process TiO_2 pigment plant. By adding the seed TiO_2 and keeping the leaching temperature at 130°C for 8 hours, iron and other impurities are selectively dissolved. The upgraded ilmenite is filtered, washed, and calcined at about 900°C , yielding an SO_3 -free product containing over 95% TiO_2 (Anon., 1971b; Kataoka and Yamada, 1973; Yamada, 1976).

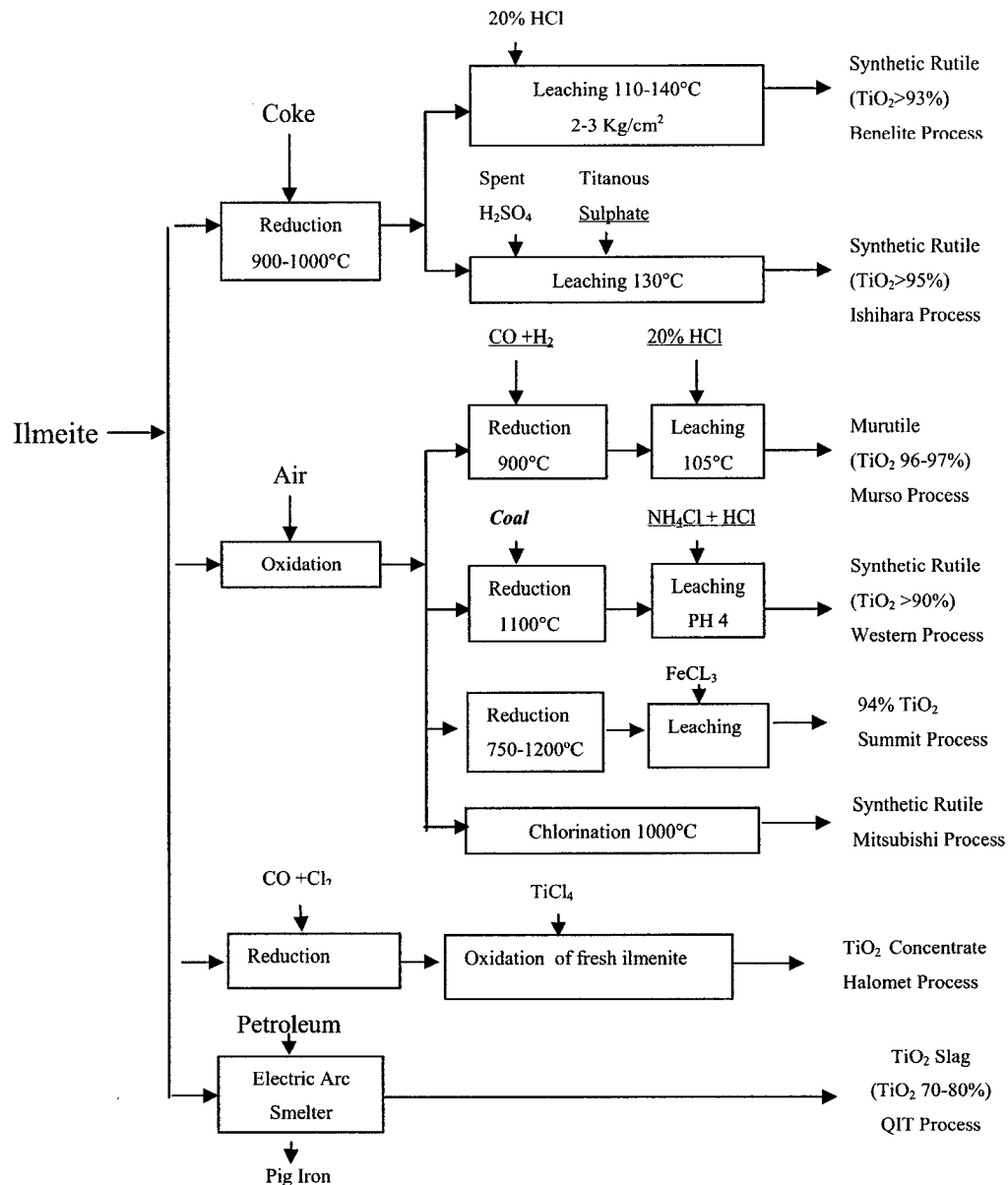


Figure 4 Synthetic Rutile Processes (Padmanabhan et al., 1990)

Murso Process, ilmenite is first oxidized at 900°C - 950°C with air, then reduced with hydrogen or hydrogen-containing gas in a fluid bed at 850°C to 900°C, reducing the ferric iron to the ferrous state with a minimum formation of metallic iron. This results in formation of a very reactive synthetic ilmenite product which is leached in 20% HCl solution at 108 to 110°C at atmosphere pressure for 3 to 4 hours, yielding a concentrate containing over 95% TiO₂. Magnetic separation may be used to remove chromium and other impurities from the final product. HCl can be regenerated from the FeCl₂ spent leach liquor by mature commercial processes and recycled (Sinha, 1972).

Western Titanium Process, this process uses high temperature oxidation to form a pseudobrookite structure, and then reduction with carbon to metallize the iron, which is then oxidized in an aerated water slurry and separated as a hydrated iron oxide suspension, yielding a beneficiated ilmenite containing 92% TiO₂. By adding as little as 2% of sulfur to the ilmenite the iron and manganese contents of the upgraded ilmenite can be further lowered, raising the TiO₂ content to 94% (Anon., 1973e, 1978c; Bracanin, 1972; Roberts, 1971).

Mitsubishi Process, in this process ilmenite is first oxidized at 950°C to 1000°C to convert all the iron to the ferric form. The oxidized material is then fed to a fluid bed chlorinator along with petroleum coke, where the iron is volatilized as ferric chloride.

The ferric chloride is then oxidized to yield ferric oxide, and chloride gas which is recycled to the chlorinator is subjected to electrostatic and magnetic separation to remove unreacted ore, coke and other impurities. About 10% of the original charge is returned to the fluidized reactor in the form of unreacted material. The final product contains 95 to 97% TiO₂ (Anon., 1972a).

Chorine Technology Process, in this process ilmenite is selectively chlorinated to remove iron and other impurities as volatile chlorides, using a fluid bed reactor under reducing conditions at about 1000°C, with the new feature of continuously removing a portion of the partially chlorinated bed, and separating it magnetically into an essentially

iron-free fraction, and a second iron-oxide-containing fraction, which is recycled to the chlorinator. Chlorine can be recovered by oxidizing the ferric chloride formed during chlorination. The final product contains 95 to 98% TiO_2 and 0.1 to 0.5% Fe_2O_3 (Dunn, 1972).

Halomet Process, partially reacted ilmenite is subjected to reduction-chlorination, with CO and Cl_2 , forming TiCl_4 and FeCl_3 , which pass to the oxidation part of the chlorinator where fresh ilmenite reacts with the TiCl_4 to form more FeCl_3 and TiO_2 . Proper metering of chlorine permits isolation of high purity ferric chloride at one end of the reactor and a titanium dioxide concentrate at the other (Anon., 1971a; Othmer and Nowak, 1972).

Summit Process, in this process ilmenite ore is oxidized in air or other oxygen-containing gases at 750°C to 1200°C to convert all the iron to the ferric state. The oxidized ore is then reduced at 750°C to 1200°C , using solid carbon fuels, carbon monoxide, hydrogen, or other reducing agents, reducing over 90% of the iron content to metal. The metallic iron is removed from the reduced ore by leaching for about 0.5 hour with an aqueous solution of ferric chloride. The residue from the leaching process is washed and dried to yield a final concentrate containing up to about 94% TiO_2 (Roberts, 1971; Shiah, 1966).

2.2.5.3 Production of titanium dioxide pigments

Titanium dioxide pigment is extracted from ilmenite and altered ilmenite (45-70% TiO_2) and Rutile (92-96% TiO_2) by two different processes referred to as the sulphate process and the chloride process. Figure 5 summarizes the possible process routes. For ilmenite ore, depending on the titanium content and the impurities, several options are available for processing. The main ones are the sulphate process, the titanium slag production and selective leaching process (e.g. HCl leaching).

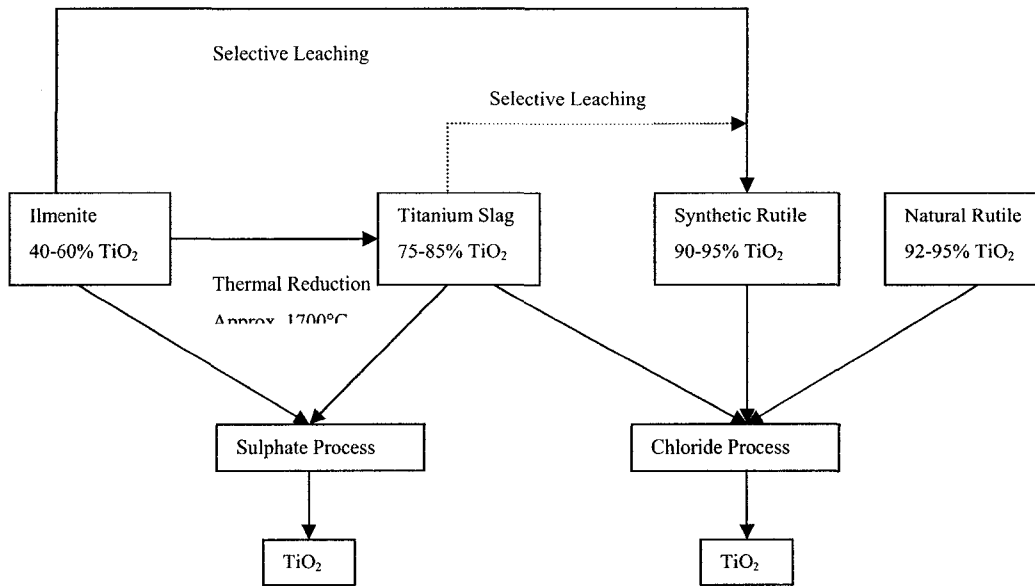
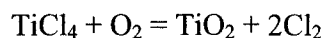
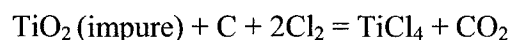


Figure 5 Production of TiO_2 from different feedstocks (Kogler and Engelhardt, 1997)

Sulphate Process: The sulphate process is the first commercial scale technology used to convert ilmenite to titanium dioxide. Finely ground ilmenite or high TiO_2 slag is digested with strong sulfuric acid, forming a solid, porous cake which is dissolved in dilute acid and water to produce a solution of titanyl sulphate (TiOSO_4) and iron sulphate. The ferric iron is reduced to ferrous iron by adding scrap iron. This is done to avoid precipitation of ferric iron later in the process and to facilitate washing the precipitated titania, because ferrous iron is less strongly adsorbed (Lefond, 1983). Some of the iron is crystallized as iron sulphate and removed. White hydrous titanium oxide is precipitated from the solution by adding water of alkali and the remaining iron washed out. The precipitate is heated, without melting, to about 1000°C to drive off contained water and allow formation of very fine crystals of raw white pigment (CRL, www.consrutile.com.au).

Chloride Process: Worldwide, there is a marked swing to the use of the chloride process with few new sulphate-process plants being established. Currently, the chloride process produces about 65 % of the 4 million tonnes of pigment produced worldwide. Most chloride process pigment producers are unable to chlorinate feedstock with titanium dioxide content below 85%. Rutile and synthetic rutile are used.

Plants using the newer chlorination process produce white pigment by calcining a mixture of synthetic rutile, coke and chlorine to form gaseous titanium tetrachloride (TiCl_4) (Yang and Hlavcek, 1998). Ilmenite cannot be used as a raw material as its titanium content is too low. The titanium tetrachloride is condensed to a liquid and most of the impurities separate as solids. It is then reheated to a gas and mixed with hot oxygen to form very fine crystalline rutile (raw white pigment). The displaced chlorine gas is recycled to the start of the process (CRL, www.consrutile.com.au).



Aluminum chloride is added to the titanium tetrachloride to assure that all the titanium is oxidized to the rutile crystalline form. The chlorine formed during oxidation is recovered and recycled (Lefond, 1983). Spray calcinations can also be used to yield TiO_2 pigment particles between 150-250nm (Gurav et al., 1998).

Other special treatments are available to improve the qualities of the pigment depending on the end use of the pigment. These involve special coatings such as aluminum phosphate coatings for improving its light fastness in laminates (Banford et al., 1998), and silica, alumina and zirconia phosphates for improving its durability and gloss (Hiew et al., 2002). Treatments by organic chemicals can improve the wettability, disperibility and gloss characteristics of pigment that is particularly suitable for use in water-thinnable systems (Orth-Gerber et al., 2002).

2.2.5.5 Production of titanium metal

Titanium is produced mainly by magnesium reduction, the Kroll process, or sodium reduction, the Hunter process (Gerdemann et al., 1997).

At the plant of Titanium Metals Corp. of American, reduction of $TiCl_4$ is conducted with magnesium in steel pots in gas-fired furnaces, under an inert helium atmosphere, at a temperature above the melting point of magnesium chloride, but below the melting point of titanium metal, which forms as a sponge-like mass. The sponge is removed from the reactor in a dry room to avoid absorption of moisture and is crushed and leached with acid to remove residual magnesium and magnesium chloride. The magnesium chloride drained from the reactor is transported molten to the magnesium plant, where magnesium and chloride are recovered by electrolysis (Lloyd, 1956).

Titanium sponge can be converted to ingot by compacting and double or triple vacuum arc melting, along with scrap and alloying constitutes as a consumable electrode, using a water-cooled copper crucible. Vacuum melting removes hydrogen, residual magnesium chloride, and other volatile impurities (Lefond, 1983; Deura et al., 1998).

2.3 Zirconium: Resources and Utilizations

2.3.1 Zirconium Minerals

2.3.1.1 Mineralogy

Zircon and baddelyite are the major sources of zirconium on the earth. In addition to zircon and baddelyite, zirconium and hafnium also occur as silicates in combination with iron, calcium, sodium, manganese, and other elements. Zircon is extremely resistant to weathering; therefore, it can be found in many ancient beach sands and placer deposits. Although resistant to alteration from external sources, zircon does go through internal alteration (metamictization) as thorium and uranium (usually <500ppm) substitute for zirconium either in the zircon lattice or in solid solution (Lefond, 1983).

Internal alteration of zircon takes place as radioactive emanations from these elements disorder the crystal lattice. This process is accompanied by hydration, reduction in specific gravity, and change in color. The effects of zircon's internal alteration and darkened color can be corrected by heating to 1000°C for 30 min or so. An appropriate combination of time and temperature makes it possible for decolorization and reordering of the crystal lattice to take place when zircon is heated at higher temperatures for shorter periods or at lower temperatures for longer periods. After the mineral is heated, X-ray diffraction patterns are sharper, the grains may be harder, and except for particles of malacon, the grains will be white or colorless in the absence of surface coatings. The color change is only temporary and the particles slowly darken again with time (Lefond, 1983).

2.3.1.2 Occurrence of zircon and baddeleyite

Zircon originates as an accessory mineral in a variety of igneous and metamorphic rocks, especially those containing sodic feldspars such as granite, syenite, and diorite. It is one of the earliest minerals to crystallize from a cooling magma and sometimes found in metamorphic rocks such as gneiss and schists. One occurrence has been reported in a meteorite.

Before the zircon particles can become part of a beach sand deposit, their host rocks must go through a series of events that will ultimately liberate the zircon for transportation to a seacoast. After subaerial weathering, the rocks are broken down into smaller fragments and after further weathering decomposes to the point at which the smaller zircon grains are liberated. The mineral particles are transported by streams and ultimately are deposited along a marine shoreline. Here, the action of the waves, tidal currents, and wind may remove lighter quartz and form a heavy mineral deposit rich in zircon. Some of the older beach sand deposits have been consolidated and the grains cemented together to form sandstones containing concentrations of titanium minerals, zircon, monazite, and other heavy minerals. At present, all commercial zircon products are mined and separated

from relatively young (Pleistocene or younger) beach sand deposits on or near active coastlines (Lefond, 1983).

2.3.2 Concentration Methods for Zirconium Minerals

Most of the heavy mineral operations in the world are similar. The alluvial ores are mined with dredges, cutter-suction or bucket line. In areas where there is not sufficient water for dredging, ores are mined using elevating scrapers and bulldozers.

The heavy minerals are concentrated by removing the quartz and other light minerals in gravity concentrators. The gravity concentrates are scrubbed to remove any surface coatings which might interfere with dry processing. The concentrates are then dried and separated into ilmenite, leucoxene, and rutile by magnetic and high-tension techniques. The remaining materials are further treated by a combination of spirals, gravity tables, high-tension separators, magnets, and air tables to produce zircon concentrate. Typical processing flow sheets are shown in Figure 4 and Figure 5.

2.3.3 World Zirconium Resources and Demand

Table 9 shows the world zirconium production (Hedrick, 2002). The world zirconium mineral resources total about 100 million tons of ZrO_2 with Australia and South Africa as the dominant producers. It is also noted that there is currently no zirconium mineral production in Canada.

Table 9 Production of zirconium minerals by country (Hedrick, 2002)

Unit: thousand metric tons

	Zirconium (ZrO ₂)				Hafnium (HfO ₂)	
	Mine production		Reserves	Reserve base	Reserves	Reserve base
	2000	2001 ^c				
United States	100	100	3400	5300	68	97
Australia	400	400	9100	30080	180	600
Brazil	19	30	1900	1900	7	7
China	^c 15	15	500	1000	NA	NA
India	19	19	3400	3800	42	46
South Africa	400	300	14000	14000	260	260
Ukraine	^c 65	75	4000	6000	NA	NA
Other countries	23	30	900	4100	NA	NA
World total	1040	1070	36000	65000	560	1000

2.3.4 Use of Zirconium Minerals and Products Derived from Zircon

Zircon sands are used in a variety of market ranging from foundry sands to zirconium-metal production. The major uses are: foundry uses, basic steel production, refractory use, abrasives, zircon-flour opacifier, zirconium metal, zirconium compounds, other zircon products and uses, hafnium metal and hafnium compounds. The following more detailed descriptions are referred from Lefond (1983):

Foundry use: the low thermal expansion and clean rounded grains of zircon that requires less binder and neutral or slightly acid pH make it ideal foundry sand. Zircon sand is used in foundry as shell cores and mold linings. It is also dry ground to flour and used to make mold washes which are painted on mold facings to give castings a smoother surface finish. The investment casting industry uses zircon sand as stucco grain and the flour for smoother finishes.

Basic steel production: zircon sand is used in basic steel production in ladle brick because it can reduce erosion and extend ladle-lining life. It is used in coatings, mortars, and as ladle-nozzle fill.

Refractory use: zircon sands can be fused to make refractory brick, which are used to line kilns, glass-melting furnaces, etc. Zircon sands can also be fused to make high temperature boats, dishes, and other laboratory ware. ZrO_2 refractories can be used at temperatures up to $1960^\circ C$ (ZrO_2 melts completely at $2760^\circ C$).

Abrasives: zircon sand is converted into ZrO_2 and used to produce zirconia and aluminum-zircon abrasives products. Zircon sand is also used to clean turbines in electrical generating plants.

Zircon-flour opacifier: zircon sand is wet ground, spray dried and sold as an opacifier for porcelain glazes. Because of its high index of refraction, it acts like TiO_2 pigment in paint, in which material of a much low index of refraction gives it an opaque white appearance.

Zirconium metal: zirconium is a hard and shiny metal. It is resistant to corrosion by water, mineral acids, strong alkalis, organic acids and salt solutions except hydrofluoric acid. Zirconium is produced from zircon sand by reacting chlorine in the presence of carbon and then converting the tetrachloride to sponge metal, which can be further worked to various shapes such as plate and bolts. The sponge metal contains about 2.5% hafnium which is closely related to zirconium and very difficult to separate. The commercial metal usually contains hafnium but reactor-grade zirconium for use in atomic reactors must be hafnium-free. Because of its low neutron-capture cross section, thermal stability, and corrosion resistance, pure zirconium is valued for atomic construction purposes. Small amounts of zirconium are used in steel. Steel with small amounts of zirconium is fine grained and has good shock and fatigue resistance.

Zirconium compound: Zirconium compounds are prepared and marketed for the following uses:

Zirconium oxychloride -----Textile coatings

Zirconium carbide-----Abrasive

Zirconium tetrachloride-----Refine Al and Mg

Sodium zirconium sulfate-----Precipitation of proteins, pigments stabilizer, and paper opacifer

Zirconium carbonate----- Poison ivy ointment

Zirconium hydride-----Neutron moderator

Other zircon products and uses: some zircon is used as special welding rod coatings which, together with other ingredients, form slag to shield the weld pool.

Hafnium metal: hafnium is sparsely disseminated and very expensive to extract although it is relatively abundant in nature. Zircon sand is the only commercial source of this metal. Hafnium's melting point is 2200°C, which is higher than that of zirconium. Heat-resisting parts for special purposes are made by compacting hafnium powder to a density of 98%. Hafnium has excellent resistance to a wide range of corrosive environments. Hafnium is also useful in unalloyed form in nuclear reactors because of its high thermal neutron-capture cross section and excellent strength up to 540°C.

Hafnium compounds: hafnium oxide is a better refractory ceramic than zirconia, but is more expensive. The inversion of the crystal from the monoclinic to the tetragonal form occurs at 1700 °C with a 3.4% expansion compared to 1090 °C and 7.5% in zirconia. Hafnium carbide has a melting point of 2290°C, making it one of the most refractory materials. Hafnium carbide is produced by reacting hafnium oxide and carbon at high temperatures.

2.4 Previous Studies to Recover Heavy Minerals from the Athabasca Oil Sands

The major difference between processing oil sands tailings and processing conventional beach sands is that solids in the oil sands tailings are coated with residual bitumen. The residual bitumen needs to be removed prior to any mineral beneficiation processes. The methods that can be used to remove the residual bitumen should affect the mineral separation efficiencies. Surprisingly, little attention has been paid to such effects.

The main purpose of mineral processing is to produce individual concentrates of desired grades before further processing. Mineral processing exploits the differences in the physical and chemical properties between desired minerals and gangue minerals to achieve the separation. These properties include specific gravity, magnetic susceptibility, electrical conductivity and surface wettability, etc.

Table 10 lists the separation characteristics of heavy minerals typically contained in alluvial mineral deposits such as the Alberta oil sands.

As can be seen, heavy minerals and the associated gangues have different separation characteristics, in addition to the significant differences in their specific gravity. Some minerals are magnetic, others are electrical conductors, and still others are both magnetic and electrical conductors.

Table 10 Separation characteristics of heavy minerals

Mineral	Specific Gravity	Magnetic Property	Electrical Conductivity
Ilmenite	4.5-5.0	Magnetic	Conductor
Altered Ilmenite	4.0-5.0	Magnetic	Conductor
Leucoxene	3.5-4.5	Weakly Magnetic	Conductor
Rutile	4.2	Non-magnetic	Conductor
Anatase	4.2	Non-magnetic	Conductor
Zircon	4.6-4.7	Non-magnetic	Non-conductor
Pyrite	4.9-5.2	Weakly Magnetic	Conductor
Tourmaline	3.0-3.2	Weakly Magnetic	Non-conductor
Garnet	3.4-4.2	Weakly Magnetic	Non-conductor
Staurolite	3.7-3.8	Weakly Magnetic	Non-conductor
Monazite	4.9-5.4	Weakly Magnetic	Non-conductor
Quartz	2.65	Non-magnetic	Non-conductor

2.4.2 Typical Separation Methods Used in Heavy Mineral Separation

2.4.2.1 Gravity concentration

Gravity concentration methods separate minerals of different specific gravity by their relative movement in response to gravity and one or more other forces, the latter often

being the resistance to motion caused by a viscous fluid, such as water or air. In order to effect a separation there must be a sufficient difference in the specific gravity between the mineral and the gangue.

There are many different types of gravity concentration equipment for various sizes of particle or types of feed. Gravity concentration equipment for heavy minerals include pinched sluices, cones, spirals, shaking tables and centrifugal equipments such as hydrocyclones and centrifugal separators.

Pinched Sluice

Pinched sluices of various forms have been used for heavy mineral separation for centuries. Its simplest form is an inclined launder about 1 m long, narrowing from about 200 mm in width at the feed to about 25 mm at the discharge. Pulp of between 50 and 60% solids enters gently and stratifies as it descends; at the discharge end these strata are separated by various methods, such as by splitters, or by some type of tray.

Reichert Cone

Reichert cone is a wet gravity concentrating device designed for high-capacity application. Its principle of operation is similar to that of a pinched sluice, but the pulp flow is not restricted or influenced by sidewall effect. The single unit comprises several cone sections stacked vertically so as to permit several stages of upgrading. The efficiency of the separation process is relatively low and is repeated a number of times within a single machine to achieve effective performance.

Spiral

The most extensive usage of spiral concentrators has been in the treatment of heavy mineral sand deposits, such as those carrying ilmenite, rutile, zircon, and monazite. Its feed is between 15-45% solids by weight and in the size range 3 mm to 0.075 mm.

Shaking Table

Shaking table is the most efficient form of gravity concentrator, and is used to treat the smaller, more difficult flow-streams, and to produce finished concentrates from the products of other forms of gravity system.

Hydrocyclone

Hydrocyclone has found many applications in mineral processing industry. Its principle applications are: thickening, solids recovery, liquids recovery, fractionation, counter washing, degrading, desliming, classification, selective classification and pre-concentration (Trawinsk 1976; Burt, 1984).

Centrifugal Concentrator

There have been a number of centrifugal gravity separation devices designed to treat ultra-fine particles since 1980s. The Falcon Centrifugal Concentrator is one of the latest developments. It takes advantage of the difference in specific gravity between heavy minerals and light minerals to effect a separation (Falcon Concentrator Inc., 1996).

2.4.2.2 Magnetic separation

Magnetic separation exploits the difference in magnetic properties of minerals. This technique can be used to separate magnetic minerals from non-magnetic minerals, or minerals of different degree of magnetic susceptibilities.

2.4.2.3 Electrostatic and high-tension separation

Both electrostatic and high-tension separations utilize the difference in electrical conductivity among the various minerals in the ore feed to effect a separation. The greatest application has been in the processing of heavy mineral sands.

2.4.2.4 Froth flotation

Although flotation is the most important and versatile mineral processing technique today, it is a relatively new technique for the separation of heavy minerals. Most heavy mineral deposits mined until now are alluvial or placer deposits and have consisted of well-liberated and well-rounded grains of minerals. It is easy to recover these minerals by gravity, electrostatic and magnetic separation techniques. As ore bodies become more disseminated and particle sizes get finer, the conventional gravity/magnetic/electrostatic combinations may gradually lose their efficiencies and froth flotation has been studied recently (Mao, et al, 1999; Bulatovic, 2000). At present flotation is not being used on a commercial scale to float any heavy minerals from the beach sands.

2.4.3 *Previous Studies to Recover Heavy Minerals from Alberta Oil Sands Tailings*

Despite the available heavy mineral resources and the favorable economic potentials, there is currently no commercial process to recover the heavy minerals. Several studies have been carried out since the 1970s, but none was able to produce saleable heavy mineral concentrates.

The previous heavy mineral extraction studies were focused mostly on the process flow sheet development, which could be broken into two major process stages: 1) removal of residual bitumen and slimes, and 2) mineral separation and upgrading.

2.4.3.1 Removal of residual bitumen and slimes

The initial stage in processing the tailings usually involves: 1) the removal of residual bitumen, 2) the removal of slimes (–325 mesh materials) which cause problems in subsequent separation of individual minerals, and 3) the reduction of the content of low-density (light) minerals such as quartz. To achieve these objectives, the following three procedures were tested in previous studies.

Burn-off and gravity concentration

Figure 6 shows a scheme to remove the residual bitumen and slimes in early studies. When the feed contained 13.3% TiO₂ and 5.4% ZrO₂, the finisher spiral concentrate contained approximately 30% TiO₂, 12.1% ZrO₂, 12% iron oxides and overall 71% heavy minerals.

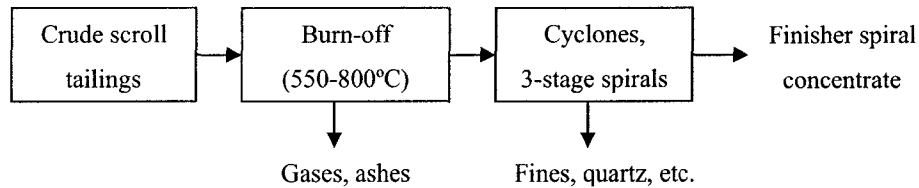


Figure 6 Schematic flow sheet of bitumen and slime removal (Trevoy et al., 1978; Trevoy and Schutte, 1981)

Typically, the product from the 3-stage spiral circuit consisted of solids of which 86% were in the -100+325 mesh size range. Recovery of Ti was close to 80% and recovery of Zr was above 90% in the 3-stage spiral circuit (Trevoy et al., 1978; Trevoy and Schutte, 1981).

Flotation and burn-off

In this process, the tailings were subject to a bulk flotation which floated the heavy minerals into a bulk concentrate together with the residual bitumen. The light minerals were rejected into the float tails. The optimum pH for heavy mineral flotation was in the range of 8.3 to 11.7. Optimum frother dosage was found to be 0.15 vol. % of pine oil. With a feed analyzing 10 - 12% TiO₂ and 4 - 5% zircon, a concentrate assaying 28 - 30% TiO₂ and 10 - 12% zircon was obtained at 85 - 95% recovery of both minerals (Ityokumbul et al., 1985).

In the mid-1990s, a modification was made to this process. A hydrocyclone was employed prior to the flotation. This modified process showed that the hydrocyclone could produce an underflow with enrichment ratios of 1.15 to 1.2 while removing over 80% of the water and bitumen from the feed. Cycloning at optimum settings recovered

approximately 85% of the heavy minerals (Owen and Tipman, 1999). Figure 7 shows the process flow sheet.

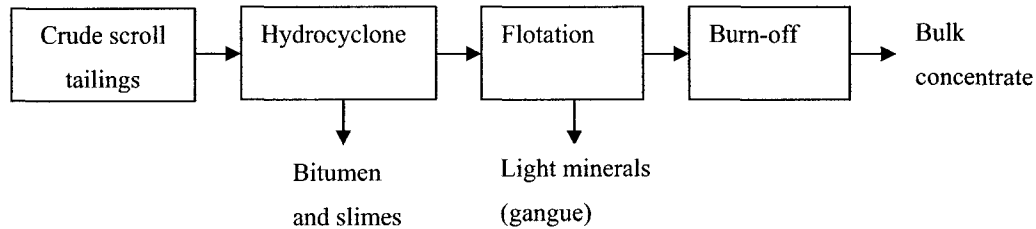


Figure 7 Removal of residual bitumen/slimes/gangue by hydrocyclone, flotation and burn off (Owen and Tipman, 1999)

Flotation and burn-off (or solvent washing)

Recently, a high pulp temperature flotation followed by burn-off (or solvent washing) was developed by Syncrude Canada Ltd and Lakefield Research Ltd. During the bulk flotation process, high recoveries could be obtained at high pH (above pH 11). The minimum flotation temperature required to obtain high heavy mineral recoveries was 70°C. The maximum recovery was obtained at 80°C. With a feed analyzing 13.6% TiO₂ and 3.38% ZrO₂, a bulk concentrate assaying 27.6% TiO₂ and 7.10% ZrO₂, with recoveries of 97% for TiO₂ and 99.4% for ZrO₂, was obtained. During the semi-bulk flotation process, the conditions were similar to those used in bulk flotation, except that starch was used to depress leucoxene. Leucoxene was recovered from the semi-bulk tailing after de-sliming and flotation using an ester collector at acidic pH. The solvent washing process involved scrubbing the bulk concentrate in the presence of naphtha and a surfactant, followed by removal of naphtha/bitumen fraction in a hydrocyclone. Successful removal of bitumen depended on the naphtha/bitumen ratio and the level of surfactant additions. Effective bitumen removal was achieved at high surfactant additions and high naphtha/bitumen ratios (Bulatovic, 1999 and 2000).

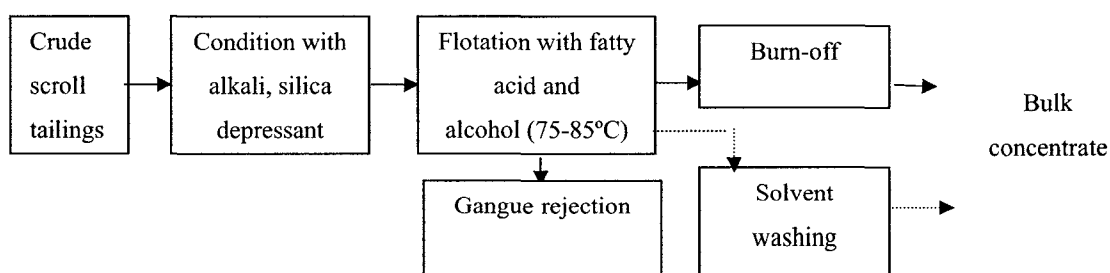


Figure 8 Schematic flow sheet of bulk flotation and burn-off (Bulatovic, 1999 and 2000)

2.4.3.2 Mineral separation and upgrading

Separation of zircon from titanium minerals

After removing residual bitumen, slimes and some of the light gangue minerals, the heavy mineral stream is then separated into zircon and titanium mineral concentrates. In this stage, high-tension separation, magnetic separation, gravity separation plus magnetic separation, and sequential zircon–titanium mineral flotation, were used.

1. High-tension separation process. This is a typical process used in beach sand processing to separate zircon, which is a non-conductor, from titanium minerals, which are conductors. When it was used in oil sands tailings, it was shown that when the feed contained 31.7% TiO_2 , 10.8% ZrO_2 , 11.4% Fe_2O_3 and 7.6% Al_2O_3 , using two stages of high tension separation and recycling the products from the second stage, two concentrates were obtained: a titanium minerals concentrate with a grade of 57% TiO_2 , 19% Fe_2O_3 , 4% Al_2O_3 and 5% zircon; and a zircon concentrate which analyzed 39% zircon, 4% TiO_2 , 3% Fe_2O_3 and 8% Al_2O_3 . Sink-float analysis with methylene iodine showed that the titanium mineral concentrate consisted of 99.2% heavy minerals, while the zircon concentrate contained only 56% heavy minerals, thus requiring further upgrading (Trevoy et al., 1978, Trevoy, 1979).
2. Gravity separation process. Spirals were used to separate the titanium minerals from zircon. After passing through a Humphrey spiral concentrator, zircon and rare earth

minerals reported to heavy product; the middlings included rutile, silica, tourmaline and leucoxene while the light product contained primarily quartz (Alberta Chamber of Resources, 1996).

3. Flotation separation process. In this process, the zircon was floated with a cationic collector and the titanium minerals were depressed with starches. Oxidized cornstarch was found to be the most effective titanium mineral depressant. Among the examined collector types of primary amines and modified mixtures of primary and secondary amines, the latter gave a higher rate of zircon flotation. In addition, tourmaline and garnet group minerals, which are magnetic, floated together with zircon that is non-magnetic. This is desirable since otherwise these minerals would interfere with the upgrading of the titanium minerals if they stayed in the float tails (Bulatovic, 1999 and 2000).
4. Magnetic separation plus high-tension separation. After removing the strongly magnetic minerals by low intensity magnetic separation, the bulk concentrate was further separated by high intensity magnetic separation on a Frantz Isodynamic Separator by setting the electric current at 0.35 A, 0.70 A, 0.95 A and 1.50 A. Major mineral concentrates produced at the corresponding current are ilmenite, xenotime, monazite and rutile. The non-magnetic fraction at 1.50 A was considered to be zircon (Ityokumbul et al., 1987). However, none of the mineral concentrates had satisfactory grades.

Upgrading of zircon concentrate

The rougher zircon concentrate obtained was of relatively low grade. Further upgrading was required. Two near-market grade zircon concentrates were obtained by the following processes:

1. Gravity separation plus high gradient magnetic separation. By using a flow sheet containing three-stage gravity separation and high-gradient magnetic separation, a

final concentrate assaying 65.1% ZrO₂, 1.16% Hf, 0.15% Fe₂O₃ and 0.23% TiO₂ was obtained (Bulatovic, 1999 and 2000).

2. Combination of gravity, high intensity magnetic and high-tension separation. By using this process, a final zircon concentrate consisting of 66.0% ZrO₂ with 0.47% TiO₂, 0.11% Fe₂O₃ and 0.72% Al₂O₃ was obtained. Minerals that are most difficult to separate from zircon are two aluminum-containing minerals, corundum and kyanite (Trevoy et al., 1978, Trevoy, 1979).

Fractionation of the titanium mineral concentrates

Unlike zirconium, which exists in the oil sands as the mineral zircon, titanium exists in the oil sands as several heavy mineral species: rutile, anatase, ilmenite, and leucoxene (which is an altered ilmenite with varying concentrations of Fe). These minerals have different TiO₂ contents and their values are significantly different. Rutile and anatase are the most valuable. Separation of the titanium minerals into individual concentrates would be desirable, especially considering the high transportation costs required for the heavy mineral concentrates if any potential heavy mineral processing plants would be built in Fort McMurray, Alberta.

The following processes have been tested on the fractionation of the titanium minerals:

1. Magnetic separation. One process used the Stearns High Intensity Separator. Using this separator, a titanium mineral concentrate (99% heavy minerals by sink-float analysis), which assayed 55% TiO₂, 21.4% Fe₂O₃, 4.7% ZrO₂ and 3.8% Al₂O₃, was separated into fifteen magnetic fractions and a nonmagnetic fraction. The initial magnetic fractions were ilmenite (containing 46.7% - 50.0% TiO₂ and 38.6% - 21.4% Fe₂O₃); the next, leucoxene (containing 50.0% - 63.4% TiO₂ and 21.4% - 7.1% Fe₂O₃). The non-magnetic fraction was claimed to be a crude rutile concentrate (containing 75.1% TiO₂ and 2.3% Fe₂O₃) (Trevoy et al., 1978, Trevoy, 1979).

2. Magnetic separation. The strongly magnetic minerals were removed by low intensity magnetic separation. The bulk concentrate was then further fractionated by high intensity magnetic separation on a Frantz Isodynamic Separator by setting the electric current to 0.35 A, 0.70 A, 0.95 A and 1.50 A. The major minerals corresponding to the current settings are ilmenite, xenotime, monazite and rutile (Ityokumbul et al., 1987).
3. Low intensity magnetic separation and electrostatic separation. Three products were produced. About 18.5% of the titanium present in the concentrate occurred as magnetic concentrate, which was believed to be ilmenite, assaying 64.4% TiO₂, 30.1% Fe₂O₃ and 1.3% SiO₂. The largest portion of titanium occurred as a conductor, a pseudorutile plus rutile mixture and assayed 74.6% TiO₂. The third fraction of titanium (leucoxene) was a non-conductor, comprised 23.5% of the total titanium and assayed 65% TiO₂, 6.56% Fe₂O₃ and 11.7% SiO₂ (Bulatovic, 1999 and 2000).

It is clear that the previous studies focused on the process development testwork. No studies were conducted to examine the ultimate limit of upgrading the zircon and titanium mineral concentrates given the mineralogical composition of the oil sands tailings.

2.4.4 *Unsolved Issues*

2.4.4.1 At the bitumen/slime removal stage

The residual bitumen present in the oil sands tailings interferes with the mineral separation operations. It needs to be removed before any mineral beneficiation is possible. Two questions that remain unanswered in this regards are: 1) what is the best process to remove the residual bitumen? and 2) is the residual bitumen worth recovering?

The two methods to remove the residual bitumen that have been studied were burn-off and solvent extraction. Burning off the residual bitumen (at 600~700°C) is a straightforward operation. The heat generated may be utilized and all the organic matter,

both the “extractable” and “combustible” hydrocarbons (Majid and Ripmeester, 1986), can be removed. The process also has the advantage that most of the secondary minerals, such as pyrite and siderite, will be decomposed. However, the separation characteristics of the heavy minerals (such as the magnetic properties of some titanium minerals) may be altered as well, which may not be desirable for the subsequent separation processes.

Using solvent extraction to remove the residual bitumen may increase the bitumen recovery if the extracted bitumen can be recovered. Usually, the froth treatment tailings need to be de-slimes before the solvent extraction. However, the residual bitumen is mostly associated with the slimes in the tailings. Removal of the slimes can cause significant losses of the residual bitumen, nullifying the benefit of additional bitumen recovery. Furthermore, solvent washing can change the surface wettability of the minerals, which affects the subsequent mineral separation if froth flotation is to be used.

In fact, if the majority of the residual bitumen could be removed together with the water and slimes in a pre-treatment process, then the slime products can probably be used as a fuel and the coarse sands may be further processed without burn-off or solvent washing of large tonnage of materials.

Whether the residual bitumen should be burnt or extracted with solvent depends on whether it is worthwhile to be recovered. The bitumen contained in the oil sands feed are known to have both the “extractable” and the “combustible” forms. It is possible that most of the “extractable” bitumen has been recovered in the hot water extraction processes and the residual bitumen in the tailings are mainly the “combustible” types. It is further noticed that solvent washing may only remove the “extractable” bitumen but not the “combustible” ones, so that not all the organic matters are removed from the oil sands tailings using the solvent washing processes.

2.4.4.2 At the mineral separation/upgrading stage

The heavy mineral concentrates produced from previous studies, i.e., zircon, rutile (anatase), leucoxene and ilmenite, contained high concentrations of misplaced minerals and were not of saleable grades. The rutile (anatase) concentrates were usually contaminated by the Fe-bearing titanium minerals (ilmenite and leucoxene). The ilmenite and leucoxene concentrates, on the other hand, contained excessive amount of radioactive elements (uranium and thorium). All the titanium mineral concentrates had high quartz content.

The zircon concentrates previously produced were closer to market-grades. Still, the Fe and Ti concentrations exceeded the maximum limits. Besides, all the zircon concentrates produced so far were off-white – in fact, they were of a dark color that was not typical of the zircon mineral and hindered the high-end applications of the mineral (such as zirconium glazes, etc.).

Table 11 to Table 13 show the grades of the heavy mineral concentrates produced from several prior metallurgical studies, together with typical market-grade heavy mineral concentrates.

Table 11 Grades of rutile concentrates produced in previous studies

Compound	Weight % in rutile concentrate				
	MDL*	WOU	MDA	LRL	Typical market grade
TiO ₂	92.9	63.3	73.3	74.2	96.1
ZrO ₂	0.6	12.2	2.3	0.42	0.6
Fe ₂ O ₃	1.5	< 1.43	1.0	17.2	0.5
Al ₂ O ₃	0.6	NA [#]	NA	NA	0.4
SiO ₂	1.85	21.3	15.0	1.8	0.6

Table 12 Grades of ilmenite and leucoxene concentrates produced in previous studies

Comp.	Weight % in ilmenite concentrate					Weight % in leucoxene concentrate				
	MDL*	WOU	MDA	LRL	Market grade	MDL*	WOU	MDA	LRL	Market grade
TiO ₂	31.5	66.7	33.3	64.4	54.0	72.0	53.3	60.0	65.4	60.0
ZrO ₂	NA	< 0.07	0.5	0.24	NA	NA	< 0.07	0.5	2.45	NA
Fe ₂ O ₃	45.9	20.0	43.6	30.1	19.0	20.9	18.6	24.3	6.56	32.5
Al ₂ O ₃	5.8	NA	NA	NA	0.4	1.6	NA	NA	NA	1.2
SiO ₂	14.8	13.0	9.6	1.3	0.5	2.9	14.9	3.2	11.7	0.85
Cr ₂ O ₃	0.6	NA	NA	NA	0.4	0.6	NA	NA	NA	0.11

Table 13 Grades of zircon concentrates produced in previous studies

Compound	Weight % in zircon concentrate				
	MDL*	WOU	MDA	LRL	Typical market grade
ZrO ₂	66.3	39.0	59.5	65.1	66.2
TiO ₂	0.1	16.0	10.0	0.23	0.1
Fe ₂ O ₃	0.05	1.4	1.0	0.15	0.02
Al ₂ O ₃	0.3	NA	NA	NA	0.2

* The mineral analysis for this sample conducted by Mineral Deposits Ltd differs significantly from all analyses before and since. It is not known if this is a result of differing analytical techniques or differences in the sample.

NA – not available.

MDL – Mineral Deposits Ltd., Australia, (Balderson, 1982)

WOU – Western Ontario University, Canada, (Ityokumbul, et al., 1985)

MDA – Mineral Agreement Study, (Alberta Chamber of Resources, 1996)

LRL – Syncrude Canada Ltd and Lakefield Research Ltd, (Oxenford et al., 2001).

3 OBJECTIVE

The objective of the proposed research program is to study the effect of residual bitumen removal methods on the separation of individual minerals contained in the oil sands tailings. This study aims at a fundamental understanding of the separation properties and separation limits of different minerals. The research program includes the following major items.

- Characterization of oil sands tailings and pretreatment of oil sands tailings by flotation and centrifugal separation.
- The effects of bitumen removal by roasting on the separation of minerals in oil sands tailings.
- The effects of bitumen removal by solvent washing on the separation.
- The effects of bitumen removal by mechanical attrition on the separation.

4 EXPERIMENTAL

4.1 Materials

4.1.1 Mineral Samples

Oil sands tailings are mixtures of different minerals. In order to understand the behavior of individual minerals, several high purity single minerals were used in this study. These included ilmenite ($\text{TiO}_2 \cdot \text{FeO}$), hematite (Fe_2O_3), pyrite (FeS_2) and ZY Rutile. Also, a rutile concentrate and a zircon concentrate previously produced from the oil sands tailings by Lakefield Research Ltd were used. The latter two were referred to as LR Rutile and LR Zircon. Ilmenite, hematite and pyrite were purchased from Ward's Natural Sciences Ltd. Lumps of the minerals were crushed with a laboratory jaw crusher, followed by a Brinkman pulverizer. Different size fractions were then screened out for different tests. For ilmenite and hematite, the $-180+74 \mu\text{m}$ size fraction was screened out for roasting tests. For pyrite, the $-154+74 \mu\text{m}$ size fraction was used for roasting and flotation tests. An "aged" pyrite sample was also used – this was essentially the same pyrite but had been stored in plastic bottles for about two years. It was known that pyrite surfaces slowly oxidize during storage and its flotation behavior changes as a result. It was thought that this aged pyrite probably better represented the pyrite in oil sands tailings since it must have been oxidized to some degree after the bitumen extraction operations. Table 14 shows chemical analysis of the three samples.

Table 14 Chemical analysis of mineral samples

Sample Name	Al_2O_3 %	BaO %	CaO %	Fe_2O_3 %	K_2O %	MgO %	MnO %	Na_2O %	P_2O_5 %	SiO_2 %	TiO_2 %	LOI %	Zr %
Hematite	0.74	<0.01	0.25	86.36	<0.01	0.02	0.02	0.37	0.14	6.85	0.12	0.59	
Ilmenite	1.01	0.01	0.34	58.87	0.38	2.41	0.22	0.42	<0.01	1.57	35.17	<0.01	
Pyrite	0.02	0.01	1.11	63.49	0.01	0.07	0.01	0.01	0.18	0.14	N/A	32.31	
LR Rutile	1.03	0.29	0.27	18.71	0.18	0.32	0.60	0.27	0.43	1.94	75.54		
LR Zircon	0.97	0.10	0.19	0.20	0.09	<0.01	0.01	0.29	0.30	34.64	0.27	0.47	51.49

ZY Rutile was a powdered concentrate produced by the Zaoyang Rutile Mine in China. The concentrate assayed over 93% TiO₂ which was all in the form of rutile. The concentrate was produced through gravity and magnetic separation techniques. The sample was screened and the -105 + 74 µm size fraction was used in the electric conductivity measurement.

The LR Rutile was used directly without size treatment since its dominant particle size was about 120 µm, and its 80% passing size was 145 µm. A mineralogical analysis indicated that it contained about 10 - 17% rutile (anatase), and the remaining titanium was in the form of leucoxene.

LR Zircon was also used directly without size treatment since its dominant particle size was about 100 µm.

4.1.2 Oil Sands Tailings Samples

The froth treatment tailings samples were collected from Syncrude's Fort McMurray operations. The first batch of sample was collected and shipped to the University of Alberta in four 20-L plastic pails in January 2001. The sample was homogenized by decanting the clear water, combining the sediments and bitumen and stirring vigorously to re-disperse the solids. After taking a head sample, the homogenized sample was evenly distributed in five 20-L plastic pails. This was labelled as sample No. 5.

Sample No. 5 was very dilute and there were not enough solids to perform the testwork. Therefore, a second batch of samples was collected in June 2001. It again consisted of four 20-L plastic pails, but each pail had much higher solid content. These four pails were labelled No. 1 to No. 4. Table 15 shows the water, solid and bitumen content of the five samples. Results of detailed characterization of the oil sands tailings will be presented in section 5.1.

Table 15 TLX of oil sand tailings and MCR of bitumen

Sample	Water %	Solids %	Bitumen %	Bitumen* in solids %	MCR of bitumen %
No.1	32.5	63.8	3.7	11.8	
No.2	29.5	67.3	3.0	9.8	14.95
No.3	39.9	51.6	4.0	14.2	
No.4	42.6	47.9	4.6	16.7	14.51
No.5	73.0	20.8	6.2	27.0	

* Bitumen content was determined by burning at 340°C for 48 hours.

4.1.3 Reagents

Table 16 lists the reagents that were used in this study.

Table 16 Reagents used in the test work

Reagent	Supplier
Dodecylamine	Aldrich Chemicals
Potassium amyl xanthate	Charles Tennant & Co/CIE
Sodium dithophosphate	Charles Tennant & Co/CIE
Swab	Charles Tennant & Co/CIE
Na ₂ SiO ₃	Fisher Scientific
NaOH	Fisher Scientific
Na ₂ S·9H ₂ O	Fisher Scientific
NaF	Fisher Scientific
HCl	Fisher Scientific
H ₂ SO ₄	Fisher Scientific
(NaPO ₃) ₁₃ ·Na ₂ O	Fisher Scientific
CuSO ₄ ·5H ₂ O	Fisher Scientific
NaHS·9H ₂ O	Fisher Scientific
MIBC	Sigma Chemicals
Cornstarch	Sigma Chemicals
Sodium oleate	Sigma Chemicals
Naphtha	Syncrude Canada
Toluene	Syncrude Canada
Kerosene	Syncrude Canada
Charcoal	Weight Products Co.

The stock solution of dodecylamine was prepared by blending in a stoichiometric amount of acetic acid and then diluting to the mark on the volumetric flask.

Cornstarch was prepared by making a paste with cold water, then dissolving with boiling water. It was observed that starch solutions prepared in this way still contained un-

dissolved precipitates. In later stages of the testwork, 0.5 N sodium hydroxide (20 g/L) solutions were used to fully digest the starch.

Charcoal was used as a reducing agent in the reduction roasting. This was an Antelope Ranch charcoal supplied by The Weight Products Co. The charcoal was screened and 850+250 μm size fraction was used. The use of coarser sized charcoal provided a simple indicator for the maintenance of reducing environment during the roasting since the unreacted charcoal could be screened out.

4.2 Equipment

Table 17 lists the equipment that was used in this study.

Table 17 Equipment used in this study

Equipment	Manufacturer
Allis-Ohalmers 00 Laboratory Jaw Crusher	Milwaukee Wis., USA
B Furnace	Denver Fire Clay Company
Corning Hot Plate Stirrer	EMI Inc., USA
DC Magnetometer	AlphaLab Inc
Deister Deck Concentration Table	Deister Concentrator Company
Digital Multimeter 8520A	John Fluke Mfg. Co., Inc.
FA1730 Laboratory Muffle Furnace	Thermolyne Corporation, USA
Falcon SB40 Centrifugal Concentrator	Falcon Concentrator Inc., Canada
Fisher Stereomaster Microscope	Fisher Scientific
Isotherm 3028H Circulating Water Bath	Fisher Scientific
Laboratory Carpco Dry Roll Magnetic Separator	Carpco Manufacture Inc., USA
Laboratory Carpco Electrostatic Separator	Carpco Manufacture Inc., USA
Laboratory Frantz Isodynamic Separator	S.G. Frantz Co., Inc., USA
Laboratory 2 L Denver Flotation Machine	Denver Mineral Engineers Inc., USA
Mechanical attrition cell	Assembled in lab
Microwave 150 HT	VRW Scientific Products
Modified Microflotation Tube	Assembled in lab
Ro-Tap Testing Sieve Shaker	Tyler Combustion Engineering Inc., USA
Suspension-cell Flotation Machine	Assembled in lab
Sybron Brinkmann Pulverizer	Brinkmann Instruments Division, Sybron Canada Limited.
UV/VIS 6505 spectrophotometer	Jenway Ltd., UK

4.3 Experimental Procedures

4.3.1 *Sample Characterization*

Head samples of the froth treatment tailings were sent to Syncrude Research Center for TLX and MCR analysis. The bitumen contents in solids were also determined by burning the dried (105°C for 24 hours) head samples at 340°C for 48 hours. The bitumen-removed solid samples were then screened for particle size distribution analysis.

The head samples were also washed with toluene to completely remove the residual bitumen, and then sent to International Plasma Laboratory Ltd in Vancouver, BC, for chemical analysis, and to Harris Exploration Inc, for mineralogical analysis. Its magnetic susceptibility was measured in our lab.

4.3.2 *Bench Flotation of Froth Treatment Tailings*

Flotation was used as one of the pre-treatment test options. These tests were conducted at Syncrude Research Center in a Denver laboratory flotation machine with a 2-L flotation cell in which pulp temperature can be controlled through a water jacket. The diameter of the impeller was 10 cm. The variables for flotation tests were: flotation time, pulp temperature, aeration rate, and agitation speed. TLX, EAS and particle size distribution measurements were performed on the flotation products at Syncrude Research Center.

4.3.3 *Centrifugal Concentration of Froth Treatment Tailings*

Centrifugal concentration was tested as another pre-treatment option. These tests were conducted with a Falcon SB40 batch centrifugal concentrator (Figure 9). This machine separates the heavy minerals from the light minerals (quartz and clays) and bitumen based on differences in their specific gravity. The sample slurry was fed into a rotor rotating in vertical direction at various speeds to generate the desired centrifugal forces. This centrifugal force magnifies the difference in specific gravity and the rotor geometry

facilitates retention of heavy particles in preference to light particles that are rejected with the process water. Back water is injected between the riffle rings in the top part of the rotor from behind to allow heavy particles to migrate into the upgrading concentrate retention zone. At the end of the sample or at predetermined intervals when the feed slurry is discontinued the rotor is stopped and concentrates are collected.

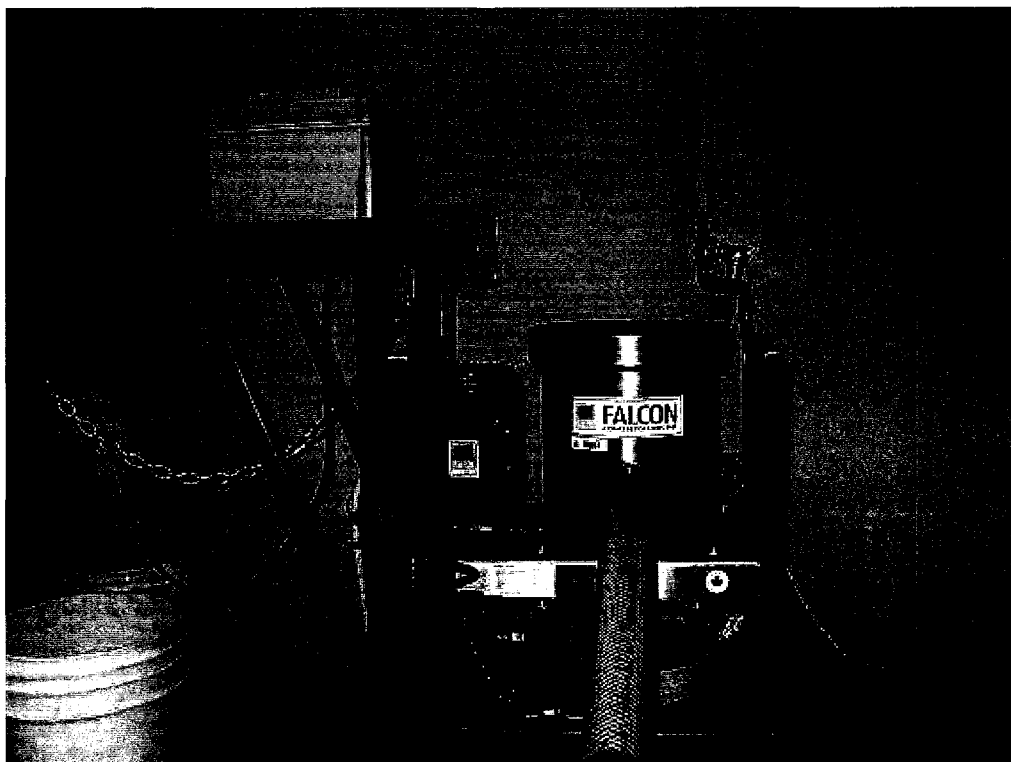


Figure 9 Falcon SB40 Centrifugal Concentrator

Before being fed to the centrifugal concentrator, the oil sand tailings slurry sample was heated to 50°C. Back water was either ambient (~20°C) or hot (50°C). The Falcon concentrator was adjusted to the pre-determined rotor speed and back water pressure. The sample was fed to the machine at about the same consistent feed rate and slurry density. After separation, the heavy product was filtered and dried at 105°C for 24 hours, and then heated in a muffle furnace at 340°C for a further 48 hours. The bitumen content was calculated by the weight losses of the dried samples. Selected Falcon heavy products

were washed with toluene to remove the residual bitumen, and then were sent to International Plasma Laboratory at Vancouver, BC, for whole rock and chemical analyses. Selected samples were also sent to Harris Exploration Services, Vancouver, BC, for mineralogical analyses to identify the types of minerals contained in those samples. The light product from the separation contained large amount of water, slimes and bitumen froths. The froths were skimmed and assayed and the remaining slurry was decanted, dried and heated as described earlier, the heated solid samples were assayed for titanium and zirconium, which was done by International Plasma Laboratory Ltd in Vancouver, BC.

Some of the light products from SB40 tests were subject to settling tests to observe their solid-liquid separation characteristics. This was done to see if the additional water, added to the light product as back water during SB40 tests, could be recycled. The settling tests were conducted with a 1- L graduated cylinder. For comparison, the SB40 feed (i.e., the original froth treatment tailings) was also tested. The absorbance of the clarified supernatant during the settling tests was measured with a UV/VIS spectrophotometer at 465nm.

The particle size distribution of the products was determined with standard sieve analysis between 70 to 400 meshes (212 to 38 μm).

To prepare the SB40 centrifugal separator product samples for bitumen characterization, the Falcon SB40 centrifuge separation tests were repeatedly conducted on sample No. 2 and No. 4 at the optimum conditions established. For sample No. 2, two products were produced and they were the heavy product and the slime product. For sample No. 4, three products were produced, i.e., the heavy product, the slimes product and the froth product which was skimmed from the slime product after standing for ~30 minutes. All the samples were sent to Syncrude Research Center for bitumen content by TLX and bitumen quality analysis by MCR (Micro Carbon Residue).

4.3.4 Roasting

The roasting of ilmenite, hematite, LR Rutile and LR Zircon was conducted in a laboratory muffle furnace. The furnace was heated to a predetermined temperature before the sample was introduced. A ceramic crucible, measuring 7.6 cm in diameter and 9.0 cm in depth, was used. Oxidation roasting was conducted in the crucible open to air. Reduction roasting was performed by heating a blend of 1 g of charcoal and 5 g mineral (i.e., a weight ratio of 1:5). This ratio was used in most of the reduction roasting tests, although a ratio of 1:10 was also used in some tests. The mineral and charcoal mixture was placed at the bottom of the crucible and was covered by a small ceramic hemisphere. The crucible was not completely sealed.

The roasting of bitumen-bearing froth treatment tailings, SB40 heavy products and pyrite was conducted in a furnace manufactured by Denver Fire Clay Company. The furnace was heated to a predetermined temperature before the sample was introduced. A dish-like crucible was used to hold the sample, which was 10 g in each batch. Chemical assays of sulfur in the roast calcine were performed by International Plasma Laboratory in Vancouver, BC.

4.3.5 Magnetic Susceptibility Measurement

Magnetic susceptibilities of the samples were measured with a Frantz Isodynamic Separator. The electric current in the magnetizing coil was adjusted from 0 to 1.9 A. The magnetic field strength of the separator was measured with a DC Magnetometer (AlphaLab Inc.) and the maximum was found to be 1.2 Tesla at the current of 1.9 A. The transverse slope (θ) of the separator was set at 14.5° . According to McAndrew (1957), the magnetic susceptibility χ of a material tested in the Frantz Isodynamic Separator is expressed as:

$$\chi = \frac{\sin\theta}{KI^2}$$

Where K is a constant and I is the electric current that results in a 50%: 50% split of the sample at the exit chute of the Separator. K was found to be 3.15×10^6 when using ferrous ammonium sulfate, $\text{Fe}(\text{NH}_4)_2(\text{SO}_4)_2 \cdot 6\text{H}_2\text{O}$ ($\chi = 32.4 \times 10^{-6} \text{ m}^3/\text{kg}$), and copper sulfate, $\text{CuSO}_4 \cdot 5\text{H}_2\text{O}$ ($\chi = 5.88 \times 10^{-6} \text{ m}^3/\text{kg}$), as standards to calibrate the Separator. To measure the magnetic susceptibility of a sample, the sample powder was separated in the Frantz Isodynamic Separator at different applied electric current. The recovery of the magnetic fraction was then plotted against the applied current, from which the current corresponding to 50% recovery was found. This was then used to calculate the magnetic susceptibility χ using the above equation.

4.3.6 Magnetic Separation

Separator. Magnetic separation of roasted SB40 heavy products was conducted with a Carpc Dry Roll Magnetic separator, following the procedure shown in Figure 10. The electrical current settings are shown in the figure as well. The rotating speed of the separation drum was controlled by setting the dial at the 40% position. Dry magnetic separation of bitumen removed oil sands tailings was also performed in a Frantz Isodynamic Separator. The maximum electric current in this separator was 1.9 A, which corresponded to a magnetic field strength of 1.2 Tesla. Magnetic separation of roasted single minerals, such as ilmenite, hematite, LR Rutile, was done on the Frantz Isodynamic

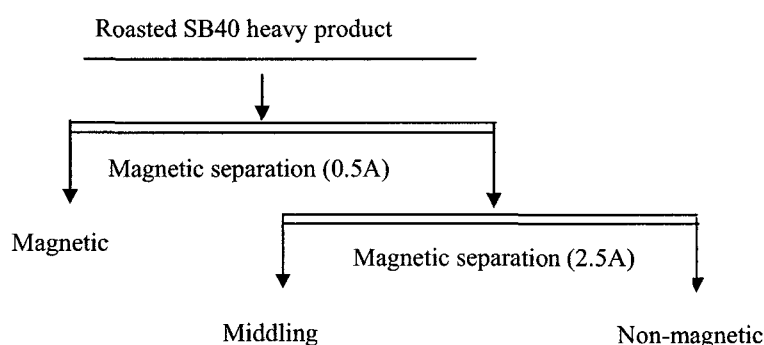


Figure 10 Magnetic separation flow sheet of roasted SB40 heavy products

4.3.7 *Small-scale Flotation Tests*

Suspension-cell Flotation

Small-scale flotation tests were conducted in a laboratory suspension-cell flotation machine. The cell volume was 30 ml and the impeller speed was set at 1980 rpm. In each test 4 g of test sample was used. In single mineral flotation the recovery was calculated as weight yield. In the flotation of SB40 heavy products and 1:1 mixtures of LR Rutile and LR Zircon, the flotation results were calculated based on chemical analyses of the flotation products, which were performed by International Plasma Laboratory at Vancouver, BC.

Modified Microflotation Tube Flotation

The flotation tests were conducted in a modified microflotation tube (Figure 11) where nitrogen gas was used as a carrying gas. In each test, 4 g solid sample was mixed with 110 ml solution and conditioned in a 250 ml beaker. The conditioning time was 3 minutes for each reagent. After conditioning, the pulp was transferred to the flotation tube and floated for 7 minutes. Dried flotation products were weighed and examined with a Stereomaster Microscope, and some of the samples were sent out to International Plasma Laboratory at Vancouver, BC, for elemental analysis.

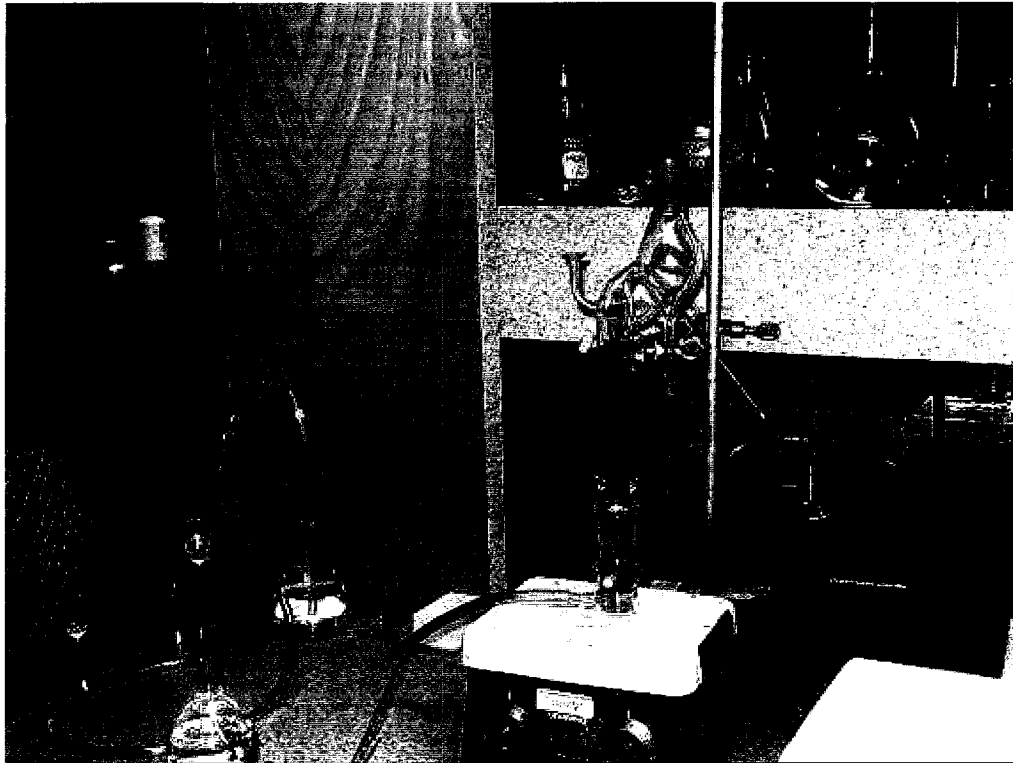


Figure 11 Modified Microflotation Tube

Flotation tests were also conducted on pyrite with and without prior roasting. The tests were conducted in the modified flotation tube. The effective tube volume was 110 ml which was used to test 4 g sample in each batch. Prior to flotation the sample was conditioned in a 250 ml beaker. After mixing the solid sample with tap water, a flotation modifier was added if used, followed by 3 minutes of conditioning. Afterwards, potassium amyl xanthate was added and the conditioning continued for another 3 minutes. As soon as the pH of the pulp was measured, the pulp was transferred to the flotation tube. Nitrogen was used to carry out the flotation except when Na_2S was used, in which case air was used to oxidize the excess Na_2S . Flotation time was generally 7 minutes. Again, when Na_2S was used, the total flotation time was 14 minutes. The flotation froth and tail were filtered, dried and weighed to calculate the yield.

4.3.7 Solvent Washing of Falcon SB40 Heavy Product

Naphtha washing was conducted by mixing 100 g Falcon SB40 heavy product with 300 ml naphtha, stirring for 30 minutes, then decanting the naphtha. The solids were washed with naphtha for three times. The washed solids were filtered and dried in air in a fume hood. The residual bitumen content of the sample was determined by washing 10 g sample with 100 ml toluene.

4.3.8 Mechanical Attrition

Since the naphtha-washed solid did not respond well to flotation, mechanical attrition was tested to remove the residual bitumen. For this purpose, a Plexiglass attrition cell was made. It was essentially a hollow cylinder with four baffle plates installed around the inside wall, which was wrapped by a water jacket (to maintain temperature) and a cap on the top (Figure 12). Internal diameter was 76 mm and the height was 90 mm. The diameter of the mixing impeller was 50 mm. In the attrition tests, a stirring speed of up to 2200 rpm was applied and the pulp temperature was tested between 20°C and 80°C, and temperature was maintained by running the water from a circulation bath to the water jacket. The preliminary attrition tests were carried out in three stages with an agitation time of 30, 20, 20 minutes, respectively. In the first stage, 100 g solid was used, and the ratio of solids to liquid was 1:1. Sodium hydroxide and sodium silicate were used in the attrition tests. The residual bitumen content was determined by washing 10 g attritioned sample with 100 ml toluene for 30 minutes.

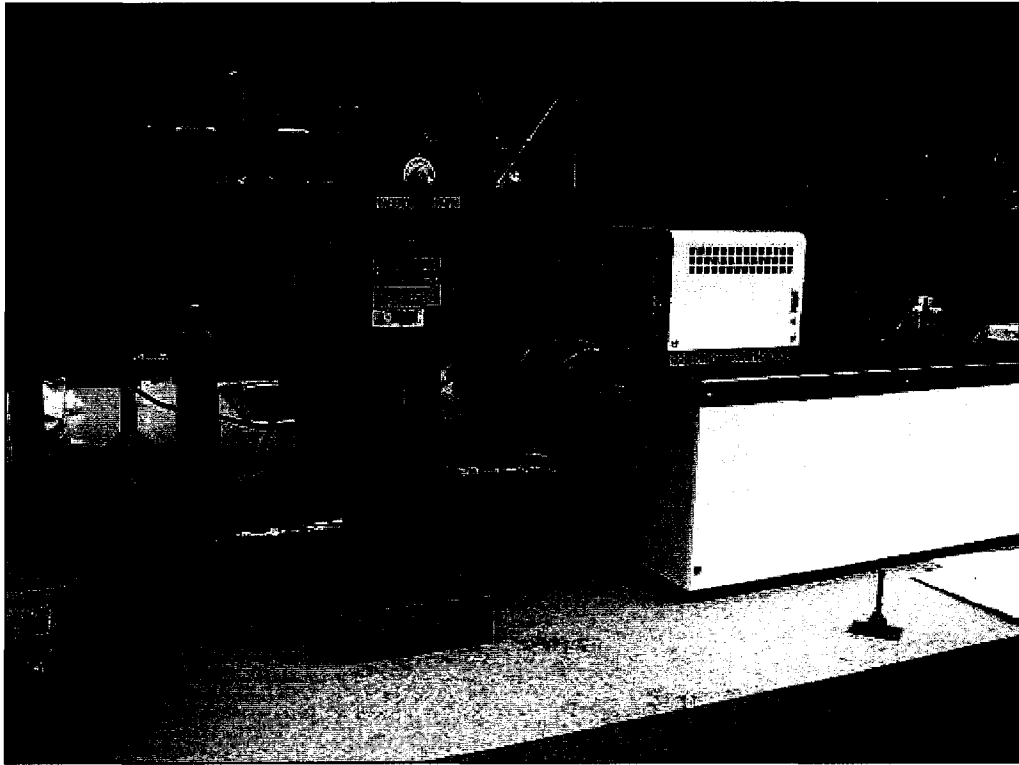


Figure 12 Mechanical attrition equipment (including Isotherm 3028H Circulating Water Bath, Suspension Frame, and Plexiglass Attrition Cell)

4.3.9 Gravity Concentration and Heavy Liquid Separation

Gravity separation tests were conducted on toluene washed SB40 heavy product with the objective to remove quartz. Gravity separation was conducted on a Deister Deck shaking table with a length of 1200 mm and a width of 600 mm. Heavy liquid separation was done using Methylene Iodide (SG 3.3) as media. The collected products were filtered and dried, and sent to International Plasma Laboratory at Vancouver, BC, for elemental analyses.

4.3.10 Electrostatic Separation

Electrostatic separation tests were conducted using a Carpco Dry Roll Electrostatic Separator. In these tests the DC voltage applied across the electrodes was set between 20 and 40 kV. The sample was fed at a very low feed rate to ensure a monolayer of particles on the separation drum.

4.3.11 SEM/EDX Analysis

Scanning electron microscopic measurements were performed in a Hitachi S-2700 scanning electron microscope with energy dispersive x-ray analysis (EDX) capabilities. The sample was coated with carbon to make them electrically conductive. An accelerating voltage of 20.0 kV was used to obtain both back-scattered electron images and secondary back-scattered electron images. EDX analysis was used for semi-quantitative analysis to identify elemental composition of localized areas on the top layer of the sample particle surfaces.

4.3.12 Electric Conductivity Measurement

3 gram mineral sample was dried and then pressed at 9000 psi to form a disk 1.27 mm in diameter and about 8 mm in thickness. Its electric conductivity was measured using an 8520A Digital Multimeter.

5 CHARACTERIZATION AND PRE-TREATMENT OF OIL SANDS TAILINGS

This chapter describe the characteristics of the froth treatment tailings samples as determined by particle size, bitumen content, magnetic susceptibility, chemical and mineralogical analyses. It also describes some of the processing steps that rejected some of the wastes from the froth treatment tailings samples but did not completely remove the residual bitumen – hence the term “pre-treatment”.

5.1 Characterization of Oil Sand Tailings

5.1.1 Particle Size Distributions and Size Assays

The five samples had different solids, water and bitumen content. The particle size distribution analysis and the bitumen content measurements are listed in Table 18. The correlation between bitumen content and % passing 400 mesh (38 μ m) in solid phase is plotted in Figure 13. As can be seen, the bitumen content in solids increased linearly with increasing –400 mesh (38 μ m) size materials, indicating a good correlation between bitumen and fine slimes.

Table 19 shows the titanium and zirconium contents and distribution in different size fractions. In sample No. 2, the titanium and zirconium distribution in –38 μ m fraction was 11.3% and 12.4%, respectively, while in sample No. 4, the titanium and zirconium distribution in –38 μ m fraction was higher at 16.7% and 19.7%, respectively. Since minerals with particle size of less than 38 μ m are hard to recover by conventional electrostatic/or high-tension separation and magnetic separation, a very high heavy mineral recovery could not be expected.

5.1.2 Magnetic Susceptibility

A small sample of the heavy product of sample No.2 was washed with toluene to remove the residual bitumen and then its magnetic susceptibility was measured with Frantz Isodynamic Separator. It was found to be $0.73 \times 10^{-8} \text{ m}^3/\text{kg}$.

Table 18 Particle size distributions of froth treatment tailings samples

Sample number	Bitumen content in solid phase, %	Size, μm	Individual distribution, %	Cumulative distribution, %
No.1	5.5	+154	20.54	100.00
		-154 + 45	48.82	79.46
		-45 + 38	5.86	30.64
		-38	24.78	24.78
No.2	4.3	+154	15.59	100.00
		-154 + 45	55.06	84.41
		-45 + 38	7.78	29.35
		-38	21.57	21.57
No.3	7.2	+154	39.20	100.00
		-154 + 45	29.10	60.80
		-45 + 38	4.04	31.70
		-38	27.66	27.66
No.4	9.8	+154	19.36	100.00
		-154 + 45	40.11	80.64
		-45 + 38	5.65	40.53
		-38	34.88	34.88
No.5	23.0	+154	6.61	100.00
		-154 + 45	34.25	93.39
		-45 + 38	5.54	59.14
		-38	53.60	53.60

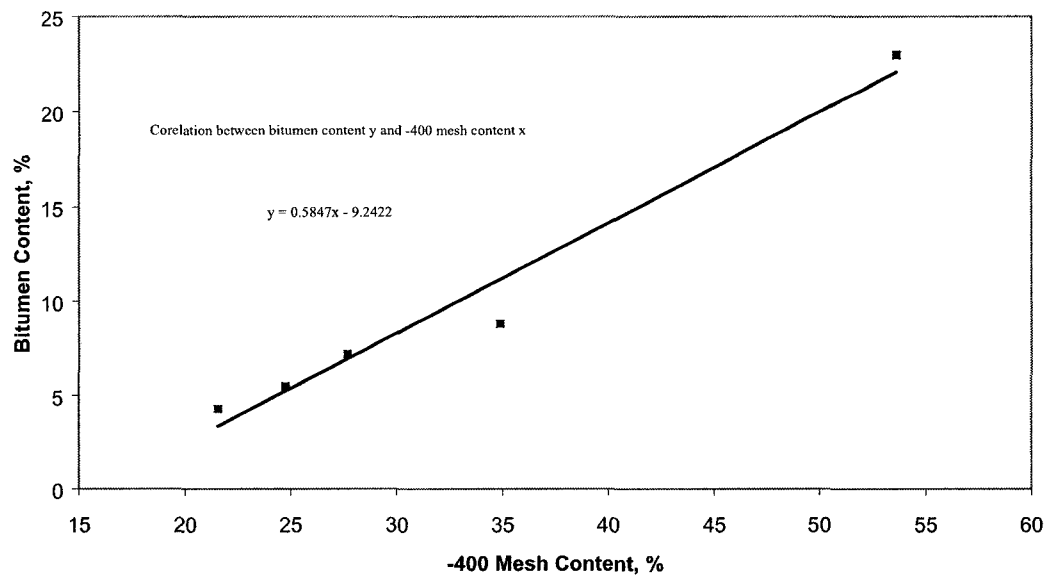


Figure 13 Bitumen content in solids of scroll tailings as a function of weight yield of - 38 μm material

Table 19 Size assay (Ti, Zr) for samples No. 2 and No. 4

Sample	Particle size range, μm	Yield, %	Ti, %	Ti distribution, %	Zr, %	Zr distribution, %
No. 2	+ 154	15.59	2.76	6.09	0.08	0.37
	-154 + 45	55.06	9.27	72.28	4.71	77.27
	-45 + 38	7.78	9.35	10.30	4.40	10.20
	-38	21.57	3.71	11.33	1.89	12.16
	Total	100.0	7.06	100.0	3.36	100.0
No. 4	+ 154	19.36	3.05	13.86	0.16	3.07
	-154 + 45	40.11	6.55	61.67	1.65	65.53
	-45 + 38	5.65	5.80	7.69	2.09	11.69
	-38	34.88	2.05	16.78	0.57	19.71
	Total	100.0	4.26	100.0	1.01	100.0

5.1.3 Whole Rock Analysis of Oil Sand Tailings Samples

Table 20 shows the elemental analysis results of bitumen-removed froth treatment tailings. Sample No. 4 assayed 7.33% TiO_2 and 1.49% ZrO_2 , while sample No. 2 assayed 13.71% TiO_2 and 4.13% ZrO_2 , respectively.

Table 20 Whole rock analysis of bitumen-removed oil sands tailings

Sample	ZrO ₂	Al ₂ O ₃	BaO	CaO	Fe ₂ O ₃	K ₂ O	MgO	MnO	Na ₂ O	P ₂ O ₅	SiO ₂	TiO ₂	LOI
No.2	4.13	6.84	0.07	2.32	9.19	0.95	1.54	0.22	0.34	0.49	54.52	13.71	4.89
No.4	1.49	9.57	0.06	3.43	9.99	0.98	1.58	0.16	0.34	0.45	56.44	7.33	7.13
No.5	2.65	12.82	0.08	1.49	11.42	1.50	1.53	0.25	0.56	0.37	44.33	9.84	11.42

5.1.4 Mineralogy

Sample No. 2 head:

Table 21 Approximate composition as determined from mineralogical analysis

Mineral	Quartz and Feldspar	Other silicates	Carbonate	Zircon	Probable Ti minerals	Pyrite
Content, %	39	11.5	2.5	8	35	4

This sample consists of mineral grains ranging in size from about 20 – 200 μm .

The dominant constituents are quartz (plus an uncertain proportion of feldspars – principally poorly twinned plagioclase). Accessory minerals include a variety of other silicate minerals (including amphibole, pyroxene, tourmaline, garnet, staurolite, kyanite and boitite); carbonates; zircon; and pyrite.

The oxide grains range from compact, well polished to porous/skeletal, and mainly show the translucency (in cross-polarized reflected light) characteristic of rutile or anatase. Few grains show the complete opacity and anisotropism characteristic of hematite or ilmenite. The negative response of the sample to the hand magnet indicates the absence of magnetite.

The zircon occurs as vari-sized, ragged grains – mostly liberated, but occasionally composite with quartz.

Overall liberation of all constituents in this sample is of a high order. Occasional examples can be seen of quartz intergrown with the skeletal/meshwork varieties of the presumed TiO_2 minerals.

Figure 14 - Figure 17 show a typical field of sample No. 2 head, at a scale of 1cm = 85 μm under four different modes of illumination.

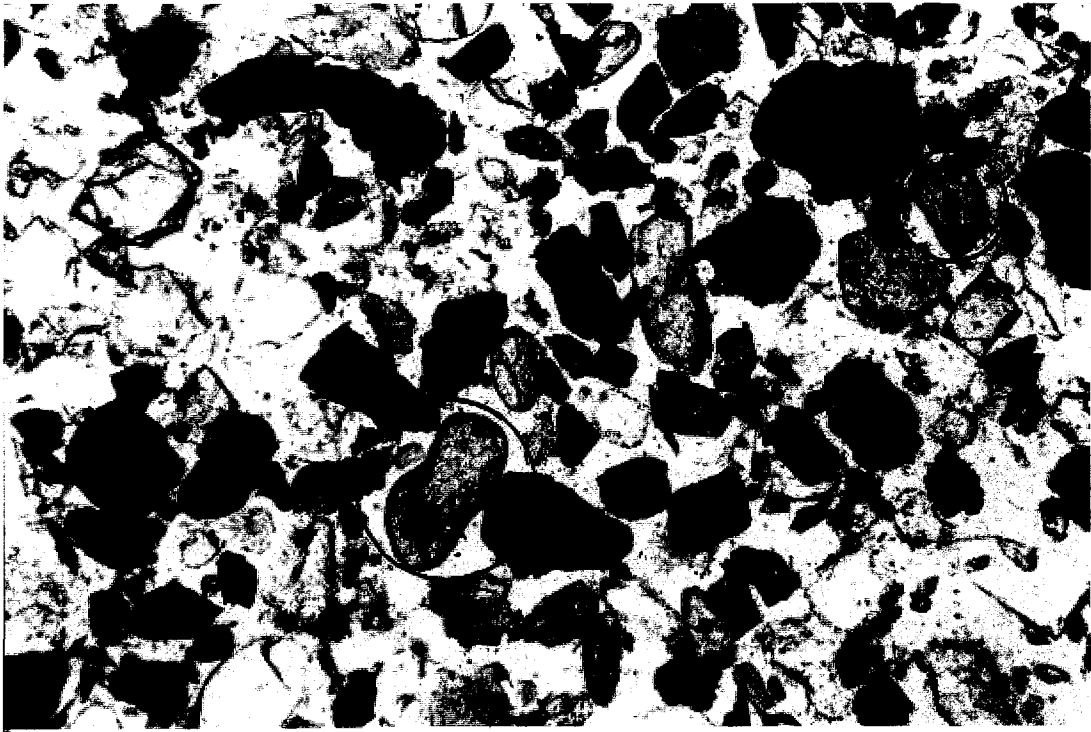


Figure 14 Sample No. 2 head under plane-polarized transmitted light

The black grains are the presumed titanium minerals. The colorless grains are quartz and feldspars. The two circled grains are zircon. Other grains are various silicates and carbonate.

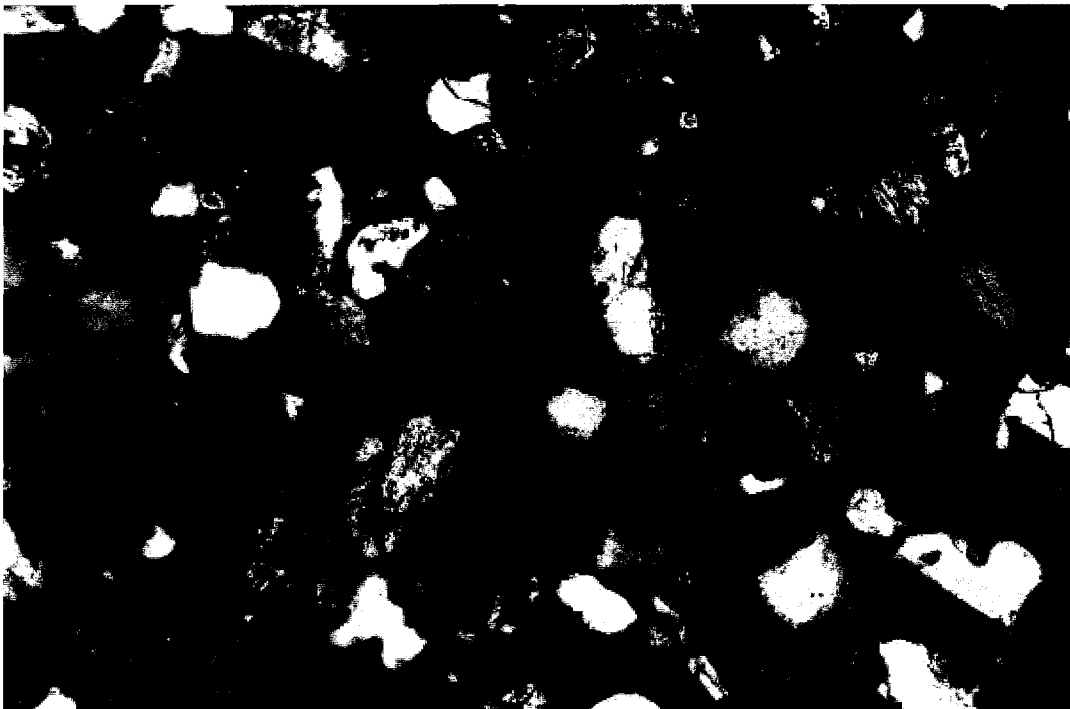


Figure 15 Same field as in Figure 14 but under cross-polarized transmitted light

The white and grey grains are quartz and feldspars. The pink and green grains are zircon.

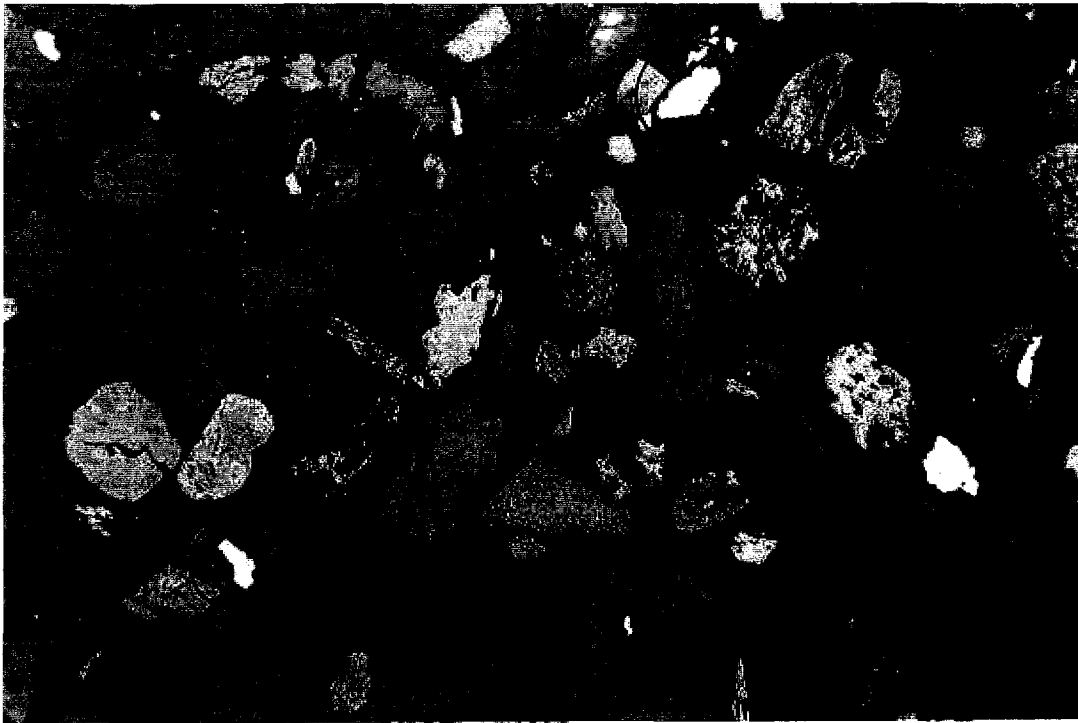


Figure 16 Same field as in Figure 14 but under reflected light

The circled small grains of high reflectivity are pyrite.

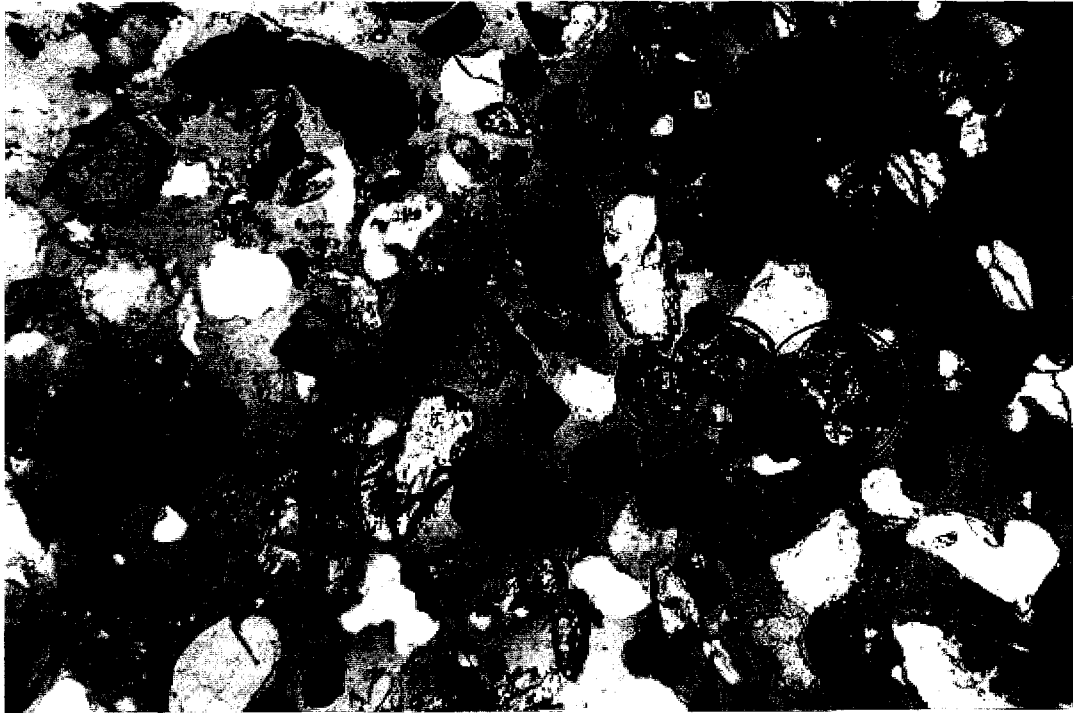


Figure 17 Same field as in Figure 14 but under cross-polarized reflected light

Compare with Figure 14, the majority of the opaque grains in that figure here appear more or less brownish translucent to sub-translucent. This is characteristic of poorly crystalline TiO_2 . The three circled grains show high order interference colors in this photo. These are probably well-crystallized rutile.

Sample No. 4 head:

Table 22 Approximate composition as determined from mineralogical analysis

Mineral	Quartz and Feldspar	Other silicates	Carbonate	Zircon	Probable Ti minerals	Pyrite
Content, %	49	10.5	5.5	5	25	5

This sample is made up of mineral grains 20 – 250 μm in size.

It shows closely similar mineralogy to the No.2 head, but the proportions of zircon and oxidic opaques/sub-opaques (presumed TiO_2 varieties) appear significantly lower relative to quartz. Among the minor constituents, carbonate is more abundant. Liberation characteristics are similar to those noted in sample No.2 head.

One difference from the No.2 head is the presence of minor proportions of a brown cryptocrystalline component, as small, discrete flecks and as diffuse coatings on other mineral grains. This is probably bituminous and/or clayey material.

5.2 Pre-treatment by Flotation

In these tests, the froth treatment tailings were subject to direct froth flotation at a pulp temperature of either 50°C or 85°C. Different types of chemicals were added during the flotation. Table 23 summarizes the results. Note that all the tests were conducted on Sample No. 2 except for tests F1 and F6 which were on sample No. 5, the flotation time were 7 minutes for each test except test F1, which was 20 minutes.

As can be seen, temperature is a very important factor that determines the flotation response of the tailings. Without the addition of any flotation reagent, the flotation at a pulp temperature of 85°C was much better than that at 50°C (e.g., compare tests F7 and F17).

However, high recoveries of the heavy minerals and residual bitumen could be obtained at the low pulp temperature (50°C) as well if appropriate reagent(s) were used. The addition of NaOH, MIBC, sodium oleate, or kerosene significantly improved the flotation. With a combination of two or three of these reagents at a low temperature (50°C), the recoveries could reach that at the higher temperature of 85°C (compare tests F19, F20, and F22 with F8).

The addition of sodium metaphosphate depressed the silicate minerals but it also reduced the recoveries of bitumen and heavy minerals (tests F11, F13, F21 and F23). The addition of KCl had a deleterious effect on the flotation at 85°C (compare tests F7 with F15) but had very little effect at 50°C. The increase of stirring intensity from 1400 rpm to 1600 rpm significantly reduced recoveries (compare tests F7 with F16) – this may signify the effect of particle size on the flotation since large particles are more likely detach from particle-bubble aggregates at high agitation speed. The increase of air flow rates from 0.692 to 1.233 L/minute had very little effect on the flotation (compare tests F7 with F14).

Table 23 Flotation of residual bitumen and heavy minerals from froth treatment tailings

Test #	Flotation conditions					Froth yield, %	Recovery, %		
	pH	Temp. °C	rpm	Air flow, L/min	Reagents		Ti	Zr	Bitumen
F1	8.3	50	1800	0.692	-	29.1	23.9	26.1	44.1
F6	8.3	85	1400	0.692	-	64.6	94.1	98.4	95.4
F7	8.3	85	1400	0.692	-	49.3	87.6	97.7	91.7
F17	8.3	50	1400	0.692	-	31.2	59.7	81.2	84.9
F8	10	85	1400	0.692	NaOH	49.0	97.8	99.0	95.5
F18	10	50	1400	0.692	NaOH	52.8	83.7	97.2	90.6
F9	10	85	1400	0.692	NaOH, MIBC	49.7	92.3	98.6	94.2
F19	10	50	1400	0.692	NaOH, MIBC	54.1	91.2	98.9	95.1
F10	10	85	1400	0.692	NaOH, Sodium oleate	56.4	97.7	97.6	91.2
F20	10	50	1400	0.692	NaOH, Sodium oleate	59.6	96.5	98.7	93.1
F11	10	85	1400	0.692	NaOH, Sodium oleate, MIBC, Sodium metaphosphate	50.2	87.3	97.1	90.9
F21	10	50	1400	0.692	NaOH, Sodium oleate, MIBC, Sodium metaphosphate	34.6	58.5	79.0	80.9
F12	10	85	1400	0.692	NaOH, MIBC, Sodium oleate	62.0	98.3	98.4	94.1
F22	10	50	1400	0.692	NaOH, MIBC, Sodium oleate	61.2	98.1	98.4	93.6
F13	8.3	85	1400	0.692	Sodium metaphosphate	38.1	50.8	83.5	83.3
F23	8.3	50	1400	0.692	Sodium metaphosphate	33.4	57.2	79.4	84.1
F15	8.3	85	1400	0.692	KCl	51.2	82.3	95.6	88.8
F24	8.3	50	1400	0.692	KCl	34.6	61.5	82.9	86.2
F26	10	85	1400	0.692	NaOH, MIBC, Kerosene	57.4	96.8	98.8	95.5
F25	10	50	1400	0.692	NaOH, MIBC, Kerosene	52.8	90.8	98.8	91.9
F14	8.3	85	1400	1.233	-	48.1	83.7	97.1	93.6
F16	8.3	85	1600	0.692	-	35.6	81.6	91.5	85.9

5.3 Pretreatment by Centrifugal Concentrator

5.3.1 Centrifugal Concentration Tests

As mentioned earlier, back water is required in the Falcon concentrators to fluidize the collected heavy minerals so that further upgrading is possible. On the plant scale operations, the use of hot water as back water would have significant economic implications, so in our tests, both hot water and “cold water” (at ambient temperature) were used in the Falcon SB40 tests, and the oils sands tailings slurry was always heated to 50°C to simulate the discharge temperature from the froth treatment plant. Table 24

shows the bitumen content and distribution in the heavy product at different G force and water temperatures. As can be seen, for sample No. 2 the back water temperature had very little effect on the bitumen content in the heavy product, while the centrifugal force had a pronounced effect on the bitumen content in the heavy product. When the G force was increased from 20 G to 300 G the bitumen content in the heavy product increased by about 2%.

For sample No. 5 the bitumen content in the heavy product was about 2% when back water temperature was 50°C, and about 6% when “cold” tap water was used. Apparently, the use of hot water reduced the viscosity of bitumen-bearing slurries and resulted in better liberation. This probably accounted for the lower entrainment of bitumen into the heavy products.

In addition, the heavy product yield increased with the increase of centrifugal force.

Table 24 Effect of back water temperature and centrifugal force on bitumen content in heavy product of sample No. 2 and No. 5 (Backwater pressure = 1psi)

Sample	Centrifugal Force, G	Back water Temperature °C	Heavy product Weight yield, %	Bitumen* Content, %	Bitumen Distribution, %
No.2	20	20	44.47	3.72	17.81
		50	52.04	3.37	18.33
No.2	60	20	64.43	3.78	25.88
		50	65.92	4.18	29.63
No.2	150	20	77.56	4.72	39.20
		50	75.95	4.41	37.30
No.2	300	20	82.30	5.26	46.70
		50	85.87	5.66	54.70
No. 5	200	20	28.87	5.96	6.30
		50	27.85	2.31	2.40
No. 5	300	20	46.33	6.16	11.20
		50	43.39	1.86	3.20

* Bitumen content was determined by burning at 340°C for 48hours.

5.3.2 Weight Yield of Heavy Product

The Falcon concentrators were initially designed to recover free gold nuggets from gold ores. Because the concentrations of gold in the gold ores are usually very low, in the ppm range, the weight yield of the heavy product in the centrifugal concentrator is typically very low. However, manufacturers of the centrifugal concentrators, such as Falcon Concentrator Ltd and Knelson Concentrator Ltd), are actively expanding the use of the concentrators into other mineral recovery systems. Their latest designs of the continuous concentrators allow the adjustment of the weight yield of the heavy products, and very high weight yield of the heavy product can be obtained. This development fit the requirement of oil sands tailings processing since the yield of the heavy product needs to be high enough to recover the heavy minerals.

Testing on the continuous centrifugal concentrators requires large amount of samples, which is not practical in this study. Our tests were therefore conducted on a smaller scale in a laboratory batch centrifugal concentrator, the Falcon SB40 concentrator. In one pass, the rotor bowl can typically retain between 50 and 100 grams of heavy product, so that the yield of the heavy product changes if the weight of feed in each batch is changed.

Tests were conducted on sample No. 2 and No. 5 at various feed weights as well as G forces and back water pressure. The recoveries of residual bitumen and TiO_2 into the heavy product are plotted against the weight yield of the heavy product in Figure 18. As can be seen, the recoveries of both TiO_2 and bitumen into the heavy product increased almost linearly with increasing weight yield of the heavy product, but the increase of TiO_2 was more pronounced and had a much higher slope than residual bitumen (1.37 vs. 0.74 for sample No. 2, and 1.56 vs. 0.45 for sample No. 5). For sample No. 2, while the TiO_2 recovery reached about 90% at 82% weight yield, the recovery of residual bitumen was around 40%. For sample No. 5 while the TiO_2 recovery reached 85% at 45% weight yield, the recovery of residual bitumen was around 10 - 15%. The results indicated that there was some degree of separation of heavy minerals from bitumen using the Falcon SB40.

5.3.3 Centrifugal Force

Tests indicated that increasing centrifugal force significantly increased the weight yield of the heavy product, thus increasing the recovery of heavy minerals. In the meantime, the bitumen recovery was also increased, but to a much lesser degree. As can be seen from Table 25, for sample No. 4 at 150 G, the recovery of Ti was 72.7%, while at 300 G the recovery reached 88.78%; for sample No. 2 at 20 G, the recovery of Ti was only 37.1%, while at 150 G the recovery reached 82.8%; for sample No. 5 at 99 G the recovery for Ti was only 59.5%, while at 300G the recovery reached 84.9%.

5.3.4 Back Water Pressure

According to the Falcon SB40 operation manual, for a given sample and a given maximum particle size, there is an optimum back water pressure to obtain the optimum separation between light minerals and heavy minerals. Since the maximum particle size of heavy minerals in the tailings is around 250 μm , the back water pressure was adjusted between 0.5 psi and 3 psi. Figure 19 shows the bitumen content in the heavy product of sample No. 5 as a function of the backwater pressure. Clearly, the minimum occurred at 1 psi. With the use of hot water, the bitumen content was lower than when cold (room temperature) water was used.

On the other hand, Figure 20 shows the bitumen and heavy minerals distribution in the heavy product of sample No. 5 as a function of the back water pressure, and it seemed that the back water pressure did not significantly change the distribution of bitumen and heavy minerals in the heavy product.

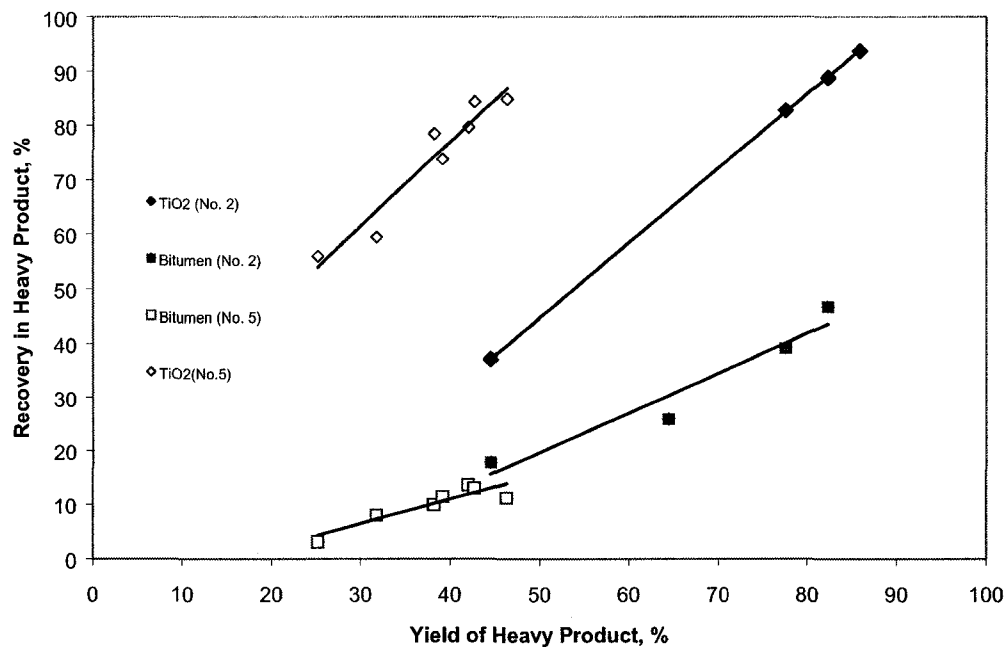


Figure 18 Recovery of heavy minerals and bitumen as a function of the weight yield of heavy products of sample No. 2 and No. 5 from SB40 tests

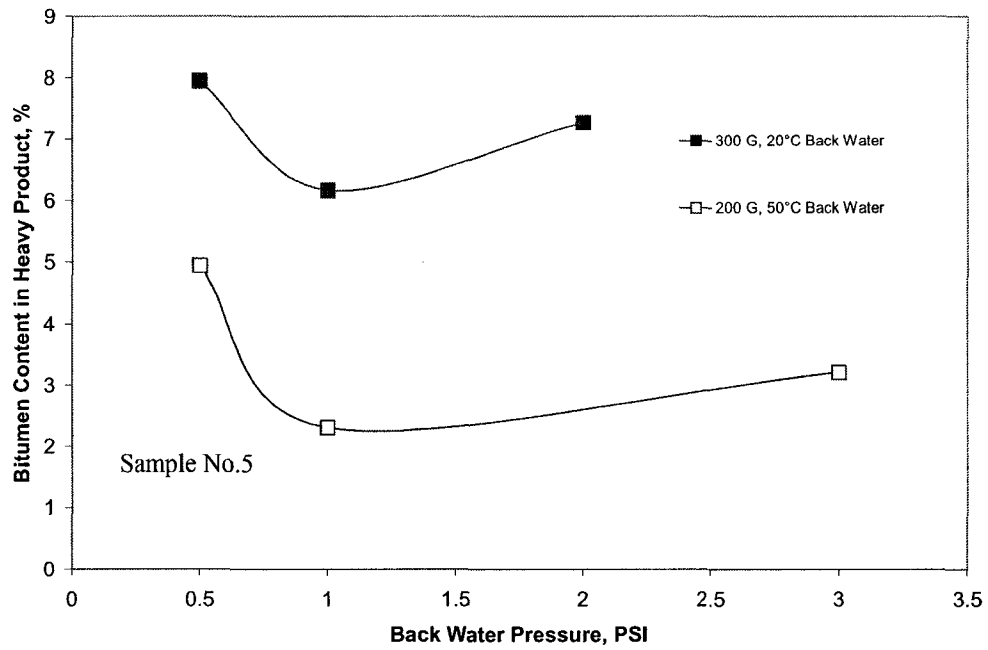


Figure 19 Bitumen content in heavy minerals as a function of back water pressure

*Bitumen content was determined by burning at 340°C for 48 hours.

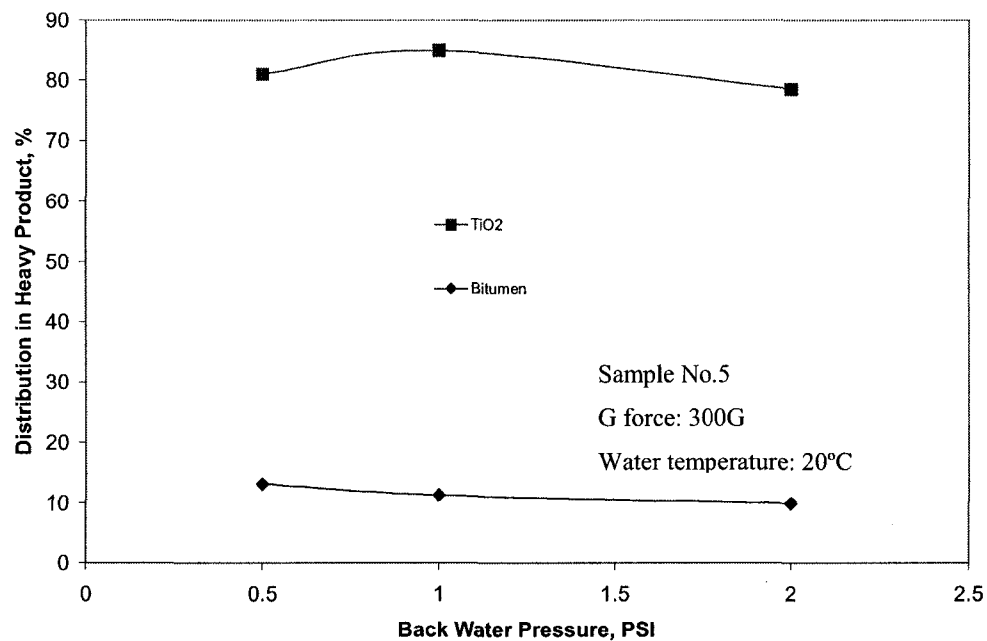


Figure 20 Bitumen and heavy mineral distributions in heavy product as a function of back water pressure

*Bitumen content was determined by burning at 340°C for 48 hours.

Table 25 Effect of centrifugal force (G) on the centrifugal separation

Sample	Conditions	G Force	Wt. yield %	Bitumen content* %	Bitumen distribution %	Ti content %	Ti distribution %
No.2	1psi 20°C back water	20	44.47	3.72	17.81	6.61	37.10
		60	64.43	3.78	25.88	6.13	44.30
		150	77.56	4.72	39.2	8.28	82.80
No.4	1psi 50°C back water	150	60.83	5.77	22.00	4.50	72.70
		300	68.29	6.74	28.70	4.98	88.78
No.5	1psi 20°C back water	99	31.84	6.85	7.98	7.68	59.50
		300	46.33	6.16	11.23	8.97	84.90

*Bitumen content was determined by burning at 340°C for 48 hours.

5.3.5 Optimum centrifugal concentrator test results

The suitable operating conditions in the SB40 tests conducted so far seemed to be: high centrifugal force (G force), 1 psi back water pressure and high weight yield of the heavy product. Several tests were conducted using these conditions and the results are presented in Table 26. It was observed that the light product contained large amount of water and bitumen. After allowing it to stand, the slimes settled and some of the bitumen formed a surface froth layer. The froth layer was skimmed off and analyzed separately.

As can be seen, under the optimum test conditions established so far, for sample No. 2, at a heavy product weight yield of 85.9%, the heavy product stream recovered 93.7% of the Ti and 91.6% of Zr, together with 54.7% bitumen. Combined with the Ti and Zr in the froth, the overall recovery was 95.4% for Ti and 94.8% for Zr. For sample No. 4, at a heavy product yield of 68.3%, the heavy product stream recovered 88.8% of the Ti and 86.7% of Zr, together with 28.7% bitumen. Combined with the Ti and Zr in the froth, the overall recovery was 91.36.43% for Ti and 92.2% for Zr. For sample No. 5, at a heavy product yield of 46.3%, the heavy product stream recovered 84.9% of the Ti, together with 11.2% bitumen. Combined with the Ti in the froth, the overall recovery of Ti was 88.6%.

Table 26 Balance of the optimum centrifugal concentrator tests

Sample	Conditions	Product	Yield, %	Bitumen* %	Bitumen Dist., %	Ti %	Ti Dist. %	Zr %	Zr Dist. %
No.2	300 G 1 psi 50°C	Heavy product	85.87	5.66	54.69	8.21	93.73	2.93	91.60
		Froth	2.40	58.44	15.77	5.33	1.70	3.66	3.19
		Slime	11.73	22.38	29.54	2.93	4.57	1.22	5.21
No.4	300 G 1 psi 50°C	Heavy product	68.29	6.74	28.70	4.98	88.78	1.21	86.70
		Froth	3.92	51.37	12.49	2.48	2.54	1.33	5.45
		Slime	27.79	33.95	58.81	1.20	8.68	0.27	7.85
No.5	300 G 1 psi 20°C	Heavy product	46.30	6.16	11.20	1.21	84.90		
		Froth	10.60	70.50	27.70	1.79	3.70		
		Slime	43.80	35.50	61.10	1.28	11.40		

*Bitumen content was determined by burning at 340°C for 48 hours.

5.4 Characterization of Separation Products

5.4.1 Particle Size Distribution and Ti/Zr Deportment in Falcon SB40 Products

The heavy mineral distribution in heavy products of tests G29 and G33 is listed in Table 27 and heavy mineral distribution in slime of tests G29 and G33 is listed in Table 28. As can be seen from Table 27, the $-38 \mu\text{m}$ content in heavy product was 15.7% for sample No. 2, whereas in the feed it was 21.6% (Table 18); the $-38 \mu\text{m}$ content in heavy product was 14.7% for sample No. 4, while in the feed it was 34.9%(Table 18). Clearly, the centrifugal separator is effective in removing the fine particles.

Table 27 Heavy mineral distributions in heavy product of test G29 and G33

Test #	Size range, μm	Weight Yield, %	TiO ₂ content, %	TiO ₂ Dist., %	ZrO ₂ content, %	ZrO ₂ Dist., %
G29	-38	15.68	6.80	7.38	2.19	11.14
	-45 + 38	8.25	17.97	10.26	9.44	25.26
	-76 + 45	15.81	19.96	21.84	7.62	39.07
	-154 + 76	45.39	17.30	54.35	1.64	24.14
	+154	14.87	5.99	6.17	0.08	0.39
	Total	100.00	14.45	100.00	3.08	100.00
G33	-38	14.72	9.43	13.33	3.46	24.38
	-45 + 38	1.71	11.19	1.84	5.88	4.81
	-76 + 45	15.11	13.73	19.93	5.55	40.15
	-154 + 76	44.89	12.11	52.22	1.40	30.09
	+154	23.57	5.60	12.68	0.05	0.56
	Total	100.00	10.41	100.00	2.09	100.00

In Table 28, it is shown that, for sample No. 2 (test 29), 4.6% of TiO₂ was lost in the slime product, and 63.8% of which was in the -38 μm fraction; 5.2% of ZrO₂ was lost in the slime product, and 35.1% of which was in the -38 μm fraction. For sample No. 4 (test 33), 8.7% of TiO₂ was lost in the slime product, and 87.4% of which was in the -38 μm fraction; 7.9% of ZrO₂ was lost in the slime product, and 56.4% of which was in the -38 μm fraction.

Table 28 Heavy mineral distribution in slime of tests G29 and G33

Test #	Size μm	Weight yield, %	TiO ₂ , content, %	TiO ₂ Dist. in Slime, %	TiO ₂ Dist. Vs. Feed, %	ZrO ₂ content, %	ZrO ₂ Dist. in Slime, %	ZrO ₂ Dist. Vs. Feed, %
G29	+38	7.52	30.12	36.21	1.65	18.30	64.91	3.38
	-38	92.48	4.36	63.79	2.92	0.80	35.09	1.83
	Total	100.00	6.30	100.00	4.57	2.12	100.00	5.21
G33	+38	1.52	25.05	12.61	1.09	15.79	43.64	3.43
	-38	98.48	2.68	87.39	7.59	0.31	56.36	4.42
	Total	100.00	3.02	100.00	8.68	0.55	100.00	7.85

5.4.2 *Settling Characteristics of the Light Product from Centrifugal Concentration*

The light product from the centrifugal concentrator was diluted with backwater in the process. In order to find out if the water could be clarified and recycled, settling tests were conducted on the light product slurries of sample No. 5. Figure 21 shows the settling curve of the slurry, together with that of the original feed sample No. 5. As can be seen, although the majority of the heavy minerals and coarse particles were removed, the light product settled in the same way as the original feed – its settling behavior was not impaired by the centrifugal separation. Both slurries settled reasonably fast. Figure 22 shows the optical absorbance of the clarified water. It is again seen that the clarity of the water was not affected by the centrifugal concentrator separation.

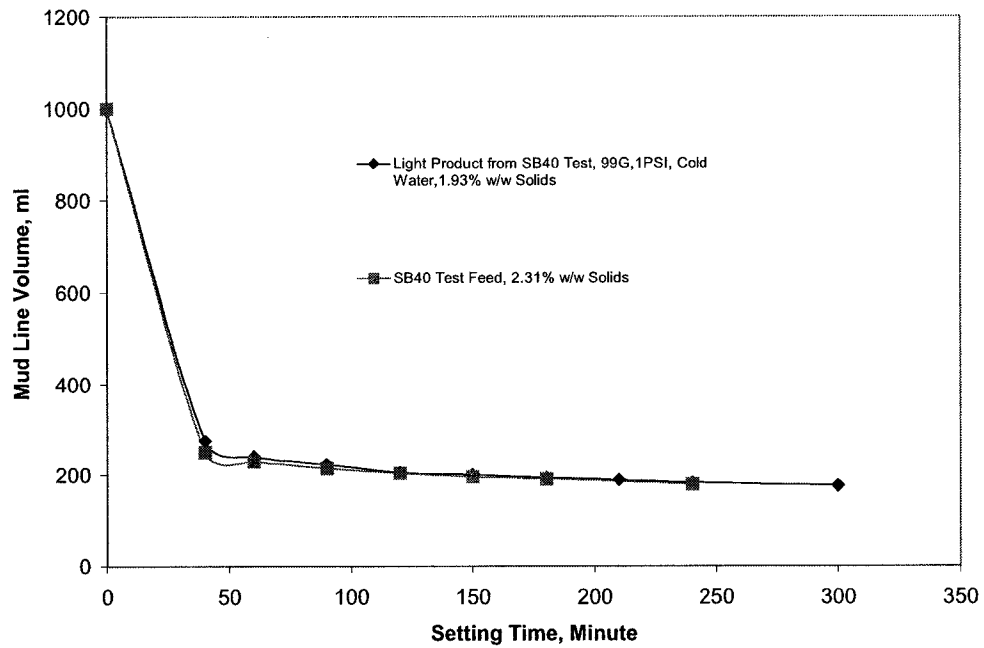


Figure 21 Settling curves of SB40 sample No.5 and the SB40 sample No. 5 light product

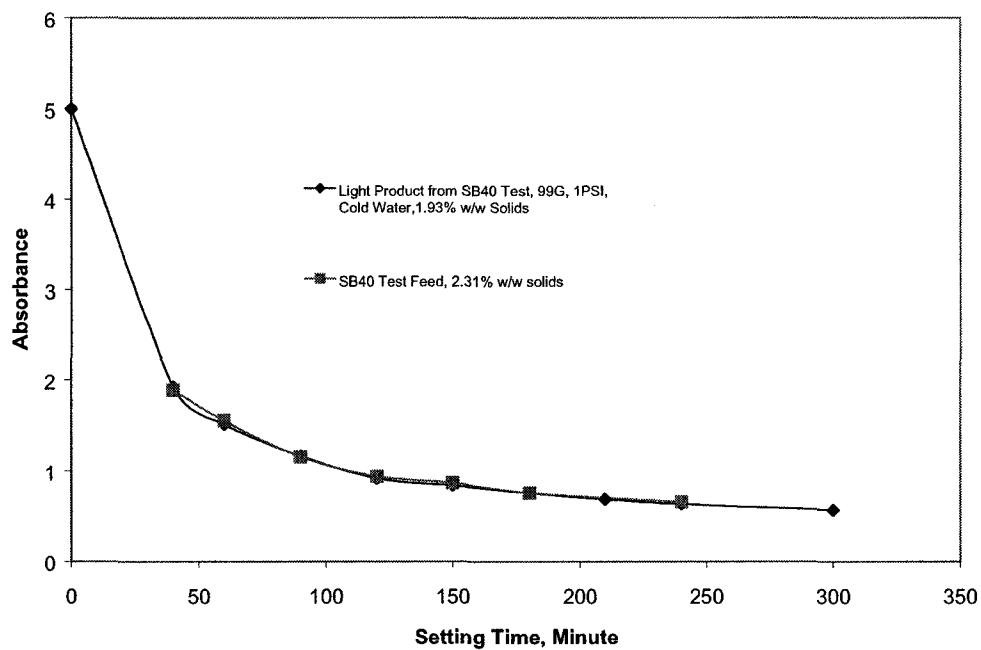


Figure 22 Optical absorbance of the clarified water from SB40 sample No.5 and the SB40 sample No.5 light product

5.4.3 Characterization of Residual Bitumen

The froth treatment tailings sample collected from the Syncrude Froth Treatment Plant was probably a decanted sample and the content of residual bitumen in the tailings was found to be close to that of the oil sand feeds. However, before embarking on recovering the residual bitumen and returning it to the extraction circuits, it is necessary to know if the residual bitumen is worth recovering. Thus, the residual bitumen needs to be characterized.

The reasoning behind conducting such tests is that perhaps the “good” bitumen has been recovered in the bitumen extraction circuits and that the residual bitumen left in the tailings was the “bad” one that is not worth recovering. Also, as shown earlier, Falcon centrifugal concentrator tests on the froth treatment tailings produced heavy products that contained very small amount of the residual bitumen, and the majority of the residual bitumen was recovered into the light products which contained mostly clays and water. It is possible that the bitumen associated with these “heavy” and “light” products were also different and thus require different down-stream treatment.

The bitumen in the oil sands is usually grouped into four fractions: the saturates, the aromatics, the resins and the asphaltenes. The asphaltene fraction is a major precursor of coke. Asphaltene content, in conjunction with carbon residue tests, is a measure of the relative bitumen quality for upgraders. Carbon residue is the residue remaining after evaporation and pyrolysis of oil under specified conditions. It indicates the relative coke-forming tendency of the oil under thermal degradation conditions. As is well known, coke is an undesirable by-product from the primary upgrading of bitumen, and it generally contains high levels of metals and sulfur that prevent it from being used as a fuel without special combustion units. Higher yields of coke imply lower yields of liquid hydrocarbon products. Therefore, bitumen with low levels of carbon residue is the more desirable feedstock for upgraders and is the “good” bitumen whereas those with a high carbon residue are the “bad” ones.

In this study, the Micro Carbon Residue (MCR) tests were conducted on the residual bitumen in the froth treatment tailings, as well as on Falcon SB40 separation products, to assess the quality of the residual bitumen.

Table 29 shows the bitumen balance for the two sets of SB40 tests. The bitumen content is converted from TLX data, which is the bitumen content in the solid phase that is free of water. The MCR of each product is also presented in the table. As a comparison, the average MCR of Syncrude oil sands feed is 13.5%.

As can be seen from Table 29, the bitumen associated with the “Slimes” fraction (with 13.6% and 13.7% MCR) had a better quality than that associated with the “Heavy” fraction (with 16.0% and 15.9% MCR). It is also interesting to note that the froth product skimmed from the “Slime” fraction had the lowest quality (with 16.3% MCR)! It is possible that this froth fraction contained organic matters such as wood chips that gave it a high MCR content. The froth treatment tailings (which are shown as “Feed” in Table 29) revealed a higher MCR (14.5% and 15.0%) than the average MCR in the oil sands feed (13.5%). However, despite the observed trend, the small variations in MCR (13.6 to 16.3%) probably indicated that the residual bitumen was still worth recovering.

As for bitumen distribution, for sample No. 2, the bitumen content in feed was 4.26%, and about 50% of bitumen was collected into the heavy product. For sample No. 4, the bitumen content in feed was 7.98%, and only 15.9% of bitumen was collected into the heavy product. As mentioned earlier under the test conditions, the recovery of heavy minerals in the heavy product was over 86% for both samples. Therefore, the results seem to indicate that when the bitumen content in the froth treatment tailings was high, there was a better separation between the heavy minerals and the residual bitumen.

Table 29 Bitumen balance for SB40 tests

Sample	Conditions	Product	Yield %	Bitumen %	Bitumen distribution %	MCR of bitumen %
No. 2	300 G 1 psi 50°C	Heavy	85.87	2.57	51.6	16.04
		Slimes	14.13	14.60	48.4	13.71
		Feed	100.00	4.26	100.0	14.95
No. 4	300 G 1 psi 50°C	Heavy	68.29	1.76	15.1	15.87
		Froth	3.92	45.20	22.2	16.33
		Slimes	27.79	18.00	62.7	13.55
		Feed	100.00	7.98	100.0	14.51

The results may suggest that the residual bitumen in the heavy product were only the one that were “wrapped” on the heavy and/or coarse mineral particle surfaces, so that its content was fixed at a relatively low level. This fraction of the bitumen would be recovered into the heavy product together with the minerals. When the froth treatment tailings had high residual bitumen content, the contributions from this “wrapped” bitumen would be small and the majority of the residual bitumen would be associated with water and clays (slimes). Therefore, after the SB40 separation, the majority of the residual bitumen would report to the slime product, resulting in a low bitumen recovery in the heavy product. On the other hand, when the froth treatment tailings had a low bitumen content, the contributions from the “wrapped” bitumen would be relatively higher, resulting in a higher bitumen recovery into the heavy product.

5.4.4 Mineralogy of Sample No. 2 Falcon SB40 Heavy Product

Table 30 Approximate composition as determined by mineralogical analysis

Mineral	Quartz and Feldspar	Other silicates	Carbonate	Zircon	Rutile and Anatase	Pyrite
Content, %	38.5	9	3.5	10	36	3

This sample shows a slightly more restricted particle size than the No.2 head, being dominantly in the range of 30 – 150 µm. This is expected since it is a heavy product from the Falcon SB40 separation.

The composition of this sample appears essentially identical to the No.2 head. Zircon may be marginally more abundant but, in light of the high variation in counts from field to field, the difference may not be significant. All constituents appear virtually fully liberated (Figure 23).

SEM/EDX analysis indicated that rare earth minerals were associated with quartz grains as shown in Figure 24.

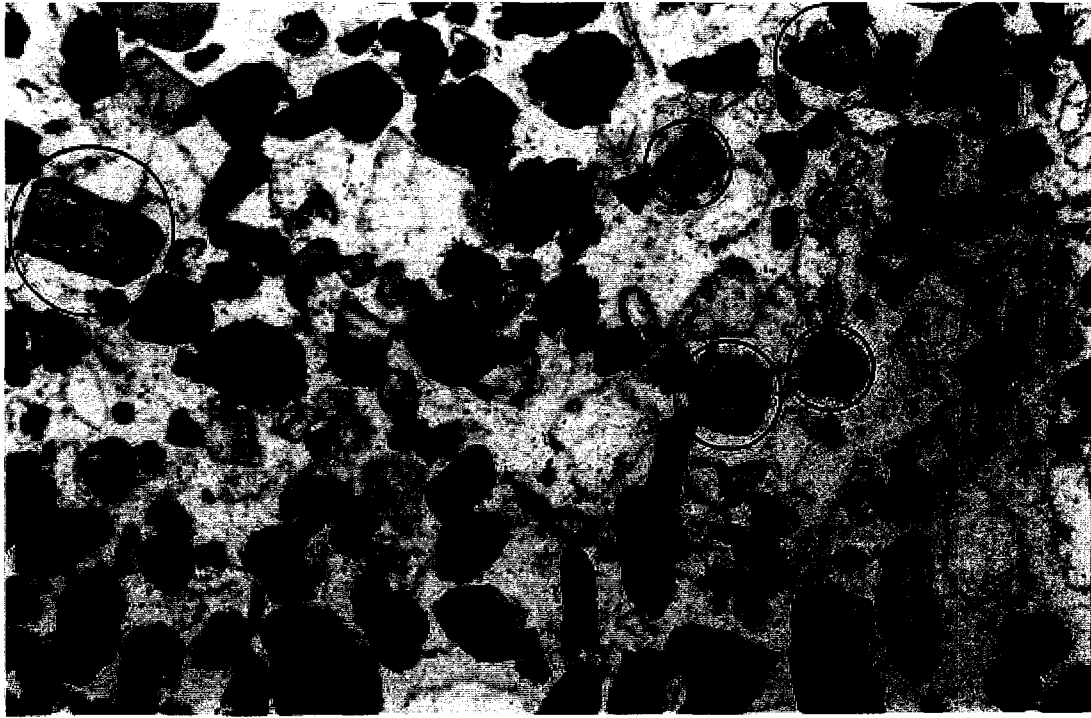


Figure 23 Sample No.2 Falcon SB40 heavy product under plane-polarized transmitted light

Circled grains are zircon, and this shows high degree of liberation of zircon.

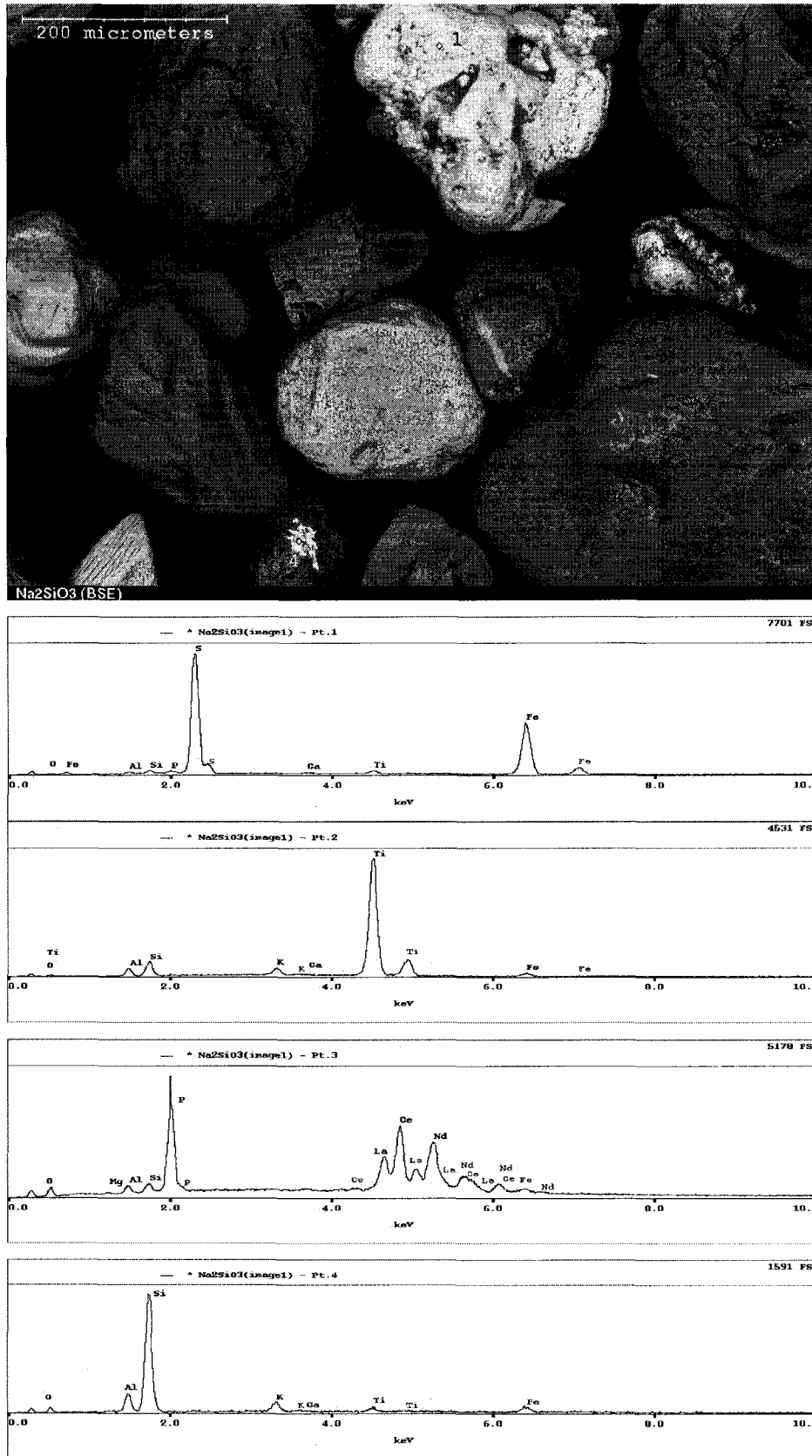


Figure 24 SEM/EDX analysis of bitumen-removed SB40 heavy product

5.4.5 Whole Rock Analysis of Centrifuge Concentration Products

Whole rock analysis results of centrifugal concentrator products are listed in Table 31. Here test G29 was on sample No. 2, test G33 was on sample No. 4, and test G15 was on sample No.5. It is interesting to note that for each sample, the assays of ZrO_2 , TiO_2 , Fe_2O_3 in the froth fraction are relatively high, some are even higher than that in the heavy product. In the slime fraction, the Al_2O_3 assay is much higher than that in the heavy fraction and froth fraction. In the heavy products, besides the titanium and zirconium minerals, the majority of composition is SiO_2 (52.88% - 64.42%), other main components include Al_2O_3 , CaO and MgO .

Table 31 Elemental analysis of centrifuge concentration products

Sample	ZrO_2	Al_2O_3	BaO	CaO	Fe_2O_3	K_2O	MgO	MnO	Na_2O	P_2O_5	SiO_2	TiO_2	LOI
G29 H	4.19	5.01	0.07	2.06	8.64	0.86	1.46	0.21	0.33	0.47	57.73	14.51	3.72
G29 F	11.88	6.06	0.12	5.16	17.76	0.40	2.50	0.37	0.40	1.18	14.46	21.40	10.88
G29 S	2.12	20.36	0.07	3.98	11.44	1.76	1.90	0.29	0.39	0.47	39.24	6.30	12.24
G33 H	1.75	4.25	0.06	3.28	8.84	0.87	1.48	0.16	0.32	0.45	64.42	8.90	3.97
G33 F	3.66	7.27	0.09	8.52	21.63	1.00	3.02	0.42	0.73	0.88	13.83	8.47	28.91
G33 S	0.55	22.96	0.06	3.10	11.18	2.13	1.63	0.12	0.32	0.37	42.82	3.02	11.83
G15 H	5.23	6.57	0.10	1.19	8.94	0.98	1.31	0.21	0.49	0.42	52.88	15.94	4.36
G15 F	4.29	7.67	0.09	3.19	26.07	0.82	2.56	0.45	0.44	0.79	13.91	10.12	29.57
G15 S	0.51	20.63	0.06	1.51	10.69	2.23	1.63	0.24	0.67	0.22	42.21	3.30	14.75

5.4.6 Comparison of Particle Size of Flotation Concentrate with that of Centrifugal Concentrate

Coarse particle sizes are more desirable for the final heavy mineral products than the fine ones. Although de-slime removed some of the fine particles, the flotation concentrate inevitably contained fine slimy particles due to the nature of this process. These fine slimy particles would still need to be rejected in later stages even though they may be the heavy minerals.

On the other hand, the fine slimy particles are rejected in the centrifugal concentrator. It is most likely that the heavy minerals lost to the light product in the Sb40 tests were of extremely fine sizes so they would not be desirable in the final heavy mineral products anyway. Their rejection at this early stage would benefit subsequent mineral separation process.

Figure 25 shows that there were more fine particles in the flotation concentrate than in the heavy product from the centrifugal concentrator. The percentage of material passing 38 μm was about 20% for the centrifugal separator heavy product, but was close to 40% for the flotation concentrate.

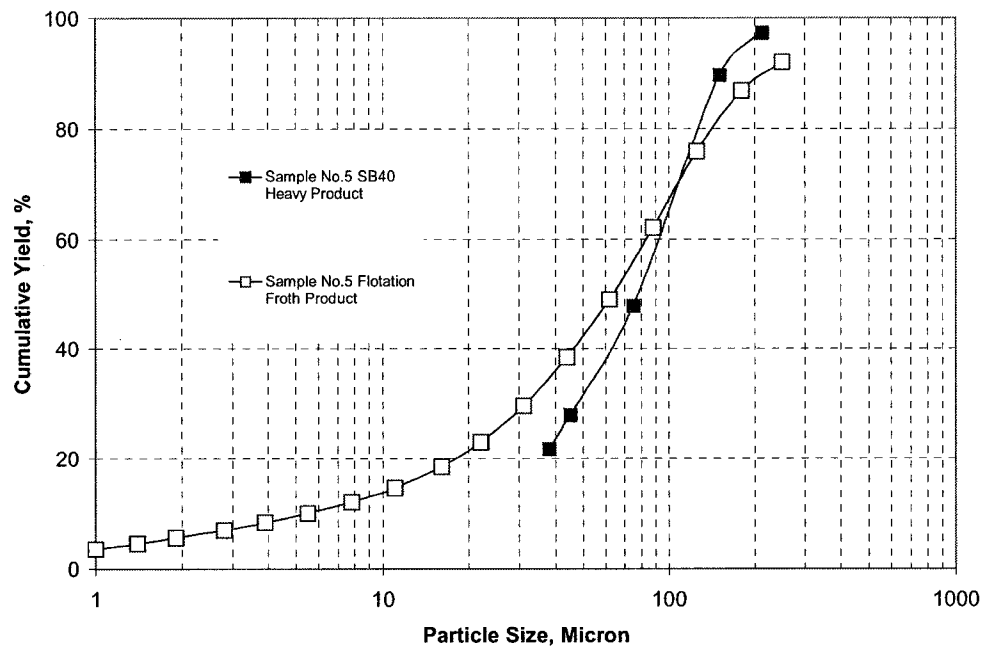


Figure 25 Particle size distribution of flotation concentrate and centrifugal concentration heavy product

5.5 Summary

Characterization of oil sands tailings

1. The residual bitumen contained in the froth treatment tailings had a slightly higher micro carbon residue, MCR, of 14.5-15.0%, than the average MCR of the oil sands feed (13.5%), indicating that the residual bitumen was of a poor quality than that in the oil sands feed.
2. The bitumen content in solids increased linearly with the -400 mesh (-38 μm) size materials.
3. In sample No. 2, the titanium and zirconium distribution in the -38 μm fraction were 11.3% and 12.4%, respectively, while in sample No. 4, the titanium and zirconium distribution in the -38 μm fraction were 16.7% and 19.7%, respectively. This indicates that even for samples taken at approximately the same time, there could be considerable variation in the particle size and heavy mineral content in the oil sands tailings.
4. The magnetic susceptibility of toluene washed sample No. 2 was $7.3 \times 10^{-9} \text{ m}^3/\text{kg}$.
5. Whole rock analysis of the bitumen-removed oil sands tailings showed that, Sample No. 4 contained 7.33% TiO_2 and 1.49% ZrO_2 , and Sample No. 2 contained 13.71% TiO_2 and 4.13% ZrO_2 .
6. Mineralogical analysis showed that Sample No. 2 consisted of mineral grains ranging in size from about 20 μm to about 200 μm . The dominant constituents were quartz and accessory minerals including a variety of other silicate minerals, carbonates, zircon, and pyrite. The oxide grains mainly showed the translucency characteristic of rutile or anatase. The negative response of the sample to the hand magnet indicated the absence of magnetite. The zircon occurred as vari-sized, ragged grains – mostly liberated, but occasionally composite with quartz. Overall liberation of all constituents in this sample was of a high order.

Flotation of oil sands tailings

1. Pulp temperature was found to be the key parameter in the flotation of oil sands froth treatment tailings: the flotation recoveries of heavy minerals and bitumen at 85°C were much higher than those at 50°C. It was shown that bitumen recovery for sample No. 5 was between 40% and 70%, and titanium mineral recovery was up to 80% and zirconium mineral recovery was up to 88% when the flotation was performed at 50°C; while the recoveries for the bitumen and heavy minerals were increased to above 94% at 85°C.
2. Similarly, at 50°C the flotation recoveries from sample No. 2 were 59.7% for bitumen, 81.2 % for titanium mineral and 84.9% for zircon. After adding NaOH, the recoveries were increased significantly. Combined use of NaOH with MIBC, and/or sodium oleate, and/or kerosene, resulted in bitumen recoveries that were comparable with the tests at a pulp temperature of 85°C.
3. For the other reagents tested: sodium metaphosphate is known to depress silicate minerals but it seemed to have also depressed the flotation of bitumen and heavy minerals. KCl had a deleterious effect on the flotation at 85°C but had very little effect at 50°C.
4. The increase of agitation intensity from 1400 rpm to 1600 rpm significantly reduced flotation recoveries. This may be due to the particle size effect. The increase of air flow rate from 0.692 to 1.233 L/minute had very little effect on the flotation.

Centrifugal concentration of oil sands tailings

1. The Falcon Centrifugal Concentrator seemed to be a better choice than flotation for the pre-treatment of the oilsands tailings. It gave a clear separation between the heavy minerals and the residual bitumen. For sample No. 5, the Falcon Concentrator produced a heavy product that recovered over 85% of the heavy minerals and 10% of the bitumen, and a light product that recovered about 15% of the heavy minerals (probably all fine heavy mineral particles) and about 90% of the bitumen.

2. The Falcon centrifugal concentrator tests on sample No. 2 showed that, under the optimum test conditions, the heavy product recovered 93.7% of the TiO_2 , 91.6% of the ZrO_2 and 54.7% of the bitumen. Overall, 4.6% of TiO_2 were lost in the light product (63.8% of them were in the $-38 \mu\text{m}$ fraction); 5.2% of the ZrO_2 were lost in the light product (35.1% of them were in the $-38\mu\text{m}$ fraction).
3. For sample No. 4, the Falcon concentrator produced a heavy product that recovered 88.8% of TiO_2 , 86.7% of the ZrO_2 and 28.7% of the bitumen. Overall, 8.7% of TiO_2 were lost in the light product (87.4% of them were in the $-38 \mu\text{m}$ fraction); 7.9% of the ZrO_2 were lost in the light product (56.4% of them were in the $-38 \mu\text{m}$ fraction).
4. The light products generated from the Falcon concentrator tests contained primarily particles that were smaller than about $38 \mu\text{m}$ (over 92% of the materials were $-38 \mu\text{m}$). Generally, from 4 to 10% of the TiO_2 and ZrO_2 were lost into the light products. But since they were of very fine sizes and would not be useful in the final Ti and Zr products, their rejection at this stage may be justified.
5. The particle size measurements indicated that the heavy products from the centrifugal concentrator were coarser than the flotation concentrate.
6. After separating the froth treatment tailings into two products using the Falcon SB40 Centrifugal Concentrator, it was observed that the bitumen contained in the heavy product had a higher MCR (15.9 – 16.0%) than those contained in the slime product (13.6 – 13.7%). This indicates that the bitumen contained in the heavy product was of a poor quality than the ones associated with the slime product.
7. The bitumen contained in the froth skimmed from the slime product had the highest MCR content (16.3%), and thus had the lowest quality. This may be due to the presence of organic matters such as wood chips, etc.
8. The bitumen content in the SB40 heavy product was low and more or less fixed. The variation in the bitumen content in the froth treatment tailings only affected the bitumen content in the SB40 slime product.
9. Due to the small variations in the MCR contents of the residual bitumen in the froth treatment tailings, as well as in different SB40 products, the residual bitumen after the SB40 centrifugal concentration should be worth recovering.

6 BITUMEN REMOVAL BY ROASTING

Burning off the residual bitumen was the method that was used in nearly all previous metallurgical studies on oil sands tailings. Surprisingly, researchers did not pay any attention to the effect of such treatment on the separation characteristics of the minerals. In this study, we examined the effect of this burning (roasting) process on the magnetic susceptibilities of minerals contained in the froth treatment tailings, as well as on other separation characters. High purity minerals were also used besides the froth treatment tailings in order to isolate the effect on individual minerals. These minerals were described in Chapter 4.

6.1 Effect of Roasting on the Magnetic Properties of Single Minerals

6.1.1 *Magnetic Susceptibility of Ilmenite*

The ilmenite used in this study was a magnetic mineral with a measured magnetic susceptibility of $2.18 \times 10^{-6} \text{ m}^3/\text{kg}$. It was subjected to both oxidation and reduction roasting to monitor changes in its magnetic susceptibility and magnetic separation behavior.

Test results indicated that oxidation roasting of the ilmenite increased the magnetic susceptibility within a certain temperature range. As can be seen from Figure 26 and Figure 27, at 500°C , even extended heating (up to 2 hours) did not cause any change in the magnetic susceptibility of the ilmenite. At higher temperatures of 650°C and 700°C , the magnetic susceptibility started to increase after 30 minutes of roasting, and continued the slight increasing trend with extended roasting time. At even higher temperatures (750°C - 1000°C), the magnetic susceptibility increased rapidly initially, reached a maximum of about $5.5 \times 10^{-5} \text{ m}^3/\text{kg}$, then dropped sharply and eventually reached a value that was lower than the original ilmenite, leveling off at about $4 \times 10^{-7} \text{ m}^3/\text{kg}$. The exact time period at which these changes occurred varied with the temperature that was used. Finally, when the temperature was above 1000°C , the magnetic susceptibility of the

ilmenite did not increase with the oxidation roasting but only decreased rapidly and quickly reached the lowest value of $4 \times 10^{-7} \text{ m}^3/\text{kg}$.

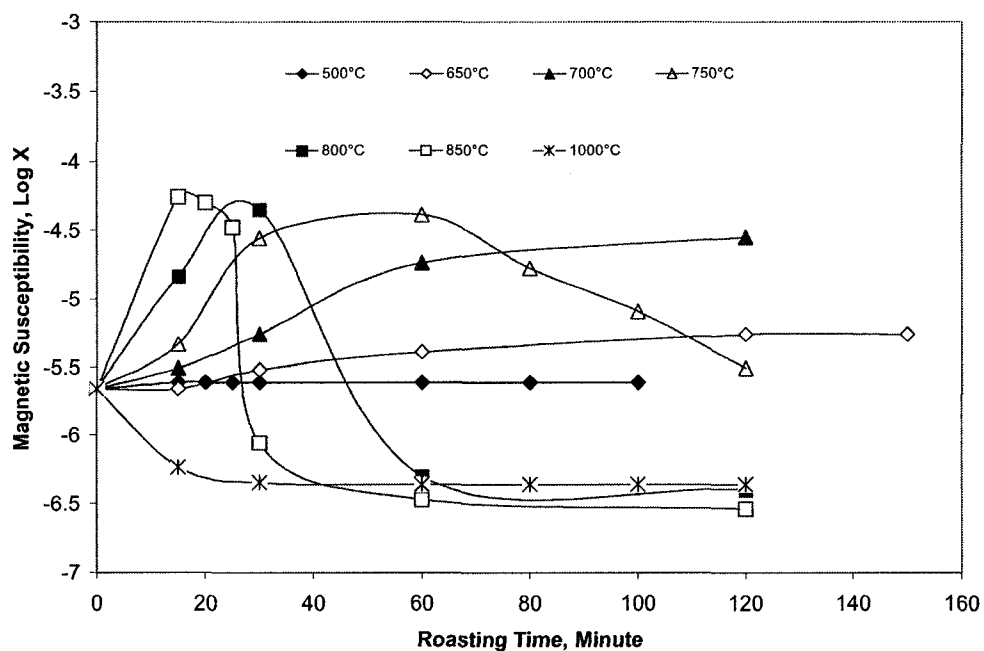


Figure 26 Oxidation roasting of ilmenite – magnetic susceptibility of ilmenite as a function of roasting time

X-ray diffraction spectra were recorded on the ilmenite samples before and after the roasting and the phases present in the samples were identified using standard spectra in the Jade database. It was found that below 850°C, oxidation roasting changed some of the ilmenite phases into hematite, rutile and reduced rutile, while after roasting for 60 minutes at 1000°C, almost all of the ilmenite phase were converted into hematite, rutile, reduced rutile and Fe_2TiO_5 .

To establish the relationship between the phase conversion and the changes in the magnetic susceptibility, the latter was plotted against the ratio of the strongest peak of hematite ($2\theta = 33.2^\circ$) and that of ilmenite ($2\theta = 32.5^\circ$) in Figure 29. As can be seen, when the ratio was between 1.5 and 3.5, the magnetic susceptibility of roasted ilmenite was much higher than that of the original unroasted ilmenite. This seems to indicate that when some of the phases in ilmenite were converted to hematite ($\alpha\text{-Fe}_2\text{O}_3$), its magnetic susceptibility significantly increased.

Interestingly, after a reduction roasting, the FeO in ilmenite was not reduced to low valence states (such as element iron, etc.), as no peaks due to elemental iron were observed in the x-ray diffraction spectra. Rather, they were converted into maghemite ($\gamma\text{-Fe}_2\text{O}_3$), causing a significant increase in its magnetic susceptibility (Figure 28) since $\gamma\text{-Fe}_2\text{O}_3$ is strongly magnetic. The mechanism of such conversion is not clear.

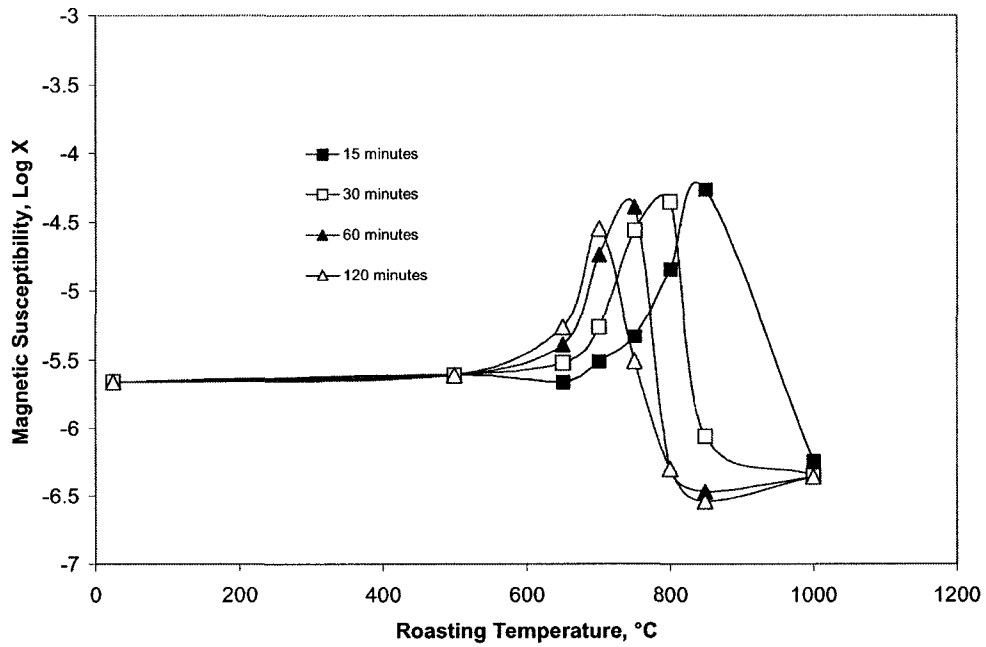


Figure 27 Oxidation roasting of ilmenite – magnetic susceptibility of ilmenite as a function of roasting temperature

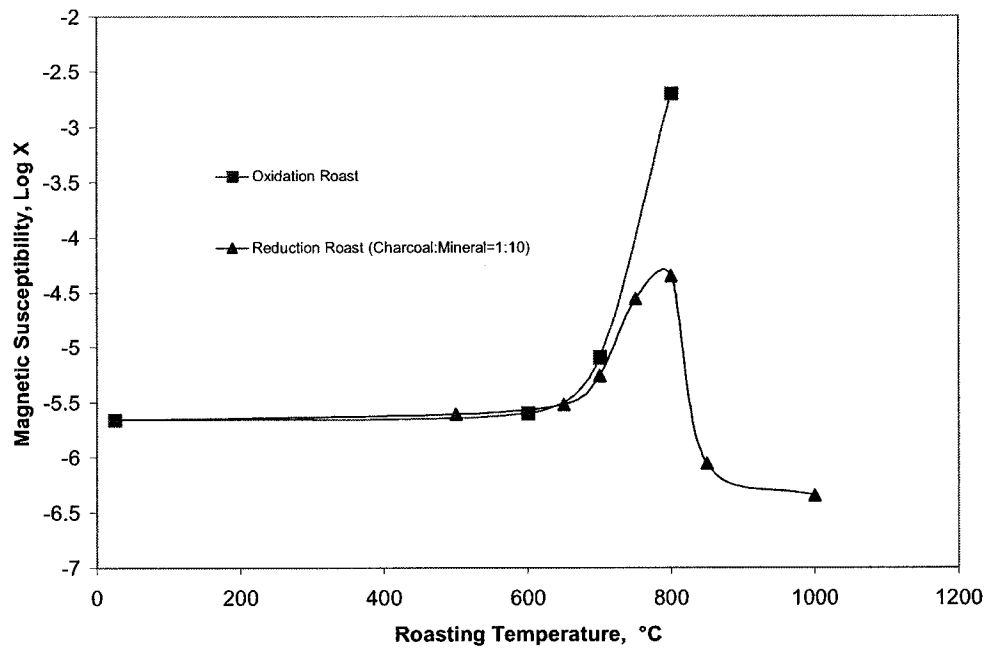


Figure 28 Magnetic susceptibility of ilmenite as a function of roasting temperature (Roasting time was fixed at 30 minutes)

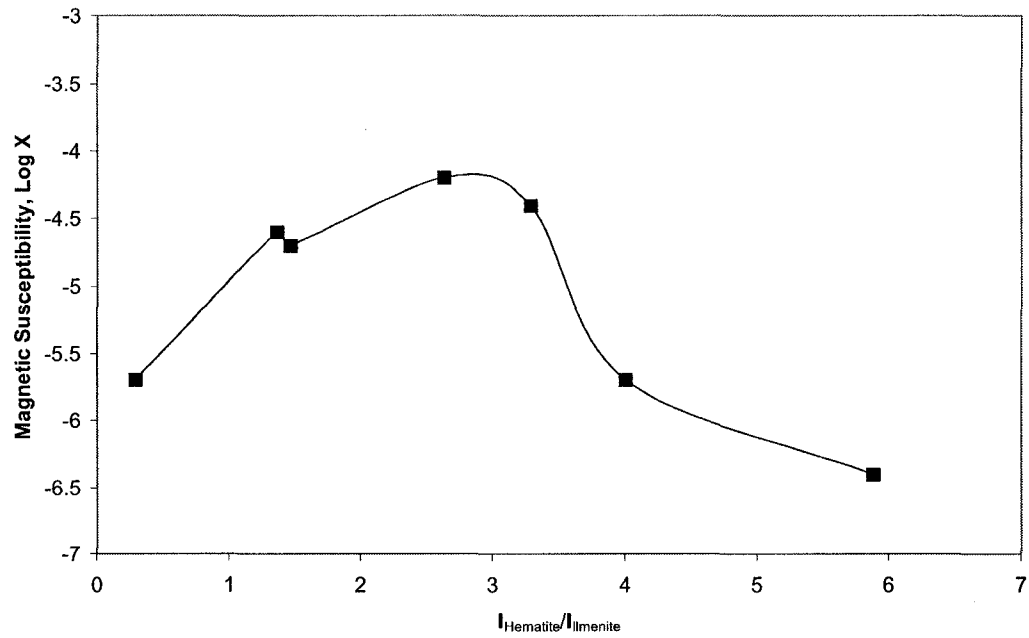


Figure 29 Magnetic susceptibility of oxidation roasted ilmenite as a function of the peak intensity ratio between hematite and ilmenite

Magnetic separation of roasted ilmenite

The roasted ilmenite was subjected to separation using the Frantz Isodynamic Separator. Two electric current settings were applied in the Separator, 0.15 A and 0.3 A, and the corresponding magnetic field strength was 0.12 and 0.24 Tesla. The separation results are presented in Figure 30 and Figure 31. Comparing Figure 30 with Figure 26, and Figure 31 with Figure 27, it is clear that at a magnetic field intensity of 0.12 Tesla, ilmenite recovery into the magnetic products coincided well with its magnetic susceptibility. Without the roasting treatment, the magnetic susceptibility of the ilmenite was $2.18 \times 10^{-6} \text{ m}^3/\text{kg}$ and only about 10% of the ilmenite reported to magnetic product at this low magnetic field intensity. After roasting, the magnetic susceptibility of ilmenite increased which resulted in a significant increase in its recovery into the magnetic product. The maximum recovery reached 90% at the maximum magnetic susceptibility of $5.5 \times 10^{-5} \text{ m}^3/\text{kg}$. Similarly, a decrease in the magnetic susceptibility resulted in a sharp drop in the recovery. At the lowest magnetic susceptibility of $4 \times 10^{-7} \text{ m}^3/\text{kg}$, the recovery was at the lowest point of about 2 - 5%.

However, when the electric current was set at 0.3 A (the corresponding magnetic field intensity was 0.24 Tesla), the recovery of the unroasted ilmenite into the magnetic product increased to about 90%. An increase in the magnetic susceptibility did not result in further increase in the recovery. However, when the magnetic susceptibility was decreased due to roasting, the recovery dropped sharply (Figure 32 and Figure 33).

Clearly, with a magnetic susceptibility of $2.18 \times 10^{-6} \text{ m}^3/\text{kg}$, the ilmenite could not be recovered by magnetic concentrators at a field intensity of 0.12 Tesla. Any increase in its magnetic susceptibility was beneficial to its recovery at this low field intensity. On the other hand, if the magnetic field intensity increased to 0.24 Tesla, the ilmenite could be recovered, but any decrease in its magnetic susceptibility would sharply lower the recovery. Since the titanium minerals contained in the Alberta oil sands tailings are rutile, ilmenite and its alteration product (leucoxene), the above fact suggested that in order to effectively recover the magnetic titanium mineral appropriate magnetic field intensity

have to be applied or the magnetic susceptibility of feed material have to be controlled or monitored

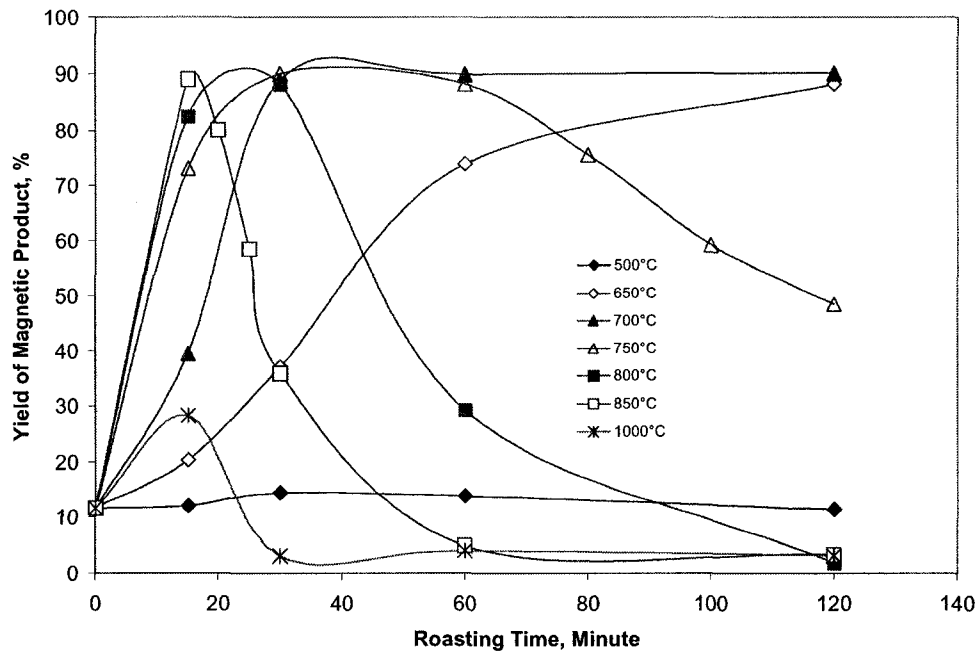


Figure 30 Yield of ilmenite into the magnetic product as a function of roasting time
(The magnetic separation was performed with a Frantz Isodynamic Separator and the electric current was set at 0.15A --- magnetic field intensity: 0.12 T)

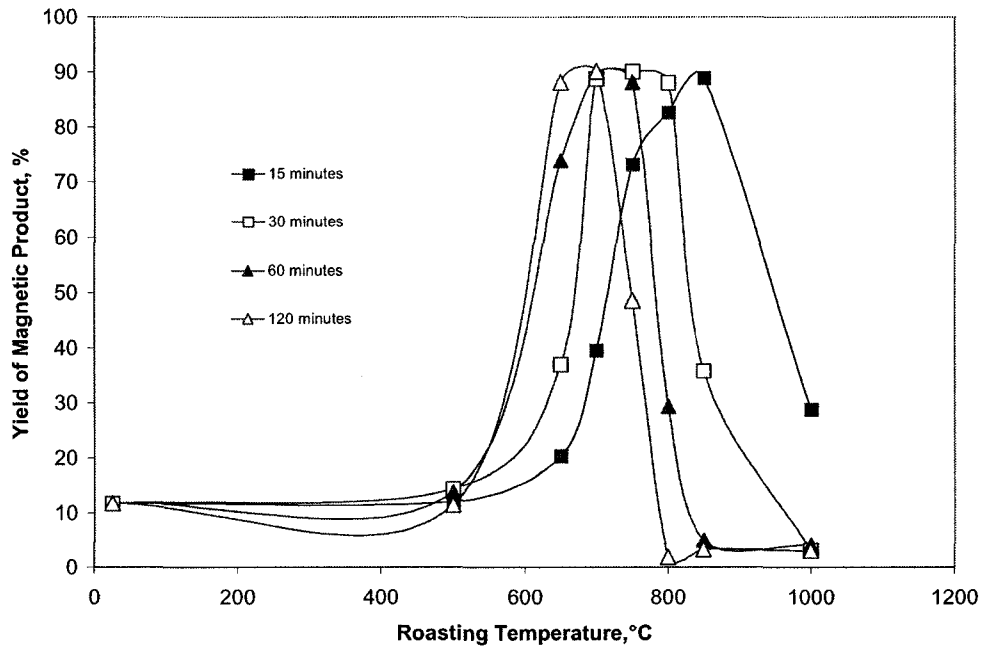


Figure 31 Yield of ilmenite into the magnetic product as a function of roasting temperature

(The magnetic separation was performed with a Frantz Isodynamic Separation and the electric current was set at 0.15A --- magnetic field intensity: 0.12 T)

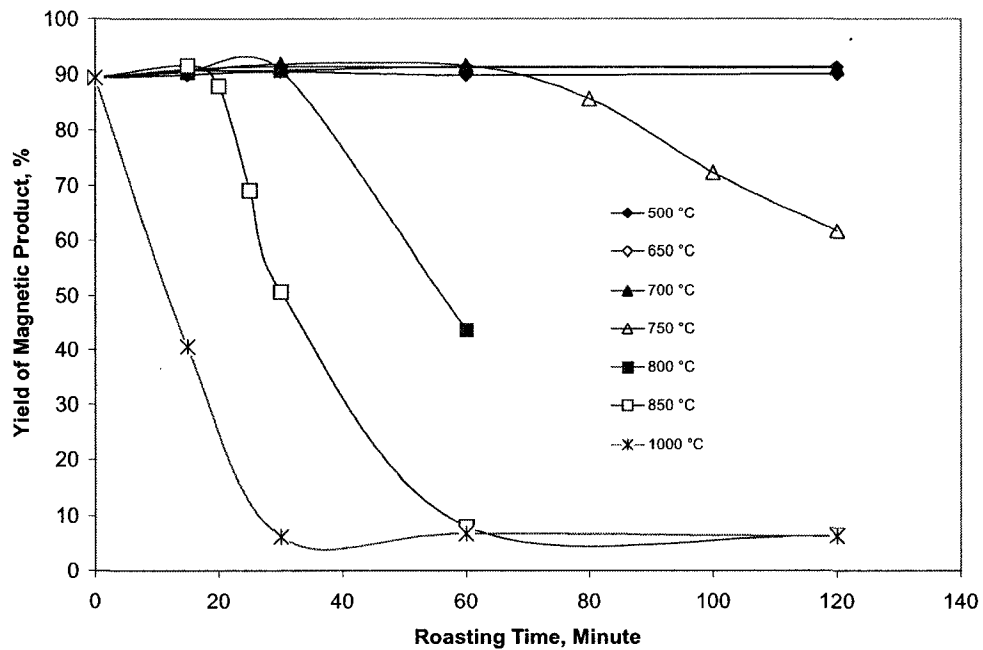


Figure 32 Yield of ilmenite into the magnetic product as a function of roasting time
(The magnetic separation was performed with a Frantz Isodynamic Separator and the electric current was set at 0.3 A (magnetic field intensity: 0.24 T))

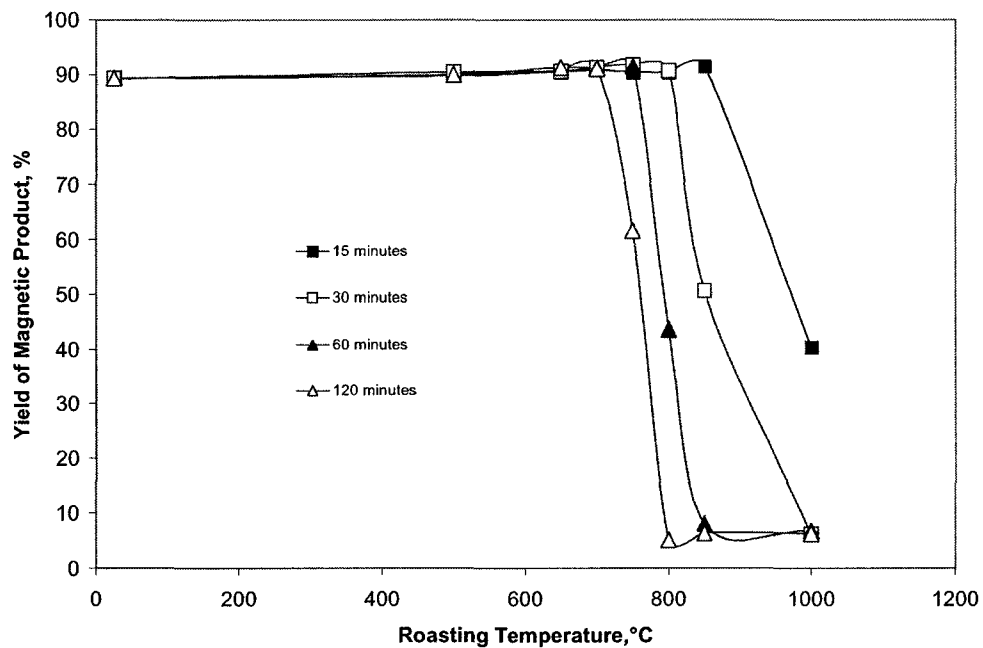


Figure 33 Yield of ilmenite into the magnetic product as a function of roasting temperature

(The magnetic separation was performed with a Frantz Isodynamic Separator and the electric current was set at 0.3 A --- magnetic field intensity: 0.24 T)

6.1.3 Effect of Roasting on the Magnetic Properties of Hematite

It is known that magnetite ($\text{Fe}_2\text{O}_3 \cdot \text{FeO}$), the most magnetic mineral, contains a blend of Fe_2O_3 and FeO phases which may have contributed to its high magnetic susceptibility. One of the most common titanium minerals in the oil sands tailings, leucoxene ($x\text{TiO}_2 \cdot y\text{Fe}_2\text{O}_3$), only had the Fe_2O_3 phases, which may be the reason for its relatively low magnetic susceptibility. If this is the case, then a reduction roasting of the oil sands tailings would convert some of the Fe_2O_3 phases in leucoxene into FeO , making the leucoxene more magnetic and therefore easier to separate from rutile using magnetic separation.

The magnetic susceptibility of the hematite (Fe_2O_3) sample used in this work, measured at $0.95 \times 10^{-6} \text{ m}^3/\text{kg}$, was lower than that of ilmenite ($2.18 \times 10^{-6} \text{ m}^3/\text{kg}$). Hematite contains ferric irons and cannot be oxidized further. In fact, oxidation roasting of hematite did not change its magnetic susceptibility. Therefore the roasting of hematite was done only in a reducing atmosphere.

Figure 34 to Figure 38 show the magnetic susceptibility of hematite after being roasted for different time periods at different temperatures and charcoal dosages. Similar to ilmenite, 500°C seemed to be a critical value, below which the magnetic susceptibility of the hematite only increased slightly even after prolonged heating. At temperatures above 500°C , the magnetic susceptibility increased significantly, and reached that of magnetite at 800°C or 1000°C . This was achieved with both a low charcoal dosage (1:10) and a high charcoal dosage (1:5). The only difference in the two different dosages is: at a low dosage, after a long period of heating (longer than 30 minutes), the magnetic susceptibility of hematite started to drop. The charcoal may have been completely consumed after prolonged heating and the partially reduced hematite started to re-oxidize. In fact, during the tests, it was observed that there was no charcoal left after more than 30 minutes of heating at the low charcoal dosage of 1:10.

Figure 37 and Figure 38 show the magnetic susceptibility of hematite as a function of roasting temperature. They again indicated that the lower limit of the temperature was about 500°C. X-ray diffraction analysis of the reduced hematite showed that some of the hematite phases were changed into maghemite ($\gamma\text{-Fe}_2\text{O}_3$), resulting in significant increase in its magnetic susceptibility. In fact, Figure 39 shows that there was a good correlation between the magnetic susceptibility of the roasted hematite and the peak intensity ratio between maghemite and hematite.

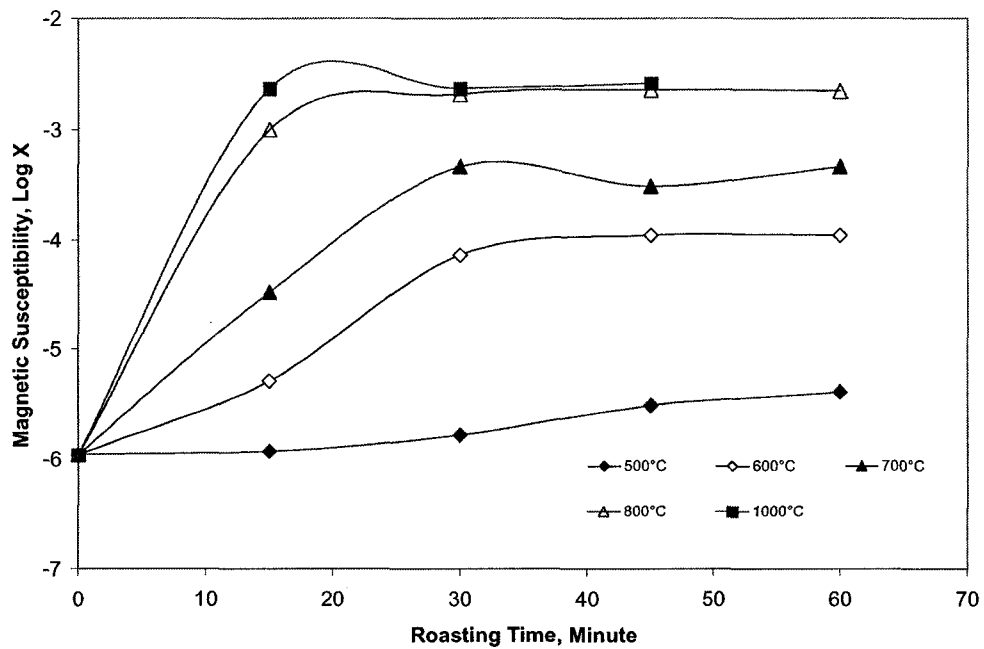


Figure 34 Magnetic susceptibility of hematite as a function of roasting time
(Charcoal and hematite were blended at a ratio of 1:5)

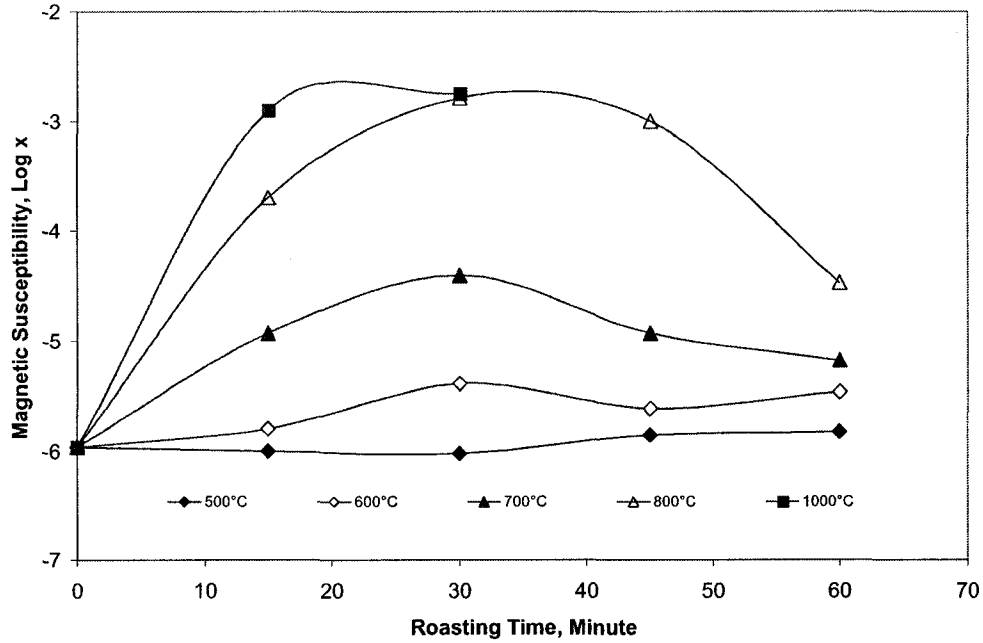


Figure 35 Magnetic susceptibility of hematite as a function of roasting time
(Charcoal and hematite were blended at a ratio of 1:10)

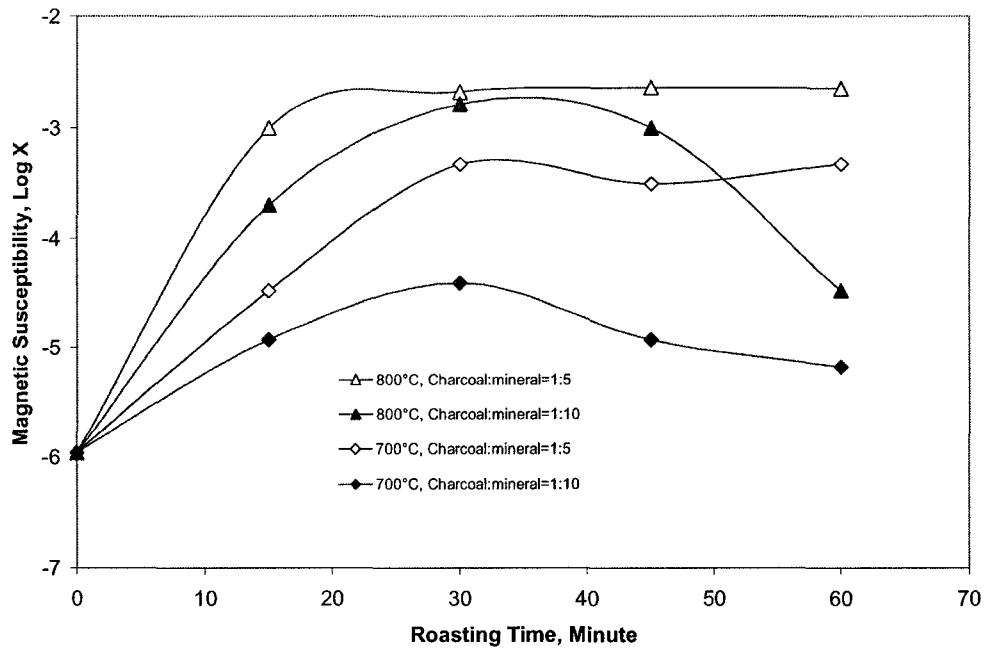


Figure 36 Comparison of reduction roasting of hematite at different charcoal dosage (Charcoal and hematite were blended at a ratio of either 1:5 or 1:10)

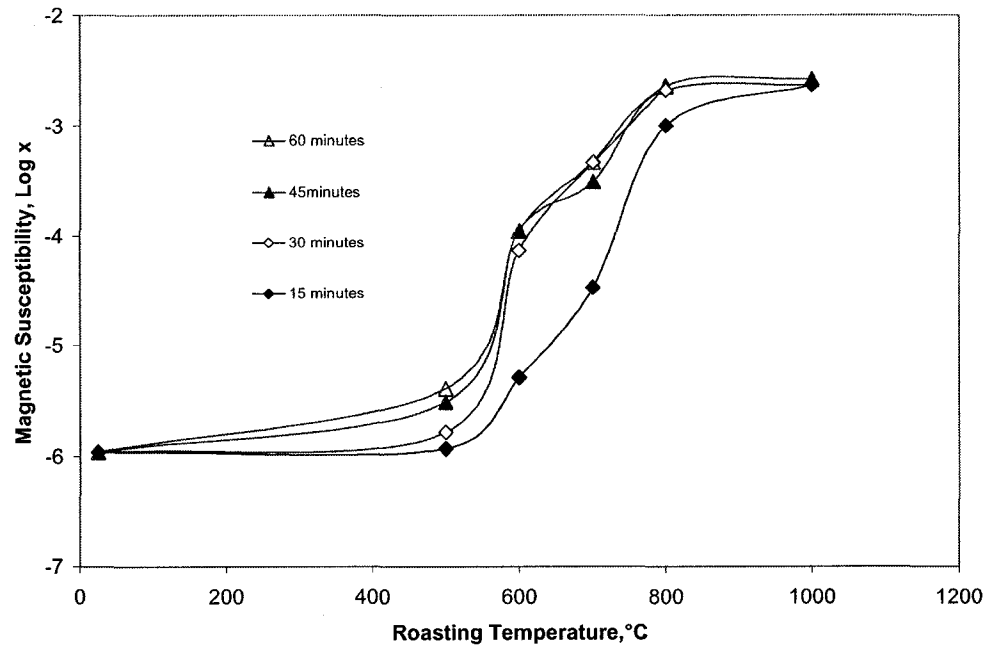


Figure 37 Magnetic susceptibility of hematite as a function of roasting temperature
(Charcoal and hematite were blended at a ratio of 1:5)

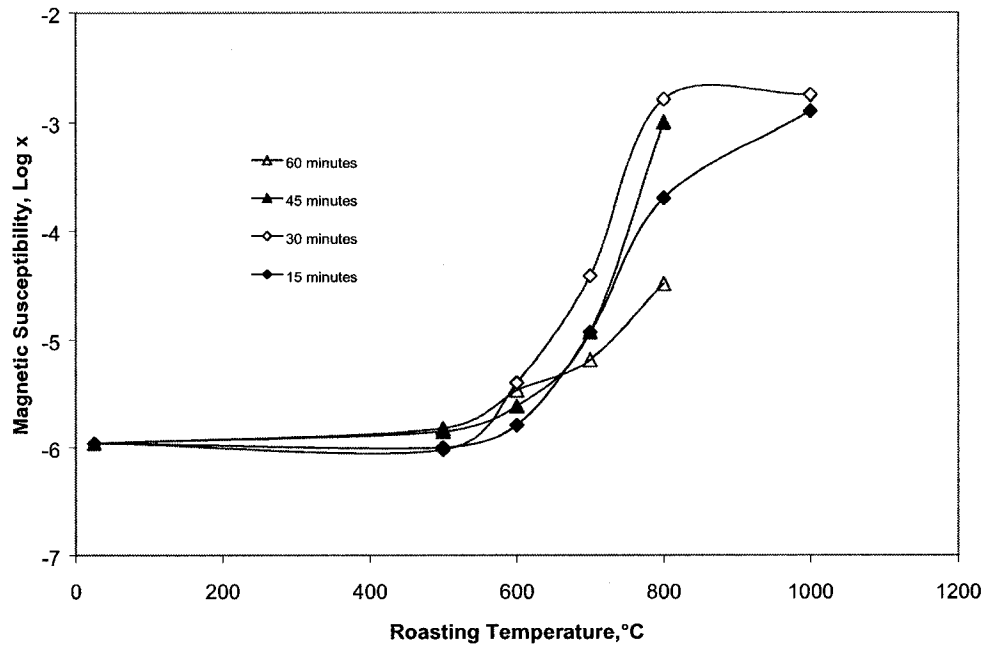


Figure 38 Magnetic susceptibility of hematite as a function of roasting temperature
(Charcoal and hematite were blended at a ratio of 1:10)

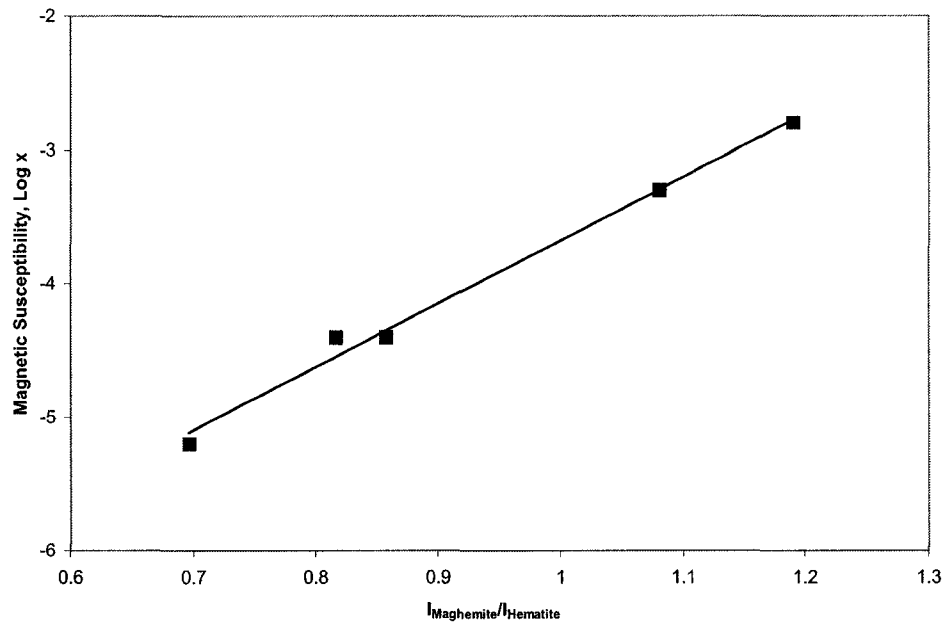


Figure 39 Magnetic susceptibility of reduction roasted hematite as a function of peak intensity ratio between maghemite and hematite

6.1.4 Effect of Roasting on the Separation of LR Rutile

The LR Rutile contained large percentages of leucoxene ($x\text{TiO}_2 \cdot y\text{Fe}_2\text{O}_3$), with only a small amount of rutile (anatase). Based on the foregoing discussion, it is expected that a reduction roasting should increase the magnetic susceptibility of the leucoxene and facilitate its removal by magnetic separation.

Table 32 shows the magnetic susceptibility of the LR Rutile after both an oxidation and a reduction roasting. Both were conducted at 800°C for 30 minutes. In the reduction roasting, charcoal was blended with the LR Rutile at a weight ratio of 1:10. As can be seen, the magnetic susceptibility of the LR Rutile dropped from $0.46 \times 10^{-6} \text{ m}^3/\text{kg}$ to $0.13 \times 10^{-6} \text{ m}^3/\text{kg}$ after the oxidation roasting, and increased to $0.58 \times 10^{-6} \text{ m}^3/\text{kg}$ after the reduction roasting.

The LR Rutile was also subjected to separation on the Frantz Isodynamic Separator at 0.5 A (0.4 Tesla), and the magnetic susceptibility of both the magnetic fraction and the non-magnetic fraction was measured. As can be seen from Table 32, while the magnetic susceptibility of the non-magnetic fraction was low and unchanged, that of the magnetic fraction nearly doubled after the reduction roasting.

Table 32 Magnetic Susceptibility of LR Rutile

Treatment	Condition	Magnetic susceptibility, $\times 10^{-6} \text{ m}^3/\text{kg}$		
		After treatment	After separation at 4000 Gauss	
			Magnetic fraction	Non-magnetic fraction
Original sample		0.46	0.66	0.05
Oxidation roasting	800°C, 30 minutes	0.13	0.16	0.03
Reduction roasting	800°C, 30 minutes, charcoal: rutile=1:5	0.58	1.15	0.05

Separation of the LR Rutile (with and without roasting) was performed with the Frantz Isodynamic Separator in the current range of 0.3 to 1.9 A (0.22 to 1.12 Tesla). The Fe_2O_3 and TiO_2 content in the non-magnetic product (which was the genuine rutile concentrate)

was assayed and expressed as a function of magnetic field intensity of the separator. The results are shown in Figure 40. Obviously, reduction roasting of the LR Rutile (at 800°C for 30 minutes with charcoal) produced a non-magnetic product with low Fe₂O₃ content and high TiO₂ assays. However, this beneficial effect was only observed in the low intensity range of up to 0.67 Tesla. At higher magnetic field intensity, the Fe₂O₃ content could be lowered without a prior reduction roasting of the LR Rutile sample.

Figure 41 shows that after grinding the LR Rutile so that the percentage passing 74 µm increased from 3% to 59%, the Fe₂O₃ content could not be significantly reduced. In fact, the figure shows that the significant size reduction did not benefit the Fe₂O₃ removal as much as a reduction roasting. This suggests that the poor separation between rutile and leucoxene in the LR Rutile concentrate was not a problem of liberation but rather a problem of the low magnetic susceptibility of the contaminating leucoxene.

The Athabasca oil sands tailings are known to contain large percentages of altered ilmenite (leucoxene)(Coward and Oxenford, 1997). It is also known that the LR Rutile had gone through a roasting process at 550°C (Oxenford et al, 2001) to remove the residual bitumen. However, it is not clear if the roasting process further converted all the ferrous iron in the oil sands into ferric (leucoxene), and lowered the magnetic susceptibilities of the Fe-bearing minerals. If this was the case, then possibilities of removing the residual bitumen at temperatures lower than 500°C should be studied. If, however, the Fe-bearing titanium minerals in the original oil sands had the low magnetic susceptibilities, then either a low intensity magnetic separation following a reduction roasting, or a direct high intensity magnetic separation, can be performed to achieve the separation. The magnetic susceptibility of the original oil sands tailings (rather than LR Rutile) was studied and will be discussed in the following.

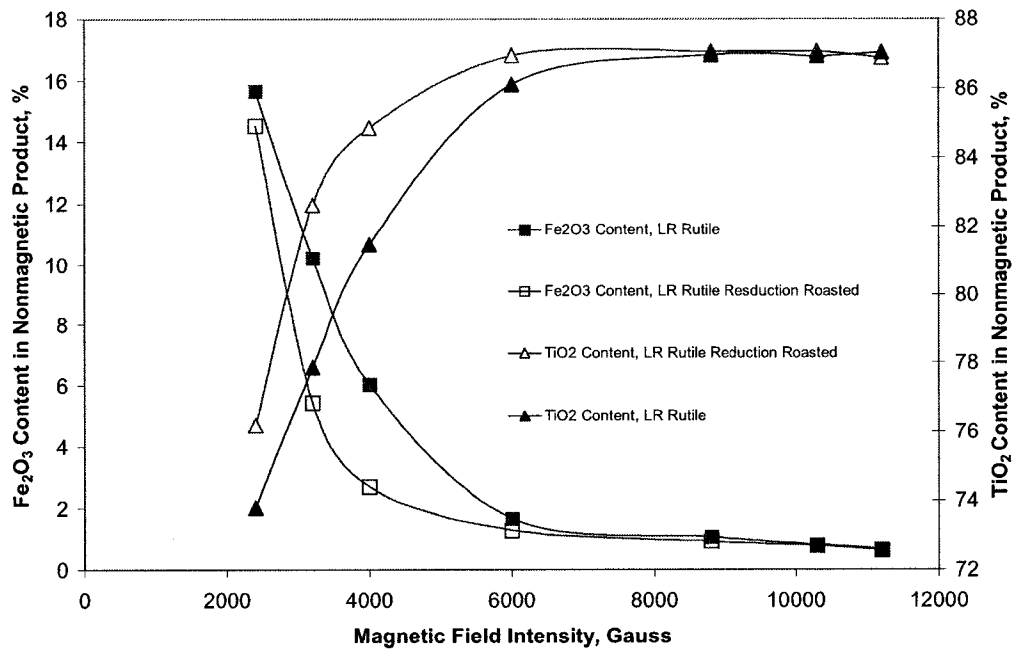


Figure 40 Fe₂O₃ and TiO₂ content in the non-magnetic product as a function of magnetic field intensity

(The non-magnetic product was obtained from separating the LR Rutile with a Frantz Isodynamic Separator)

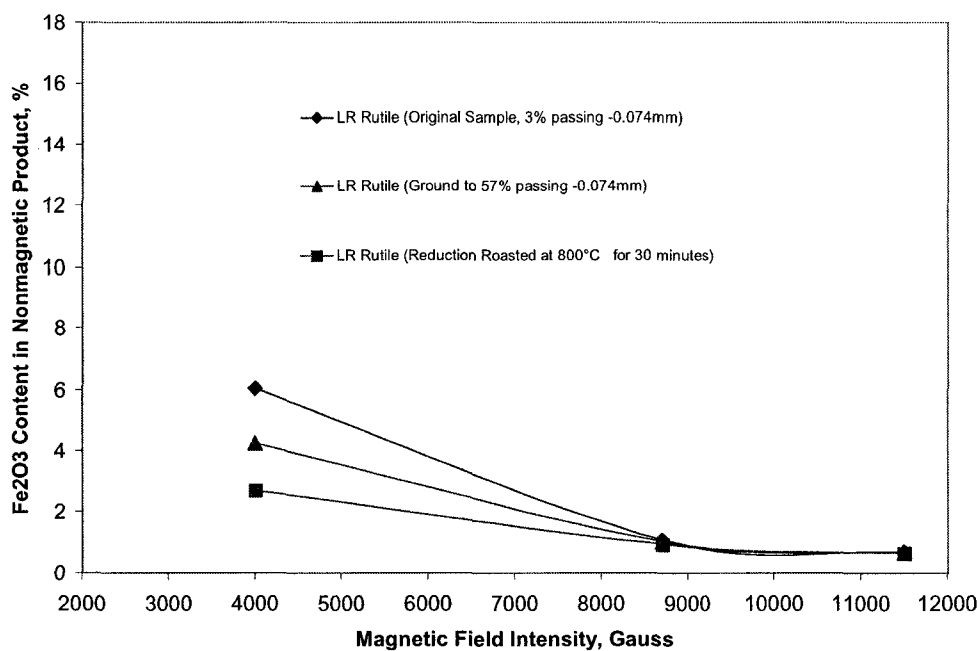


Figure 41 Fe₂O₃ content in the non-magnetic product after different pretreatment of the LR Rutile

6.2 Effect of Roasting on the Magnetic Properties of Oil Sands Tailings

6.2.1 *Magnetic Properties of Roasted SB40 Heavy Products*

Several batches of SB40 tests were conducted under the optimum conditions established before. The heavy products from each batch were combined and used in the following tests.

A small sample of the heavy product was washed with toluene to remove the residual bitumen. The magnetic susceptibility of the washed solids was measured and was found to be $0.73 \times 10^{-8} \text{ m}^3/\text{kg}$. This was taken as the magnetic susceptibility of the unroasted froth treatment tailings.

Small samples of the heavy product were also roasted to remove the residual bitumen. The magnetic susceptibility of the roasted sample was measured and plotted against the roasting temperature and roast time as shown in Figure 42 and Figure 43.

As can be seen, the magnetic susceptibility showed little variation with roasting time within the range tested (from 15 minutes to 120 minutes). It would appear that roasting temperature had a significant effect on the magnetic susceptibility of the froth treatment tailings since a dramatic increase was observed above 800°C . However, it was observed under a stereomicroscope that when the sample was heated to a high temperature, the dark opaque Fe- and Ti-bearing mineral particles tended to sinter with non-opaque minerals such as quartz by incipient fusion at points of contact. Sintering started at about 600°C and became very significant above about 700°C (Figure 45 to Figure 49). Since the magnetic susceptibility was determined with a Frantz Isodynamic Separator, which is based on recovery into a magnetic fraction, the fusion of the magnetic particles with non-opaque minerals such as quartz would increase recovery into the magnetic fraction and thus cause an incorrectly higher magnetic susceptibility reading.

Similarly, if zircon particles were sintered to the Fe- and Ti-bearing particles it would be very difficult to separate in the subsequent stages. Therefore, a favorable roasting temperature would be much lower than 800°C.

The roasted SB40 heavy products were subjected to the two-stage magnetic separation. The results are summarized in Table 33. As can be seen, as the roasting temperature increased from 500°C to 900°C, the SiO₂ content in the “Magnetic” fraction increased from 30% to 47% and the SiO₂ content in the “Middling” fraction increased from 36% to 48%. This seemed to be the direct result of the sintering of Fe-bearing titanium minerals with quartz. Similarly, the distribution of Fe₂O₃ in the “Non-magnetic” fraction decreased from 30.5% (toluene washed) to 6.2% (900°C roasted). From the Fe₂O₃ content and the TiO₂ distribution in the “Non-magnetic” fractions, it seems that about 50% of the TiO₂ was in the form of rutile and/or anatase, and the Fe₂O₃ content in the “Non-magnetic” fraction from the roasted sample was lower (from 0.67% to 1.58%) than that from toluene-washed sample (3.01%). To the extent that sintering did not occur, roasting in the presence of bitumen seemed to have a reducing effect which increased the magnetic susceptibility of the Fe-bearing minerals.

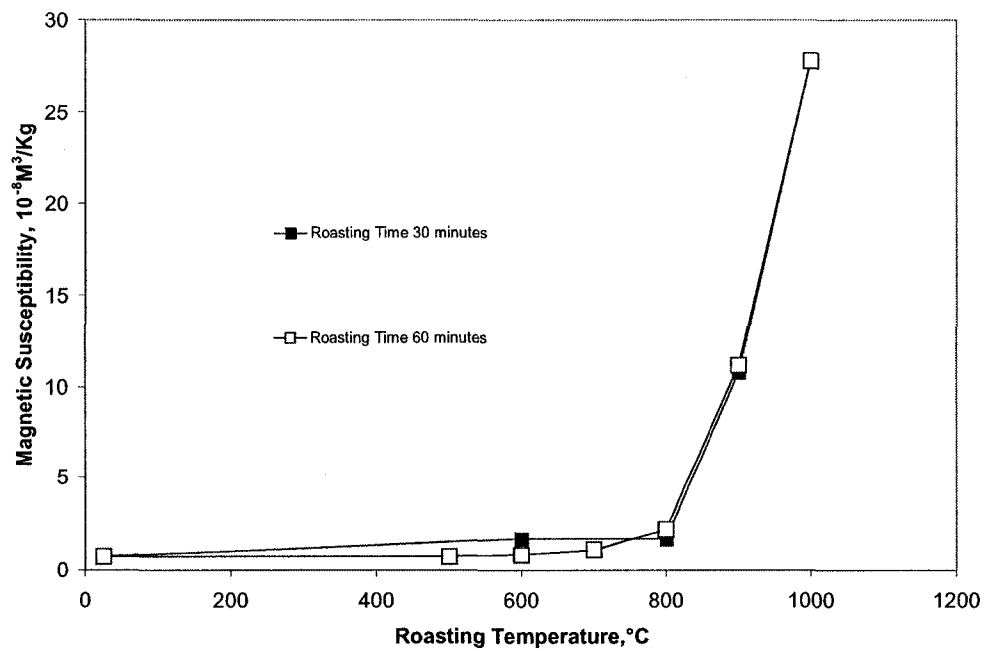


Figure 42 Magnetic susceptibility of roasted SB40 heavy products as a function of roasting temperature

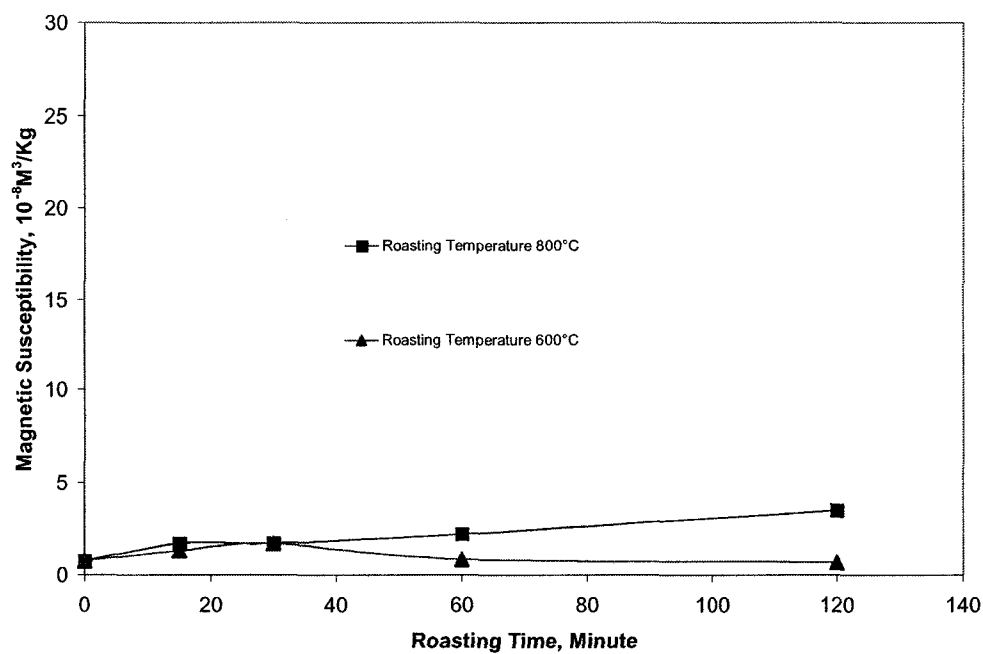


Figure 43 Magnetic susceptibility of roasted SB40 heavy product as a function of roasting time

Table 33 Summary of magnetic separation of roasted SB40 heavy products

Sample treatment	Magnetic Susceptibility *10 ⁻⁸ m ³ /kg	Product	Yield %	SiO ₂ %	Fe ₂ O ₃ %	Fe ₂ O ₃ dist., %	TiO ₂ %	TiO ₂ dist., %
Toluene washed	0.73	Magnetic	7.35	13.17	29.12	29.21	33.60	12.85
		Middling	18.37	26.38	16.07	40.28	29.53	28.22
		Non-mag	74.28	58.74	3.01	30.51	14.08	54.42
		Feed	100.00	49.45	7.33	100.00	19.22	100.00
Roasted 500°C 60'	0.73	Magnetic	17.39	30.33	20.68	57.61	25.08	23.79
		Middling	20.14	36.72	11.06	35.68	27.02	29.69
		Non-mag	62.47	67.09	0.67	6.71	15.07	51.36
		Feed	100.00	54.58	6.24	100.00	18.33	100.00
Roasted 600°C 30'	1.7	Magnetic	18.41	34.57	20.60	54.92	22.66	20.71
		Middling	19.26	37.01	11.05	30.82	27.27	26.08
		Non-mag	62.33	69.21	1.58	14.26	17.19	53.20
		Feed	100.00	56.63	6.91	100.00	20.14	100.00
Roasted 800°C 30'	1.7	Magnetic	22.70	41.94	18.78	57.60	15.41	19.60
		Middling	20.98	41.63	11.25	31.89	24.74	29.08
		Non-mag	56.32	64.36	1.38	10.50	16.27	51.33
		Feed	100.00	54.50	7.40	100.00	17.85	100.00
Roasted 800°C 120'	3.5	Magnetic	30.75	44.32	18.38	68.49	13.59	25.65
		Middling	14.00	37.35	12.93	21.94	26.22	22.53
		Non-mag	55.25	66.66	1.43	9.57	15.27	51.79
		Feed	100.00	56.69	8.25	100.00	16.29	100.00
Roasted 900°C 30'	10.8	Magnetic	34.66	47.23	14.09	66.45	16.95	32.97
		Middling	22.56	48.18	8.92	27.38	24.11	30.52
		Non-mag	42.78	68.62	1.06	6.17	15.20	36.49
		Feed	100.00	56.59	7.35	100.00	17.82	100.00



Figure 45 Stereomicroscopic image of roasted (800°C 30 minutes) SB40 heavy product under transmitted light (Magnification = 60)



Figure 46 Stereomicroscopic image of roasted (900°C 30') SB40 heavy product under transmitted light (Magnification = 60)

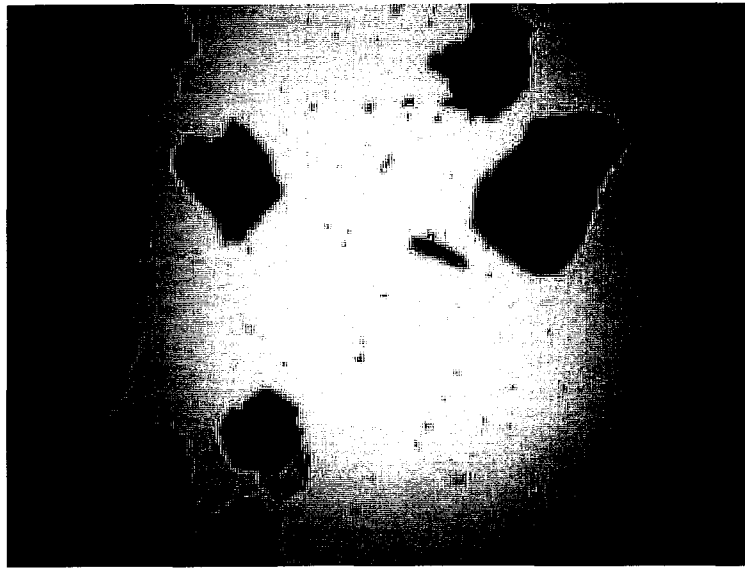


Figure 47 Stereomicroscopic image of roasted (600°C 30') SB40 heavy product under transmitted light (Magnification = 60)



Figure 48 Stereomicroscopic image of roasted (500°C 30') SB40 heavy product under transmitted light (Magnification = 60)



Figure 49 Stereomicroscopic image of roasted (1000°C 30') SB40 heavy product under transmitted light (Magnification = 60)

6.3 Low Temperature Roasting and Its Effect on Pyrite Flotation

6.3.1 Low Temperature Roasting

The SB40 heavy product was roasted at up to 500°C for up to 300 minutes and the sulfur content in roasted samples was assayed. The results were summarized in Table 34. As can be seen, since the sulfur content after roasting at 400°C for 120 minutes was almost the same as that of toluene-washed sample, a temperature of 400°C seemed to be the highest temperature at which the pyrite was not oxidized. Above 450°C the pyrite was obviously oxidized because the sulfur content was reduced to 0.35%.

Table 34 Sample sulfur assays under different roasting conditions

Roasting conditions	Sample sulfur assay, %
Toluene washed	1.46
350 °C, 300 minutes	1.74
400 °C, 120 minutes	1.40
450 °C, 120 minutes	0.35
500 °C, 120 minutes	0.32

The rate of removal of volatile matter, presumably residual bitumen, in the SB40 heavy product was measured at roasting temperature of 350°C and 400°C. The weight loss of the roasted samples against roasting time was plotted in Figure 50. As can be seen, it took about 48 hours to remove all the volatile matter at 350°C while it took about 4 hours at 400°C.

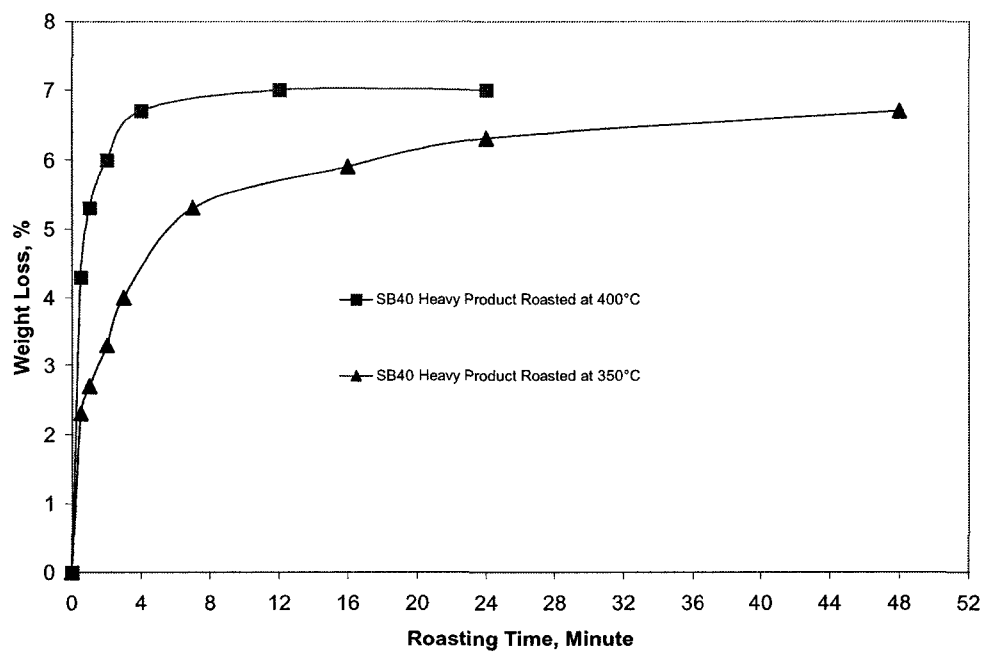


Figure 50 Weight losses of roasted SB40 heavy products as a function of roasting time

6.3.2 *The Effect of Roasting on Pyrite Flotation*

Figure 51 shows that there was a significant difference in the flotation behavior of fresh and aged pyrite. The natural pulp pH for fresh pyrite was 7.4, but it was 3.7 for aged pyrite. At the lower xanthate dosage (~250 g/t), the recovery of fresh pyrite was about 90%, but it was only 40% for aged pyrite. With an increase in xanthate dosage the difference in the recoveries between the fresh and aged pyrite became smaller.

Figure 52 shows the recovery of fresh pyrite after being roasted under different temperatures. As can be seen, as the temperature increased from 25°C to 450°C, the natural pulp pH of the pyrite slurry dropped from 7.4 to 2.8, and the recovery followed the same trend, dropping from 90% to near zero. The possible reason was that with the increase of roasting temperature the Fe^{3+} content resulting from the surface oxidation of pyrite also increase. When the sample was introduced to water, the hydrolysis of the Fe^{3+} made the pulp pH drop. At 450°C, most of the pyrite was oxidized as hematite and totally lost its floatability by xanthate.

Figure 53 and Figure 54 show the recovery of Aged Pyrite after being roasted under different temperatures and then exposed to air for different time periods. As can be seen, extending the exposure time after roasting lowered flotation recovery. However, it is interesting to note that when the roasting temperature was below 350°C and the roasted sample was exposed in air for less than 30 minutes, the recovery of the roasted Aged Pyrite was higher than that of un-roasted Aged Pyrite.

To improve the recovery of the Aged Pyrite, $\text{Na}_2\text{S} \cdot 9\text{H}_2\text{O}$ was used in the flotation. As can be seen from Figure 55, the addition of $\text{Na}_2\text{S} \cdot 9\text{H}_2\text{O}$ did not restore the flotation of the Aged Pyrite but depressed its flotation at low $\text{Na}_2\text{S} \cdot 9\text{H}_2\text{O}$ dosage.

Figure 56 shows the effect of cornstarch on the flotation of pyrite. As can be seen, the addition of cornstarch reduced the froth yield of both fresh and aged pyrite.

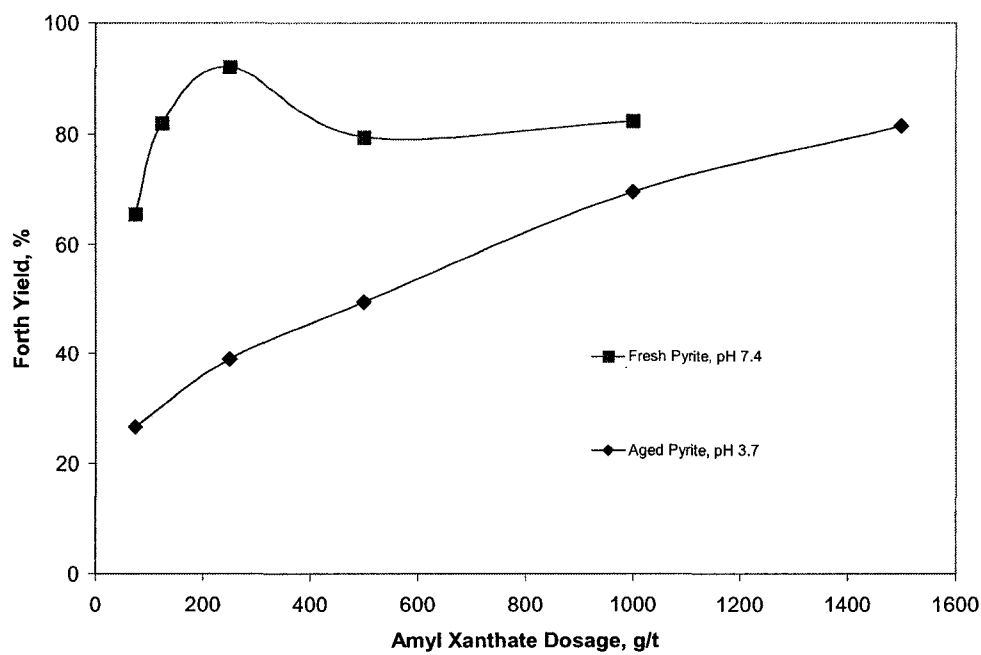


Figure 51 The yield of froth in the single mineral flotation of fresh pyrite and aged pyrite as a function of xanthate dosage

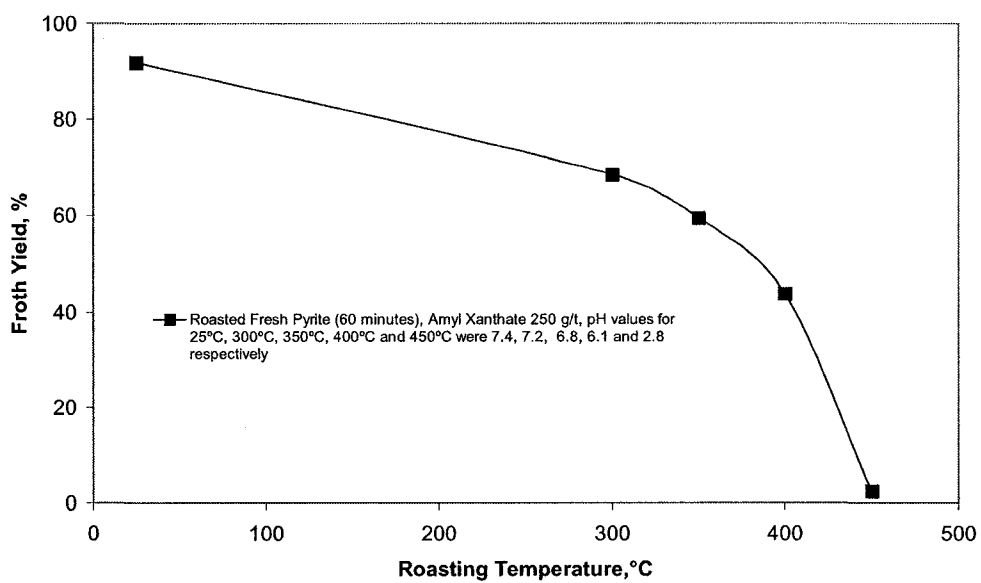


Figure 52 The yield of froth in the single mineral flotation of roasted fresh pyrite as a function of roasting temperature

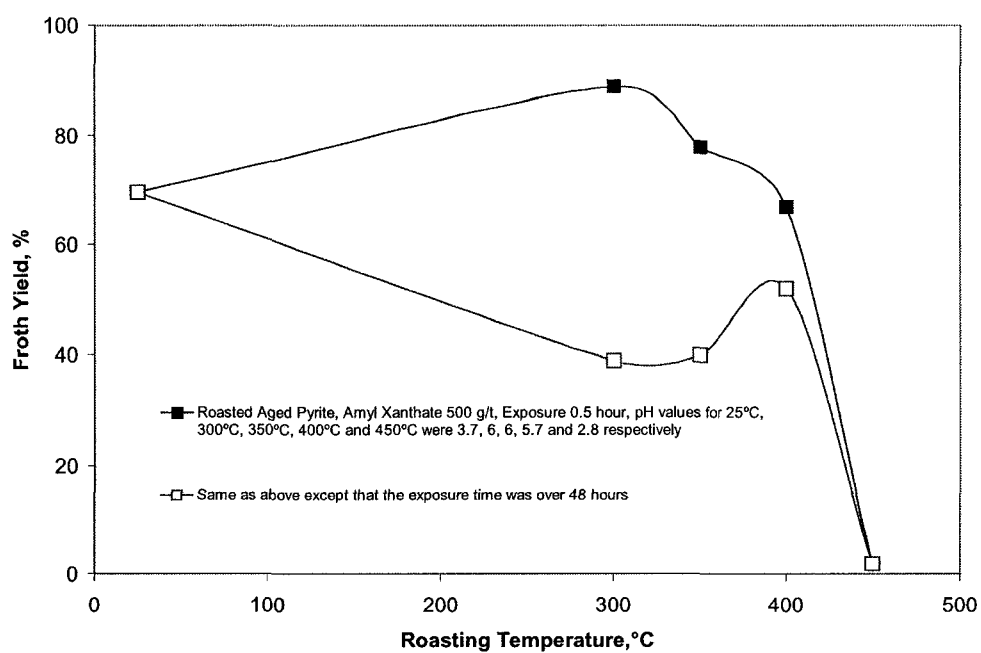


Figure 53 The yield of froth in the single mineral flotation of roasted aged pyrite as a function of roasting temperature

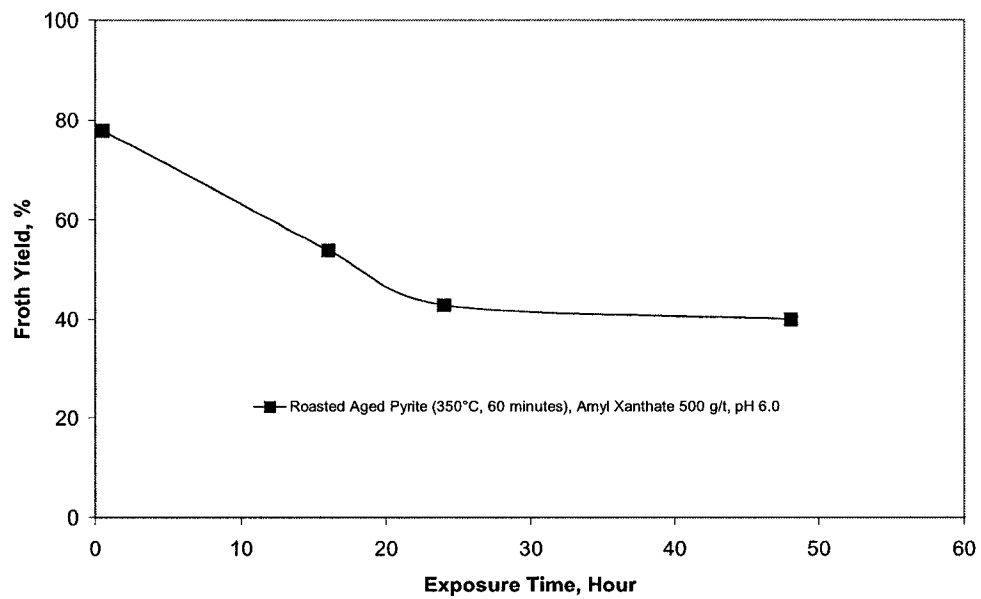


Figure 54 The yield of froth in the single mineral flotation of roasted aged pyrite as a function of exposure time

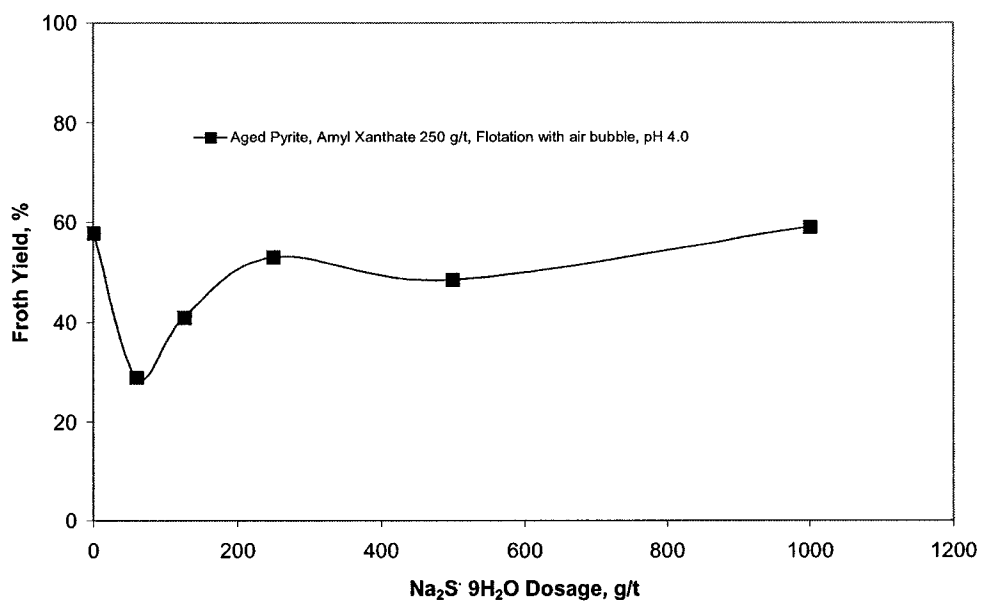


Figure 55 The yield of froth of aged pyrite as a function of Na₂S dosage

(Note: air was used during flotation and flotation time was extended to 14 minutes)

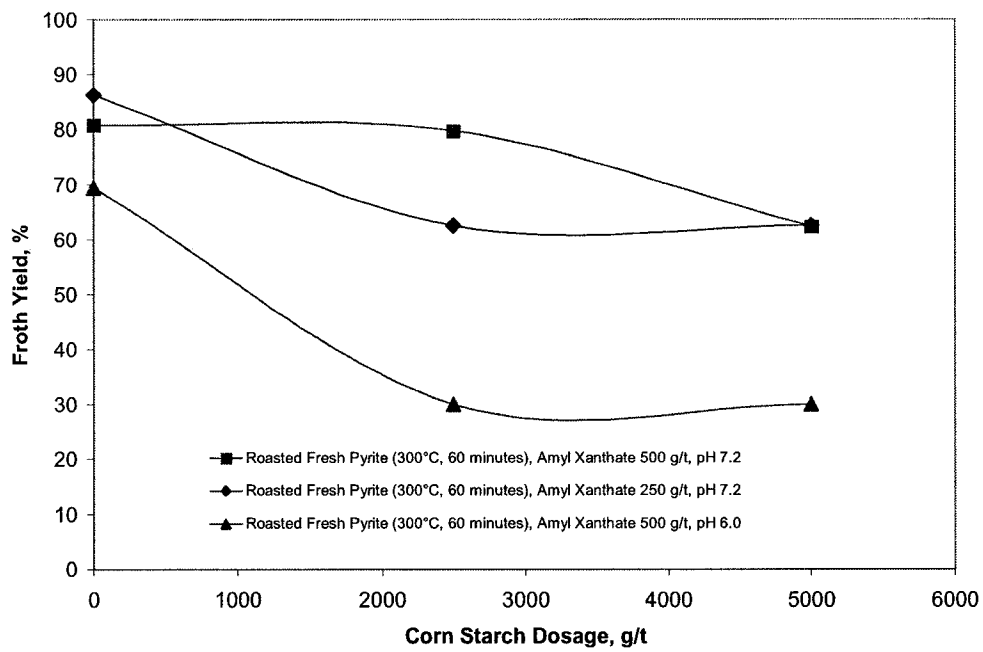


Figure 56 The yield of froth in the single mineral flotation of roasted fresh pyrite as a function of cornstarch dosage

6.4 Gravity Concentration of Roasted Oil Sand Tailings

Table 35 summarizes the gravity separation results for roasted (350°C, 60h) Falcon SB40 heavy product. As can be seen, the TiO₂ content was increased from 16% in the feed to 26.65% in the concentrate, and the Ti loss in the tailings was about 13%; the ZrO₂ content was increased from 4% in the feed to 7.7% in the concentrate, and the Zr loss in the tailings was about 10%. It is interesting to note that the titanium and zirconium contents in the tailing are higher than those in the middling. Most likely the reason was that some of the heavy mineral particle surface was hydrophobic and was floated to the tailing product.

Table 35 Shaking table concentration of roasted (350°C, 60hrs) SB40 heavy product

Product	Yield %	TiO ₂ %	TiO ₂ dist. %	ZrO ₂ %	ZrO ₂ dist. %	SiO ₂ %	SiO ₂ dist. %
Concentrate	41.6	26.65	69.29	7.68	80.76	36.90	27.28
Middling	38.4	7.18	17.23	0.95	9.22	75.76	51.70
Tailing	20.0	10.79	13.48	1.98	10.02	59.13	21.02
Feed	100.0	16.00	100.00	3.96	100.00	56.27	100.00

6.5 Flotation Concentration of Roasted SB40 Heavy Product

Based on the chemical analyses, the SB40 heavy products still contained about 60% SiO₂. Preliminary flotation tests were conducted to remove these light minerals. These tests were performed with a laboratory suspension-cell flotation machine on 10 g batches of samples or with a modified microflotation tube on 4 g batches of samples. The results are presented in Table 36 and Table 37, respectively.

Table 36 Suspension-cell flotation of roasted (600°C for 60') SB40 heavy product

Test #	Conditions				Product	Yield %	TiO ₂ %	ZrO ₂ %	TiO ₂ Dist. %	ZrO ₂ Dist. %
	pH	Collector (g/t)	Depressant (g/t)	MIBC g/t						
HF1	6.7	Sodium oleate (1000)		670	Froth	92.8	16.95	3.85	95.2	96.0
					Tail	7.2	11.19	2.08	4.8	4.0
					Feed	100.0	16.53	3.72	100.0	100.0
HF3	6.7	Sodium oleate (1000)	Sodium metaphosphate (50)	670	Froth	49.0	18.28	4.43	54.9	62.0
					Tail	51.0	14.44	2.60	45.1	38.0
					Feed	100.0	16.32	3.50	100.0	100.0
HF8*	6.7	Sodium oleate (2000)		1340	Froth	45.0	20.10	5.07	52.8	69.1
					Tail	55.0	14.69	1.85	47.2	30.9
					Feed	100.0	17.12	3.30	100.0	100.0
HF9*	6.7	Sodium oleate (2000)	Sodium metaphosphate (100)	1340	Froth	13.0	15.52	4.76	11.3	18.1
					Tail	87.0	18.27	3.22	88.7	81.9
					Feed	100.0	17.91	3.42	100.0	100.0
HF10*	6.7	Sodium oleate (2000)	NaF (100)	1340	Froth	35.4	18.18	3.90	36.8	40.3
					Tail	64.6	17.10	3.18	63.2	59.7
					Feed	100.0	17.48	3.43	100.0	100.0

*: Test samples were deslimed before flotation and the yield of slime fraction was 22.6%.

As can be seen from Table 36, flotation with sodium oleate as collector was ineffective in recovering the heavy minerals while rejecting the quartz gangue at the tested temperature of 20°C. Addition of NaF and sodium metaphosphate reduced quartz flotation but they also severely depressed the flotation of the heavy minerals. Many operating factors may be responsible for the results:

- Particle size effect: it is possible that the particle sizes of the heavy minerals are not within the optimum flotation range, especially given the intensive agitation conditions in the suspension-cell. This factor may be in effect when one compares test HF1 with HF8. After desliming, the flotation recovery of the heavy minerals dropped dramatically, even at higher collector and frother dosages.
- Surface property changes after the roasting: the flotation samples have been roasted at 600°C for 60 minutes. It is possible that the roasting have changed the sample surface properties which adversely affect the separation.

- Pulp temperature: sodium oleate is known to perform better at higher pulp temperatures. In the testwork by Lakefield Research Ltd. a much higher pulp temperature was used, which worked quite well in recovering the heavy minerals. Their flotation tests preceded the bitumen removal so that a high pulp temperature was also beneficial to reduce the viscosity of the bitumen. But the high pulp temperature should have certainly also benefited the action of the sodium oleate.

As can be seen from Table 37, flotation with sodium oleate and NaF could reject about one third of the SiO₂ with a TiO₂ recovery of up to 92% and ZrO₂ recovery of up to 98%, but the concentrate contained about 5% ZrO₂ and 20% TiO₂.

Compared with shaking table concentration, flotation concentration is less effective than gravity concentration in the upgrading of bitumen-removed SB40 heavy product.

Table 37 Microflotation tube flotation of roasted (600°C for 60') SB40 heavy product

Test #	Conditions		Product	Yield %	TiO ₂ %	TiO ₂ dist. %	ZrO ₂ %	ZrO ₂ dist. %	SiO ₂ %	SiO ₂ dist. %	
	pH	Collector (g/t)									Modifier (g/t)
HF 15	7.1	Sodium oleate (5000)	NaF (125)	Froth	61.3	20.2	82.0	6.05	92.6	49.12	52.3
				Tail	38.7	6.98	18.0	0.77	7.4	71.01	47.7
				Feed	100.0	15.08	100.0	4.01	100.0	57.59	100.0
HF 30	7.3	Sodium oleate (5000)	NaF (250)	Froth	74.3	19.3	92.0	4.37	98.1	51.61	66.5
				Tail	25.7	4.85	8.0	0.24	1.9	75.19	33.5
				Feed	100.0	15.59	100.0	3.31	100.0	57.67	100.0
HF 31	7.4	Sodium oleate (5000)	NaF (500)	Froth	71.5	18.82	89.1	4.28	96.2	52.11	65.4
				Tail	28.5	5.75	10.9	0.42	3.8	69.02	34.6
				Feed	100.0	15.10	100.0	3.18	100.0	56.93	100.0
HF 19*	7.1	Sodium oleate (2500)	NaF (125)	Froth	75.9	20.13	89.9	6.66	98.6	50.34	68.5
				Tail	24.1	7.16	10.1	0.29	1.4	72.93	31.5
				Feed	100.0	17.00	100.0	5.12	100.0	55.78	100.0
HF 33*	7.4	Sodium oleate (2500)	NaF (500)	Froth	81.4	17.84	89.5	4.62	99.1	56.01	78.5
				Tail	18.6	9.2	10.5	0.19	0.9	67.02	21.5
				Feed	100.0	16.23	100.0	3.80	100.0	58.06	100.0

* Test samples were de-slimed before flotation and the yield of slime fraction was 22.6%.

6.6 Flotation Separation of Ti Minerals from Zircon

6.6.1 Single Mineral Flotation

In these flotation tests, which was conducted in a 30 ml suspension flotation cell, dodecylamine was used as a collector and cornstarch as a rutile depressant. As can be seen from Figure 57, at around neutral pH and a dodecylamine dosage of 500 g/t, a separation window exists when the cornstarch dosage was above 3750 g/t. Figure 58 shows that at a dodecylamine dosage of 500 g/t and a cornstarch dosage of 5,000 g/t, there was a separation window between rutile and zircon in the pH range of 5.5 to 10.5.

Using these conditions, a flotation separation test was performed on a 1:1 LR Rutile/LR Zircon mixture, and the results are shown in Table 38. As can be seen, at pH 6.2, and a dodecylamine dosage of 500g/t and a corn starch dosage of 5,000 g/t, the flotation froth recovered 85% of the zircon but only 16% TiO₂ in one single stage of flotation, which showed that flotation separation between rutile and zircon was possible.

Table 38 Flotation balance for 1:1 mixture of LR Rutile and LR Zircon (pH 6.2, dodecylamine 500 g/t, cornstarch 5,000 g/t)

Component	Yield	TiO ₂	ZrO ₂	TiO ₂ Distribution	ZrO ₂ Distribution
	%	%	%	%	%
Froth	49.0	12.5	55.0	16.0	85.0
Tail	51.0	63.1	9.3	84.0	15.0
Feed	100.0	38.3	31.7	100.0	100.0

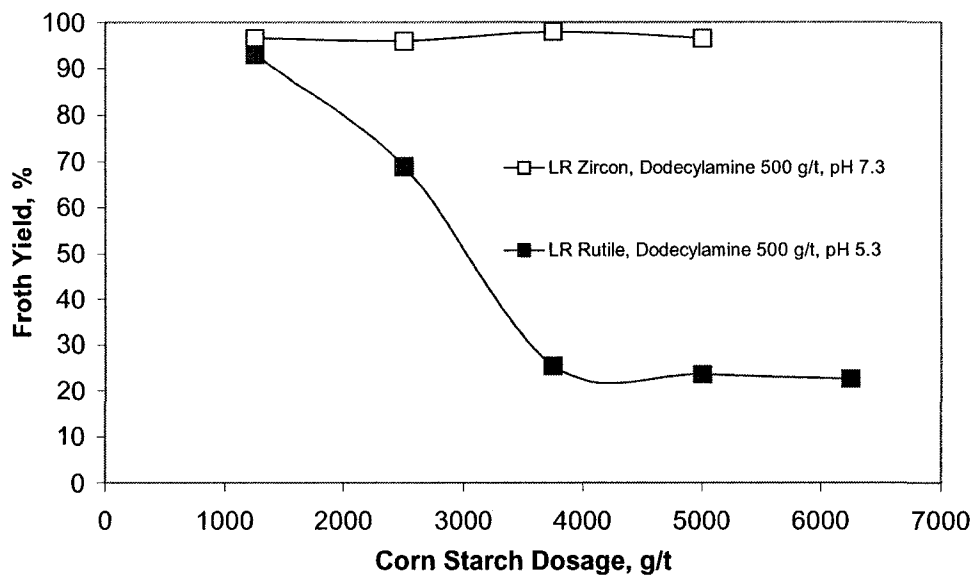


Figure 57 Yield of froth in the single mineral flotation of LR Rutile and LR Zircon as a function of cornstarch dosage

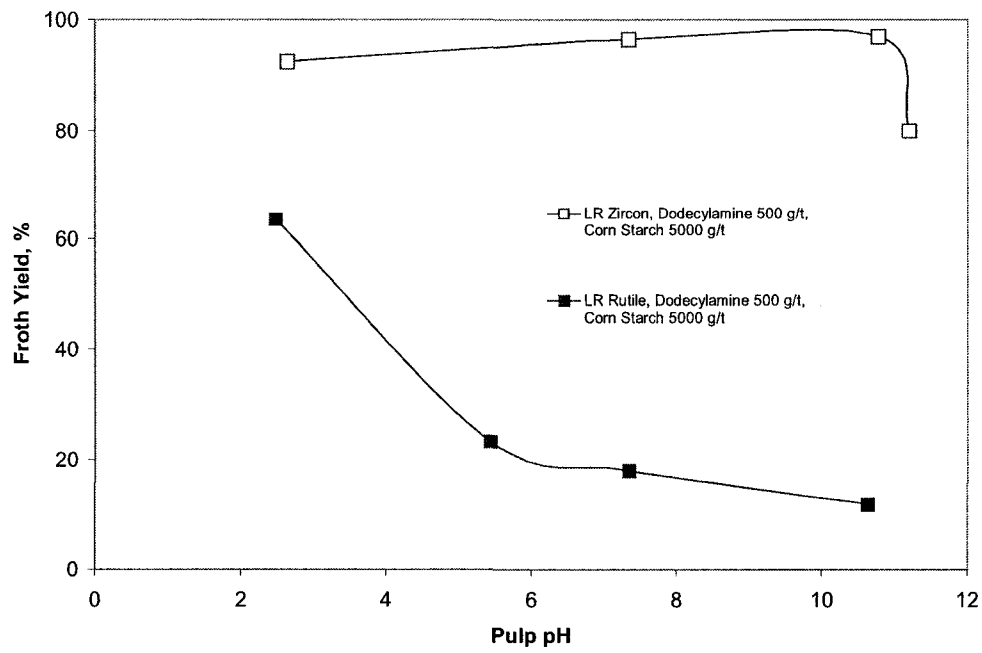


Figure 58 Yield of froth in the single mineral flotation tests of LR Rutile and LR Zircon as a function of pH

6.6.2 Roasted SB40 Heavy Product

Table 39 shows suspension-cell flotation of roasted (600°C for 60h) SB40 heavy product. Tests HF6 and HF7 showed that there was potential to separate the titanium minerals from the zirconium minerals but the flotation conditions need to be optimized.

Table 39 Suspension-cell flotation of roasted (600°C for 60) SB40 heavy product

Test #	Conditions				Product	Yield %	TiO ₂ %	ZrO ₂ %	TiO ₂ Dist. %	ZrO ₂ Dist. %
	pH	Collector (g/t)	Depressant (g/t)	MIBC g/t						
HF6	5.3	Dodecylamine (500)	NaF (100) Cornstarch (1000)		Froth	47.5	11.85	5.89	34.6	73.6
					Tail	52.5	20.31	1.90	65.4	26.4
					Feed	100.0	16.29	3.80	100.0	100.0
HF7	5.3	Dodecylamine (250) Diphenylamine (250)	NaF (100) Cornstarch (1000)	670	Froth	27.8	11.49	4.11	19.6	33.7
					Tail	72.2	18.14	3.11	80.4	66.3
					Feed	100.0	16.29	3.39	100.0	100.0

Table 40 shows microflotation tube flotation of roasted SB40 heavy product. Tests HF22, HF24 and HF35 showed that the flotation conditions for Ti-Zr separation was ineffective: TiO₂ and ZrO₂ were either floated or depressed together and there was no separation.

Table 40 Microflotation tube flotation of roasted SB40 heavy product

Test #	Conditions			Product	Yield %	TiO ₂ %	TiO ₂ dist. %	ZrO ₂ %	ZrO ₂ dist. %
	pH	Collector (g/t)	Modifier (g/t)						
HF35*	9.2	Dodecylamine (250)	Cornstarch (2500)	Froth	45.8	8.05	25.5	0.71	11.9
				Tail	54.2	19.89	74.5	4.45	88.1
				Feed	100.0	14.47	100.0	2.74	100.0
HF22	5.8	Dodecylamine (250)	Cornstarch (2500)	Froth	64.2	11.64	50.8	2.91	49.3
				Tail	35.8	20.21	49.2	5.36	50.7
				Feed	100.0	14.71	100.0	3.79	100.0
HF24	9.0	Dodecylamine (250)	Cornstarch (2500)	Froth	51.6	8.91	32.2	1.79	32.5
				Tail	48.4	20.01	67.8	3.96	67.5
				Feed	100.0	14.28	100.0	2.84	100.0

* Test samples for HF35 were de-slimed before flotation and the yield of slime fraction was 22.6%.

6.7 Summary

1. Oxidation roasting could increase the magnetic susceptibility of ilmenite within the temperature range of 500 - 1000°C. Below 500°C, the magnetic susceptibility was not affected by the roasting, whereas above 1000°C, roasting caused a sharp reduction in its magnetic susceptibility.
2. Within the temperature range of 500 - 1000°C, the magnetic susceptibility of ilmenite usually increased with the progress of oxidation roasting, reaching a maximum, which was followed by a sharp drop in the magnetic susceptibility. The time period to reach the maximum depended on the temperature, and was shorter at higher temperatures.
3. X-ray diffraction analyses showed that hematite ($\alpha\text{-Fe}_2\text{O}_3$) was the new phase formed during the oxidation roasting of ilmenite. The highest susceptibility was obtained when the peak intensity ratio between hematite and ilmenite was between 1.5 and 3.5.
4. Reduction roasting of the ilmenite with charcoal as a reducing agent at 800°C increased its magnetic susceptibility significantly, and the magnitude of the increase was higher than oxidation roasting. X-ray diffraction analyses show that some of ilmenite phases have been changed into strongly magnetic maghemite ($\gamma\text{-Fe}_2\text{O}_3$).
5. Oxidation roasting did not change the magnetic susceptibility of hematite, and reduction roasting significantly increased its magnetic susceptibility. The extent of the increase depended on the temperature, roasting time and charcoal dosages. At 800°C or 1000°C, the magnetic susceptibility of reduction roasted sample reached that of magnetite. X-ray diffraction analyses show that some of the hematite was transformed into maghemite.
6. The reduction roasting of the LR Rutile resulted in an increase in its magnetic susceptibility. It was found that the increase was mainly due to leucosene, a dominant component in LR Rutile.
7. Upgrading of the LR Rutile was possible by using magnetic separation. With a low intensity magnetic separator (field intensity below 0.67 Tesla), a reduction roasting of the sample improved the separation. However, when a high intensity magnetic separator was used, the separation could be achieved without the need for a reduction

- roasting. The separation seemed only depended on the magnetic field intensity or the magnetic susceptibility, and liberation was not a limiting factor.
8. Low temperature roasting of Falcon heavy product showed that 400°C was the highest allowable temperature above which pyrite in the oil sands tailings would be oxidized. It needs about 48 hours to remove all the bitumen at 350°C while it needs about 4 hours to remove almost all the bitumen at 400°C.
 9. Single mineral flotation of pyrite also showed that below 400°C the roasted pyrite floated relatively well, but above 450°C it did not float at all.
 10. Roasting the SB40 heavy product to remove the residual bitumen for 60 minutes at over 600°C resulted in an increase in its magnetic susceptibility. It is likely that the residual bitumen has acted as a reducing agent that converted some of the ferric iron in the leucoxene into ferrous iron. Alternatively, the oxidation of pyrite at this temperature may convert it to hematite which has a higher magnetic susceptibility.
 11. Roasting time had little effect on the magnetic susceptibility of the Falcon heavy product, but roasting temperature had a significant effect on the magnetic susceptibility. However, at temperatures above 800°C, incipient fusion of quartz with Fe-bearing minerals occur which would affect subsequent separation.
 12. Magnetic separation of roasted Falcon heavy product showed that the removal of bitumen by roasting should be conducted at relatively low (about 500°C) temperature in order to produce a high TiO₂ content product.
 13. Compared with shaking table concentration, flotation concentration is less effective than gravity concentration in the upgrading of bitumen-removed SB40 heavy product.
 14. There is a potential to separate titanium minerals from zircon by flotation separation in the pH range of 5 ~10 with dodecylamine as a collector, and cornstarch as a modifier.

7 BITUMEN REMOVAL BY SOLVENT WASHING

Although burning the residual bitumen off from the oil sands tailings was a popular choice among the majority of researchers who worked on the oil sands tailings, it was not a right choice, especially after Canada rectified the Kyoto Protocol, which limits the discharge of green house gases and other toxic gases. Therefore, other bitumen removal methods were tested. In this Chapter, the solvent washing technique is discussed, and in the next Chapter, a process using mechanical attrition is described.

7.1 Solvent Washing

Naphtha washing was conducted by mixing 100 g Falcon SB40 heavy product with 300 ml naphtha, stirring for 30 minutes, then decanting the naphtha. The solids were washed with naphtha for three times. The washed solids were filtered and dried in a fume hood. The residual bitumen of the washed solids was determined by washing 10 g sample with 100ml toluene. The residual bitumen content was found to be 0.8% after naphtha washing.

7.2 Gravity Concentration

Table 41 summarizes the heavy liquid separation of toluene-washed SB40 heavy product. As can be seen, at a heavy liquid density of 3.3, 93.6% of zircon and 79.5% of the titanium minerals were recovered in the “Sink” product. The results indicated that the degree of liberation for titanium minerals was low. This was consistent with the image analysis result by Owen (1996). His finding was that rutile was 75.3% liberated, leucoxene was 89% liberated, and zircon was 95.5% liberated.

Also, as shown in Figure 59, some of the titanium minerals were closely associated with quartz, reducing the titanium mineral liberation. This would definitely reduce the purity of ultimate titanium concentrate from physical processing methods such as magnetic, electrostatic and flotation etc.

Table 41 Heavy liquid (SG 3.3) separation of toluene-washed SB40 heavy product

Product	Yield %	ZrO ₂ %	ZrO ₂ dist. %	TiO ₂ %	TiO ₂ dist. %	SiO ₂ %	SiO ₂ dist. %	Fe ₂ O ₃ %	Fe ₂ O ₃ dist. %
Sink	31.06	11.12	93.64	34.89	79.51	14.29	7.75	16.85	72.50
Float	68.94	0.34	6.36	4.05	20.09	76.61	92.25	2.88	27.50
Feed	100.00	3.69	100.00	13.63	100.00	57.25	100.00	7.22	100.00

Table 42 summarizes the gravity separation results for toluene-washed SB40 heavy product using a shaking table. As can be seen, the TiO₂ content was increased from 14.45% in the feed to 28.41% in the concentrate, and the Ti loss in the tail was about 11%; the ZrO₂ content was increased from 4.13% in the feed to 9.4% in the concentrate, and the Zr loss in the tail was about 2%. Compared with Table 35, the separation result for toluene washed SB40 heavy product was better than that of roasted SB40 heavy product. The reason for this might be that the gravity separation of roasted SB40 heavy product was not optimized. Anyway, the gravity concentration of bitumen-removed SB40 heavy product was effective.

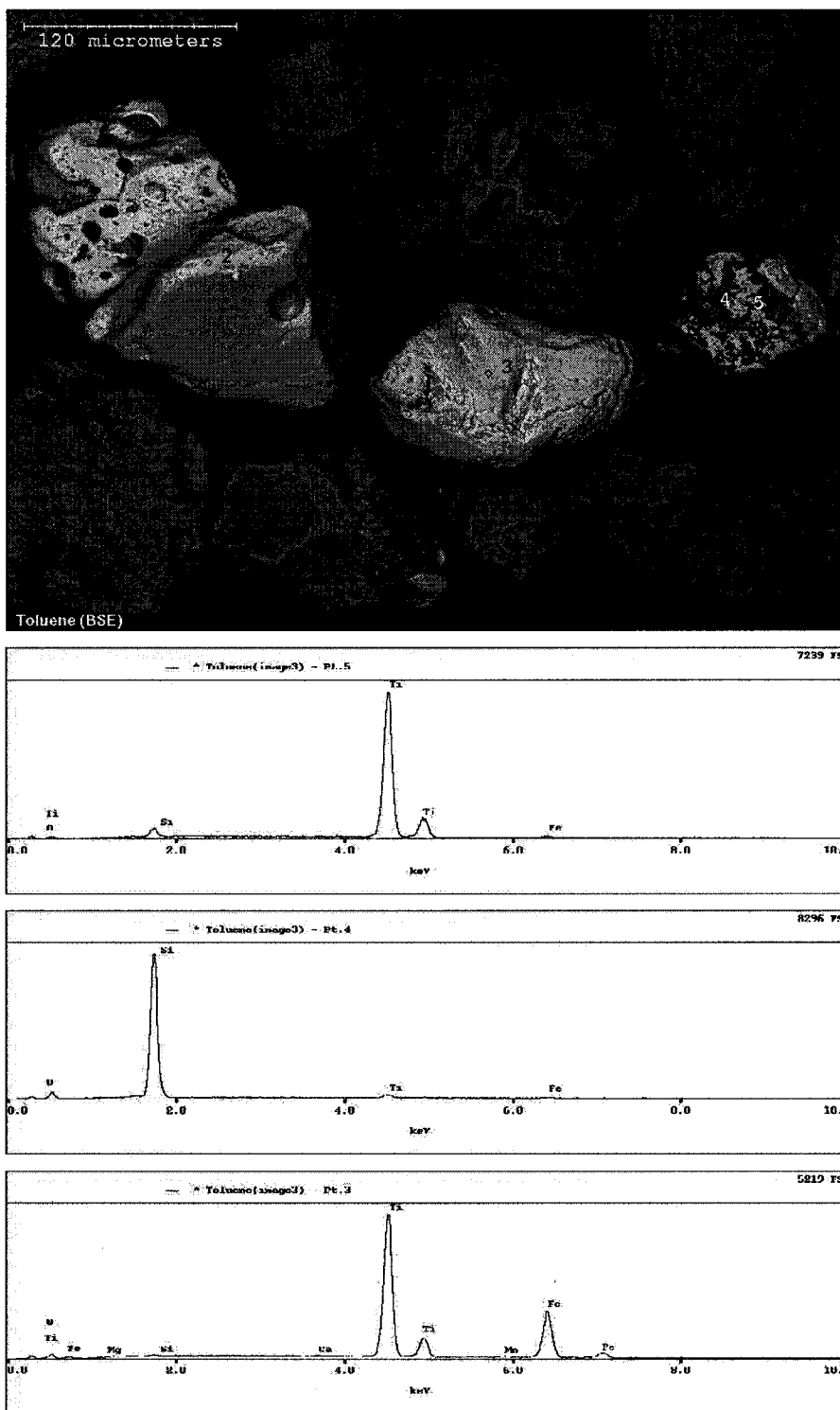


Figure 59 SEM/EDX analysis of bitumen-removed SB40 heavy product

Table 42 Shaking table concentration of toluene-washed SB40 heavy product

Product	Yield %	ZrO ₂ %	ZrO ₂ dist. %	TiO ₂ %	TiO ₂ dist. %	SiO ₂ %	SiO ₂ dist. %
ST4 Con.	42.2	9.40	96.00	28.41	82.86	26.13	18.55
ST4 Mid	8.9	1.16	2.50	9.85	6.06	71.05	10.64
ST4 Tail	48.9	0.12	1.50	3.28	11.08	86.06	70.81
Feed	100.0	4.13	100.00	14.45	100.00	58.83	100.00

Before separation the bitumen-removed SB40 heavy product was scrubbed with sulfuric acid to render the sample hydrophilic.

7.3 Flotation of Pyrite from the Bitumen-removed SB40 Heavy Products

In order to remove the pyrite in the bitumen-removed SB40 heavy product, preliminary flotation tests were carried out. Since the pyrite content in SB40 heavy product was about 4%, the expected float yield for pyrite concentrate would be 5% to 10%. Table 43 and Table 44 summarize the preliminary flotation test results on naphtha-washed Falcon SB40 heavy product. As can be seen in Table 43, without any pre-treatment, the washed sample was readily floatable without a collector between pH 2.9 and 7.5; even after drying at 100°C for 14 hours the flotation yield was still as high as 43.5%. After heating at 300°C to 400°C for 60 minutes, the flotation yield dropped significantly to less than 10% and the addition of amyl xanthate and/or NaHS did not increase the yield. On various conditions the separation of pyrite from heavy minerals was ineffective as shown in Table 44. At first it was suspected that the trace residual organic matter made the naphtha-washed sample hydrophobic; however, toluene-washed sample was also easy to float although it had much lower organic matter content. These results suggest that surface adjustment is required in order to separate the pyrite from Ti and Zr heavy minerals.

Table 43 Flotation froth yield from naphtha-washed SB40 heavy product

Test #	Pre-treatment	Flotation condition			Yield, %
		pH	Amyl xanthate, g/t	Modifier, g/t	
SF14	-	11.3	-	-	6.0
SF5	-	7.5	-	-	48.3
SF15	-	6.6	-	-	23.8
SF16	-	2.9	-	-	22.5
SF11	300°C, 60'	7.3	250	-	6.3
SF12	300°C, 60'	7.2	250	CuSO ₄ · 5H ₂ O (500)	9.5
SF13	300°C, 60'	7.3	250	NaHS · 9H ₂ O (500)	5.5
SF7	100°C, 14 hrs	7.5	-	-	43.5
SF9	300°C, 60'	7.2	-	-	9.0
SF43	350°C, 60'	6.9	-	-	4
SF44	400°C, 60'	6.8	-	-	3.8

Table 44 Pyrite flotation test results on naphtha-washed SB40 heavy product

Test #	Sample	Flotation Condition	Product	Yield %	S %	S dist. %	ZrO ₂ %	ZrO ₂ dist. %	TiO ₂ %	TiO ₂ dist. %
SF1	Washed SB40 HP (300°C, 60')	Amyl xanthate 250 g/t pH 7.6	Froth	8.8	4.20	20.9	5.79	12.6	9.21	4.8
			Tail	91.2	1.54	79.1	4.00	87.4	17.80	95.2
			Feed	100.0	1.77	100.0	4.17	100.0	17.10	100.0
SF2	Washed SB40 HP	Amyl xanthate 250 g/t pH 7.6	Froth	61.0	1.85	81.2	5.76	99.4	25.21	96.1
			Tail	39.0	0.68	18.8	0.05	0.6	1.61	3.9
			Feed	100.0	1.39	100.0	3.53	100.0	16.0	100.0
SF3	Washed SB40 HP	pH 7.6	Froth	77.0	1.73	86.2	5.06	99.6	21.67	98.1
			Tail	23.0	0.93	13.8	0.07	0.4	1.43	1.9
			Feed	100.0	1.55	100.0	3.91	100.0	17.00	100.0

Table 45 shows some of the selected pyrite flotation results of bitumen-removed SB40 heavy product with surface adjustment. As can be seen, without the addition of cornstarch, 89.5% of pyrite reported to froth, but at the same time 52.7% of TiO₂ and 58.6% of ZrO₂ also reported to the froth; with the addition of cornstarch, 76.6% of pyrite

reported to froth, at the same time only 8.6% of TiO₂ and 4.2% of ZrO₂ reported to the froth.

SEM/EDX analyses of samples for pyrite flotation are shown in Figure 60 and Figure 61. It is easy to see that some of the pyrite particles were associated with quartz particles. This may have contributed to the unsatisfactory removal of pyrite from the bitumen-removed SB40 heavy product.

Table 45 Microflotation tube flotation of pyrite from bitumen-removed SB40 heavy product

(Collector: amyl xanthate 250 g/t, dithiophosphate 250 g/t)

Sample	Condition		Product	Yield %	S %	S dist. %	TiO ₂ %	TiO ₂ dist. %	ZrO ₂ %	ZrO ₂ dist. %
	pH	Modifier (g/t)								
SF102	5.0		Froth	32.8	2.63	89.5	23.10	52.7	4.01	58.6
Toluene washed			Tails	67.2	0.15	10.5	10.17	47.3	1.38	41.4
			Feed	100.0	0.96	100.0	14.45	100.0	2.24	100.0
SF103	5.0	Cornstarch (2500)	Froth	8.3	10.47	76.6	19.82	8.6	2.13	4.2
Toluene washed			Tails	91.7	0.29	23.4	19.10	91.4	4.38	95.8
			Feed	100.0	1.13	100.0	19.16	100.0	4.19	100.0

Before separation the bitumen-removed SB40 heavy product was scrubbed with Swab to clean the pyrite surface.

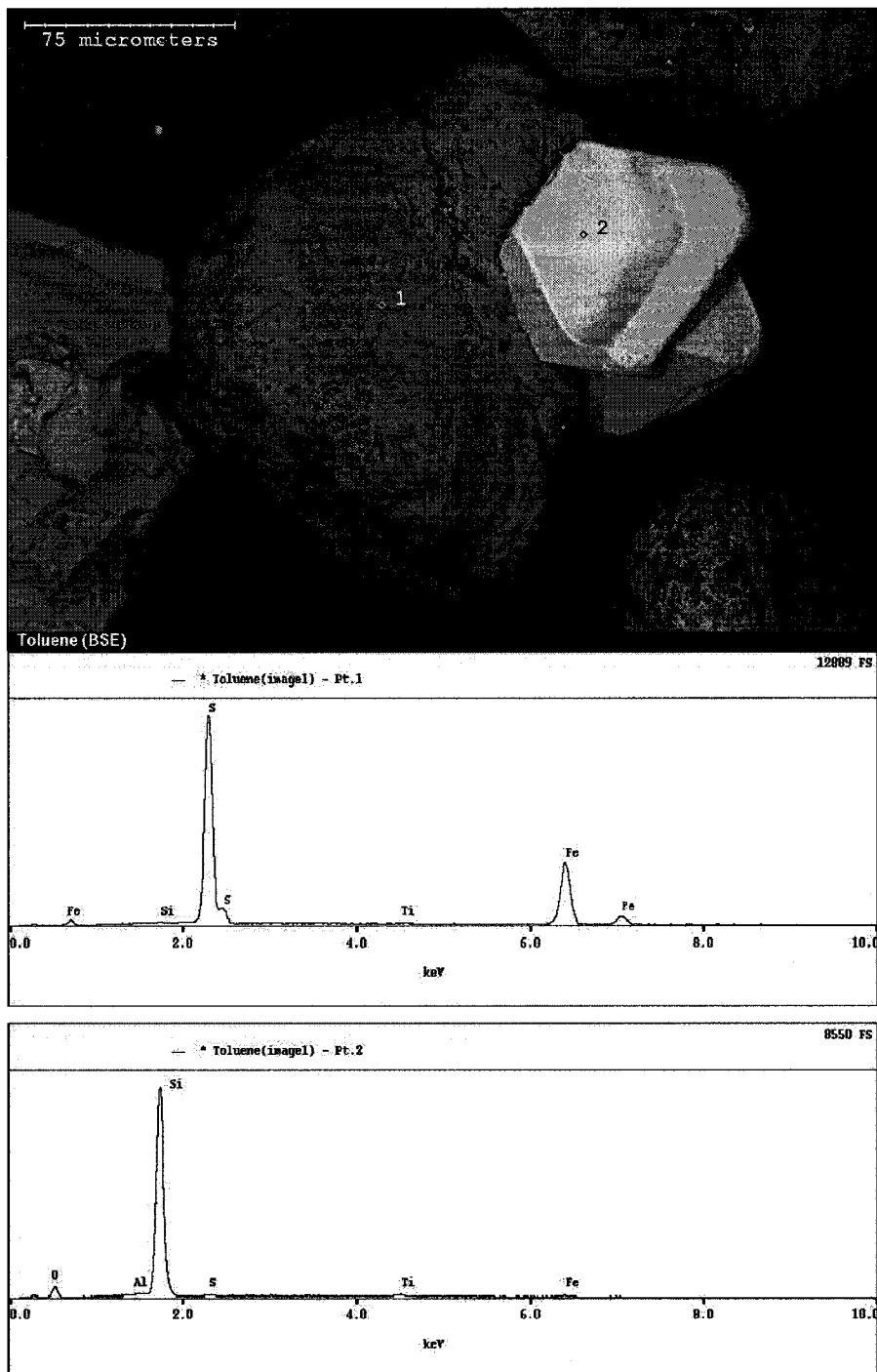


Figure 60 SEM/EDX analysis of bitumen-removed SB40 heavy product

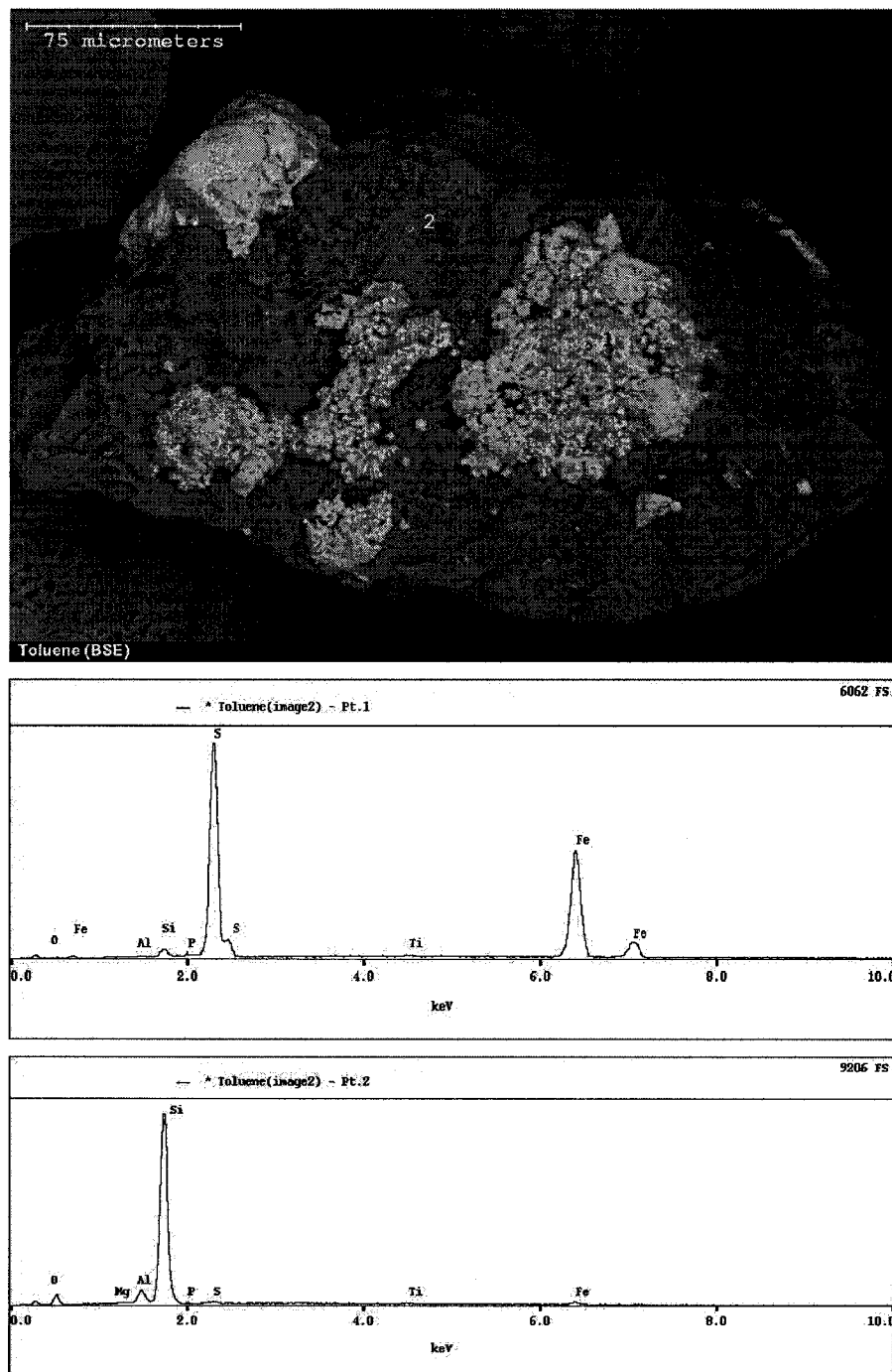


Figure 61 SEM/EDX analysis of bitumen-removed SB40 heavy product

7.4 Magnetic and Electrostatic Separation

Table 46 shows the magnetic and electrostatic separation of heavy liquid concentrate. The test flow sheet is shown in Figure 62. As can be seen, high intensity magnetic separation was effective in separating the non-magnetic zircon and low iron-bearing weak magnetic titanium minerals from high iron-bearing magnetic titanium minerals: 80.4% of the iron reported to the magnetic product together with 3.44% of the zircon and about 60% of the titanium minerals. However, the electrostatic separation was ineffective in the separation of non-magnetic zircon from the low iron-bearing weak-magnetic titanium minerals.

Table 46 Magnetic and electrostatic separation of heavy liquid concentrate

Product	Yield %	ZrO ₂ %	ZrO ₂ dist. %	TiO ₂ %	TiO ₂ dist. %	SiO ₂ %	SiO ₂ dist. %	Fe ₂ O ₃ %	Fe ₂ O ₃ dist. %
Mag cond	13.45	0.38	0.42	43.28	15.81	7.06	6.40	24.98	21.29
Mag mid	34.19	0.86	2.39	42.22	39.20	8.45	19.48	23.61	51.15
Mag N-cond	5.72	1.36	0.63	29.02	4.51	14.50	5.59	21.95	7.96
Mag subtotal	53.36	0.79	3.44	41.15	59.52	8.85	31.47	23.78	80.40
N-mag cond	9.19	22.25	16.61	28.11	7.02	20.01	12.40	12.49	7.27
N-mag mid	30.87	26.62	66.75	33.25	27.88	22.05	45.90	5.63	11.01
N-mag N-cond	6.58	24.72	13.21	31.26	5.59	23.05	10.23	3.17	1.32
N-mag subtotal	46.64	25.49	96.56	31.96	40.48	21.79	68.53	6.63	19.60
Feed	100.00	12.31	100.00	36.82	100.00	14.83	100.00	15.78	100.00

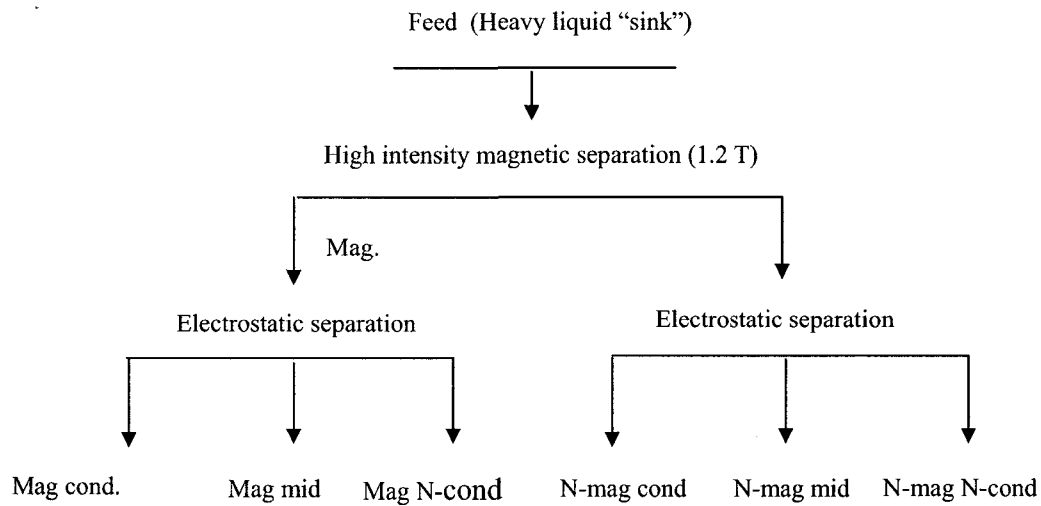


Figure 62 Magnetic and electrostatic separation flowsheet of heavy liquid heavy product

7.5 Summary

1. Three stages of naphtha washing could reduce the bitumen content of SB40 heavy product from 2.6% to 0.8%.
2. Heavy liquid separation results suggested that the liberation of titanium minerals was low.
3. Gravity concentration of bitumen-removed SB40 heavy product using a shaking table was effective: a concentrate containing 9% ZrO_2 and 28% TiO_2 with recoveries of above 90% for both titanium and zirconium minerals was obtained.
4. After bitumen removal by solvent washing, mineral surface adjustment such as sulfuric acid attrition is required in order to separate pyrite from titanium and zirconium minerals.
5. Flotation removal of pyrite from the bitumen-removed SB40 heavy product was possible. However, due to the association of some of the pyrite particles with quartz, the separation efficiency was low.

6. High intensity magnetic separation was effective in separating the non-magnetic zircon and low iron-bearing weak magnetic titanium minerals from high iron-bearing magnetic titanium minerals; however, electrostatic separation was ineffective in the separation of non-magnetic zircon from the low iron-bearing weak-magnetic titanium minerals.

8 BITUMEN REMOVAL BY MECHANICAL ATTRITION

8.1 Mechanical Attrition

A new bitumen removal method by mechanical attrition was tested besides roasting and naphtha washing. The attrition tests were conducted by high intensity agitation (2200 rpm) at high pulp pH, high % solids (50%) and high temperature (80-85°C). The preliminary results are summarized in Table 47. As can be seen, when the NaOH dosage was 10 kg/t, the scrubbed sample contained the same amount of organic matter as that of the naphtha washed sample. With the decrease of NaOH dosage the content of residual organic matter increased significantly. The addition of 10 kg/t Na_2SiO_3 generated the same results as 10 kg/t NaOH. Overall, the preliminary results showed that attrition was a promising method, because it avoided the use of solvent naphtha, and did not produce CO_2 emission as in the case of roasting.

When the Falcon SB40 heavy product was scrubbed with NaOH or Na_2SiO_3 , the scrubbed product was also easy to float. However, when it was scrubbed with HCl, or H_2SO_4 , or Swab nothing was floated without the addition of flotation collectors.

Table 47 Preliminary naphtha washing and attrition results

Reagents for each stage (100 g solids)	Dosage, kg/t	Pulp pH	Toluene dissolved matter content	% removal of bitumen
Naphtha washing 3 times		N/A	0.8%	69.2
NaOH	10	12.6	0.8%	69.2
NaOH	6	12.2	1.8%	28.6
NaOH	2	10.1	2.3%	11.5
Na_2SiO_3	10	12.1	1.0%	61.5

8.1.1 Effect of Attrition Temperature on the Residual Bitumen Content

Figure 63 shows the effect of attrition temperature on the residual bitumen content. As can be seen, with the pulp temperature increasing from 20°C to 80°C, the residual bitumen content dropped almost linearly from 1.4% to about 1%.

8.1.2 Effect of Attrition Time on the Residual Bitumen Content

Figure 64 shows the effect of attrition time on the residual bitumen content. Under the specified conditions, when the attrition time increased from 15 minutes to 30 minutes, the residual bitumen content dropped from 1.6% to about 1%. Further attrition would not lower the residual bitumen content.

8.1.3 Effect of Stirring Intensity on the Residual Bitumen Content

Figure 65 shows the effect of stirring intensity on the residual bitumen content. Under the given attrition conditions, when the stirring intensity increased from 900 rpm to 1500 rpm, the residual bitumen content dropped from 1.6% to 1%. Further increase of stirring intensity had very little effect on the bitumen content.

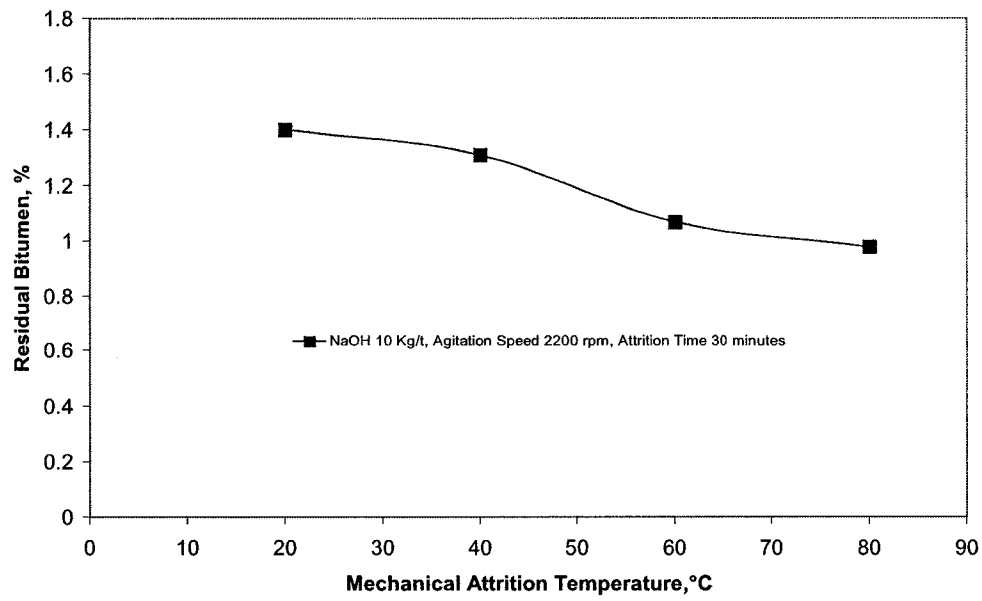


Figure 63 Residual bitumen content as a function of attrition temperature

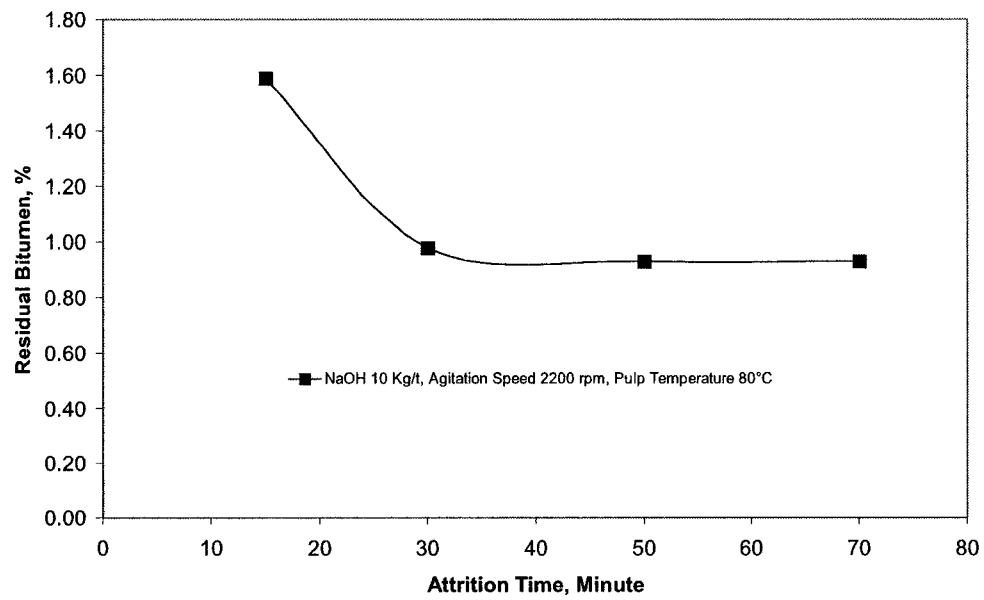


Figure 64 Residual bitumen content as a function of attrition time

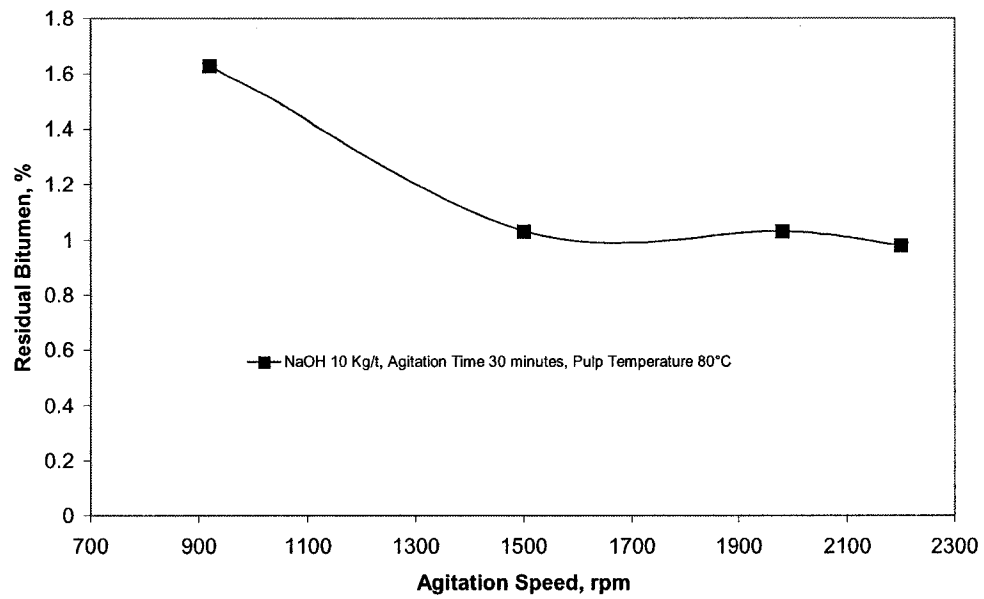


Figure 65 Residual bitumen content as a function of stirring intensity

8.2 Gravity Concentration

Table 48 summarizes the gravity separation results for mechanically scrubbed SB40 heavy product. As can be seen, the TiO_2 content was increased from 14.49% in the feed to 29.26% in the concentrate, and the Ti loss in the tail and M2 was about 6%; the ZrO_2 content was increased from 3.49 % in the feed to 8% in the concentrate, and the Zr loss in the tail and M2 was about 2.5%. Although the sample was scrubbed with sulfuric acid before separation, the titanium and zirconium contents in the tailing are still higher than those in the middling M1 and M2.

Table 48 Shaking table concentration of mechanically scrubbed SB40 heavy product

Product	Yield %	S %	S dist. %	ZrO_2 %	ZrO_2 dist. %	TiO_2 %	TiO_2 dist.%	SiO_2 %	SiO_2 dist. %
ST3-Con	38.45	1.90	74.24	8.00	88.13	29.26	77.63	29.06	18.51
ST3-M1	38.06	0.47	18.18	0.74	8.07	6.25	16.41	78.58	49.55
ST3-M2	20.91	0.19	4.04	0.37	2.22	2.72	3.92	84.62	29.31
ST3-Tail	2.58	1.35	3.54	2.15	1.59	11.38	2.03	61.53	2.63
Feed	100.00	0.98	100.00	3.49	100.00	14.49	100.00	60.36	100.00

Before separation the bitumen-removed SB40 heavy product was scrubbed with sulfuric acid to render the sample hydrophilic.

8.3 Flotation Concentration of Mechanically scrubbed SB40 Heavy Product

Table 49 and Table 50 show some selected flotation test results on bitumen-removed SB40 heavy product by mechanical attrition. The flotation results were unsatisfactory – this might be due to the remaining residual bitumen (at 1 wt%), or due to the non-optimized flotation conditions.

Table 49 Suspension-cell flotation of scrubbed SB40 heavy product (65°C)

Test #	Conditions			Product	Yield %	TiO ₂ %	TiO ₂ dist. %	S %	S dist. %	SiO ₂ %	SiO ₂ dist. %
	pH	Collector (g/t)	Depressant (g/t)								
ASF 3	7.1	Sodium oleate (2500)	NaF (500)	Froth	78.16	17.29	82.84	1.67	84.10	58.33	75.40
				Tail	21.84	12.82	17.16	1.13	15.90	68.10	24.60
				Feed	100.00	16.31	100.00	1.55	100.00	60.46	100.00
ASF 4	7.3	Sodium oleate (1250)	NaF (500)	Froth	56.88	18.38	57.69	1.55	66.94	55.16	53.79
				Tail	43.12	17.78	42.31	1.01	33.06	62.51	46.21
				Feed	100.00	18.12	100.00	1.32	100.00	58.33	100.00

Before separation the bitumen-removed SB40 heavy product was scrubbed with sulfuric acid to render the sample hydrophilic.

Table 50 Microflotation tube flotation of scrubbed SB40 heavy product

Test #	Conditions			Product	Yield %	TiO ₂ %	TiO ₂ dist. %	S %	S dist. %	SiO ₂ %	SiO ₂ dist. %
	pH	Collector (g/t)	Depressant (g/t)								
ABF 2	7.1	Sodium oleate (2500)	NaF (125)	Froth	64.79	15.91	69.12	1.79	87.51	60.66	61.02
				Tail	35.21	13.08	30.88	0.47	12.49	71.29	38.98
				Feed	100.00	14.91	100.00	1.33	100.00	64.40	100.00
ABF 3	7.3	Sodium oleate (5000)	NaF (250)	Froth	65.9	17.26	68.75	1.65	83.72	55.92	61.73
				Tail	34.1	15.16	31.25	0.62	16.28	67.01	38.27
				Feed	100.0	16.54	100.00	1.30	100.00	59.70	100.00
ABF 4	7.4	Sodium oleate (1250)	NaF (250)	Froth	40.0	20.19	47.18	2.28	74.88	46.37	31.06
				Tail	60.0	15.07	52.82	0.51	25.12	68.61	68.94
				Feed	100.0	17.12	100.00	1.22	100.00	59.71	100.00

Before separation the bitumen-removed SB40 heavy product was scrubbed with sulfuric acid to render the sample hydrophilic.

8.4 Flotation of Pyrite from the Bitumen-removed SB40 Heavy Products

Table 51 shows some of the selected pyrite flotation results of bitumen-removed SB40 heavy product with surface adjustment. As can be seen, without the addition of cornstarch, for toluene-washed sample, 89.5% of pyrite reported to froth, but at the same time 52.7% of TiO₂ and 58.6% of ZrO₂ also reported to the froth; With the addition of cornstarch, for toluene-washed sample, 76.6% of pyrite reported to froth, and only 8.6% of TiO₂ and 4.2% of ZrO₂ reported to the froth; for mechanically scrubbed sample, 62.9% of pyrite reported to froth, at the same time 9.4% of TiO₂ and 17.4% of ZrO₂ reported to the froth.

Table 51 Microflotation tube flotation of pyrite from bitumen-removed SB40 heavy product

(Collector: amyl xanthate 250 g/t, dithiophosphate 250 g/t)

Sample	Condition		Product	Yield %	S %	S dist. %	TiO ₂ %	TiO ₂ dist. %	ZrO ₂ %	ZrO ₂ dist. %
	pH	Modifier (g/t)								
SF102 Toluene washed	5.0		Froth	32.8	2.63	89.5	23.10	52.7	4.01	58.6
			Tails	67.2	0.15	10.5	10.17	47.3	1.38	41.4
			Feed	100.0	0.96	100.0	14.45	100.0	2.24	100.0
SF103 Toluene washed	5.0	Cornstarch (2500)	Froth	8.3	10.47	76.6	19.82	8.6	2.13	4.2
			Tails	91.7	0.29	23.4	19.10	91.4	4.38	95.8
			Feed	100.0	1.13	100.0	19.16	100.0	4.19	100.0
SF104 Scrubbed	5.0		Froth	14.3	5.12	77.4	19.02	14.9	8.67	37.0
			Tails	85.7	0.25	22.6	18.09	85.1	2.46	63.0
			Feed	100.0	0.95	100.0	100.00	100.0	3.35	100.0
SF105 Scrubbed	5.0	Cornstarch (2500)	Froth	8.8	6.86	62.9	18.86	9.4	7.39	17.4
			Tails	91.2	0.39	37.1	17.64	90.6	3.38	82.6
			Feed	100.0	0.96	100.0	17.75	100.0	3.73	100.0

Before separation the bitumen-removed SB40 heavy product was scrubbed with Swab to clean the pyrite surface.

8.5 Ti-Zr Separation of Mechanically Scrubbed SB40 Heavy Product

Table 52 shows microflotation tube flotation of scrubbed SB40 heavy product. Although there is about 10% difference between the distribution of zircon and titanium minerals in the froth, the flotation conditions was ineffective or the flotation separation of zircon from titanium minerals is more difficult for mechanically scrubbed SB40 heavy product than for roasted SB40 heavy product.

Table 52 Microflotation tube flotation of scrubbed SB40 heavy product

Test #	Conditions		Product	Yield %	TiO ₂ %	TiO ₂ dist. %	ZrO ₂ %	ZrO ₂ dist. %	
	pH	Collector (g/t)							Modifier (g/t)
ABF5	5.8	Dodecylamine (250)	Cornstarch (2500)	Froth	22.98	12.21	19.32	4.77	30.39
				Tail	77.02	15.21	80.68	3.26	69.61
				Feed	100.0	14.52	100.00	3.61	100.00
ABF6	5.8	Dodecylamine (500)	Cornstarch (2500)	Froth	52.6	11.49	43.70	3.00	52.43
				Tail	47.4	16.43	56.30	3.02	47.57
				Feed	100.0	13.83	100.00	3.01	100.00

Before separation the bitumen-removed SB40 heavy product was scrubbed with sulfuric acid to render the sample hydrophilic.

8.6 Magnetic and Electrostatic Separation

Table 53 shows the magnetic and electrostatic separation of tabled scrubbed SB40 heavy product. Its separation flowsheet is shown in Figure 66. As can be seen, in the first stage of electrostatic separation, about 80% of pyrite and less than 3% of zircon reported to conductor fraction; 5.57% of pyrite and about 37% of iron reported to non-conductor fraction. In the non-magnetic fraction of the conductor product, the S content is 29.50%, and S distribution is 55.53%, and this suggests that it is possible to separate the pyrite from titanium and zirconium minerals by using electrostatic separation plus magnetic separation. In the last stage of electrostatic separation, the TiO₂ contents in the middling and non-conductor were above 30%, i.e., it is very hard to separate zircon from the low iron-bearing weak-magnetic titanium minerals. In the magnetic separation of non-conductor, the magnetic fraction (ES1-4) contained above 20% of both TiO₂ and SiO₂, the possible reason is that some of the titanium minerals are associated with quartz as shown by the SEM /EDX images (Figure 59).

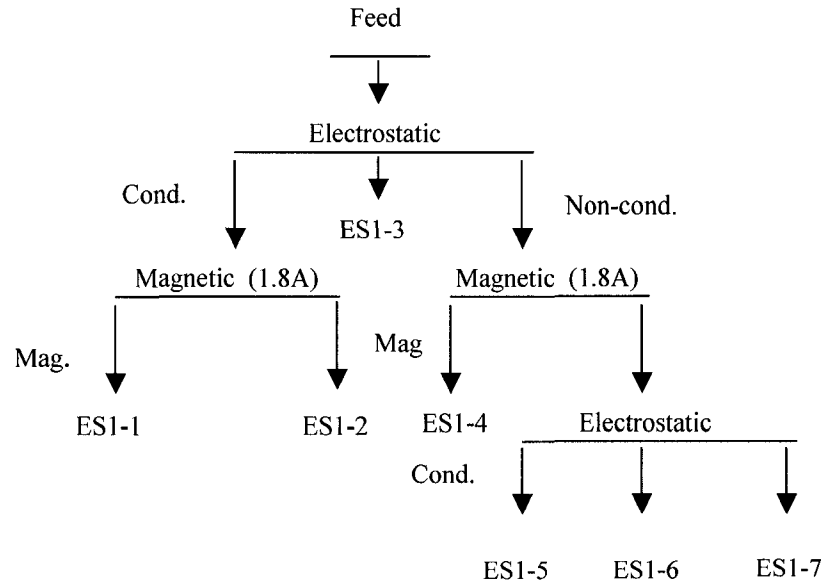


Figure 66 Magnetic and electrostatic separation flowsheet of tabled scrubbed SB40 heavy product

Table 53 Magnetic and electrostatic separation of tabled scrubbed SB40 heavy product

Product	Yield %	S %	S dist. %	ZrO ₂ %	ZrO ₂ dist. %	TiO ₂ %	TiO ₂ dist. %	SiO ₂ %	SiO ₂ dist. %	Fe ₂ O ₃ %	Fe ₂ O ₃ dist. %
ES1-1	12.48	3.78	24.26	1.23	2.03	51.89	20.26	3.63	1.63	29.43	28.63
ES1-2	3.66	29.50	55.53	1.57	0.76	18.18	2.08	23.38	3.08	35.74	10.20
ES1-3	32.21	0.41	6.79	8.46	36.12	37.63	37.92	28.09	32.56	9.69	24.33
ES1-4	29.89	0.51	7.84	5.03	19.93	22.28	20.84	24.24	26.07	14.95	34.83
ES1-5	5.92	0.46	1.40	2.12	1.66	9.69	1.79	78.44	16.71	0.87	0.40
ES1-6	10.90	0.45	2.52	18.55	26.80	33.66	11.48	37.03	14.52	1.09	0.93
ES1-7	4.94	0.65	1.65	19.40	12.70	36.37	5.62	30.56	5.43	1.76	0.68
Feed	100.00	1.94	100.00	7.55	100.00	31.96	100.00	27.79	100.00	12.83	100.00

8.7 Mineral Electric Conductivity Measurement

It is known that the following principal factors affect electrostatic separation: the contact resistance between particles and the (grounded) deposition electrode, the particle resistance, the conductivity of the treated-material components, the surface roughness of particles, their temperature, humidity and hygroscopicity, the condition of the air, the particle shape, the electric field potential, the extent of the field nonuniformity, mechanical forces, etc. (Moskva, 1957).

The particle conductivity is decisive for their discharge at the deposition electrode, i.e., for their actual separation.

Mineral electric resistance was measured to investigate the effect of particle conductivity on the separation of heavy minerals.

Table 54 shows the electric resistance of different minerals contained in oil sand tailings. As can be seen, of all the measured minerals, LR Zircon has the highest resistance, i.e. the lowest conductivity. Among the titanium minerals, high purity rutile of 93% TiO_2 has the lowest conductivity, while the ilmenite with the lowest TiO_2 has the highest conductivity. Since the conductivity difference between zircon and high TiO_2 titanium minerals is very small, electrostatic separation of those minerals would be difficult.

Table 54 Electric resistance of minerals

Mineral	Mineral purity	Bulk resistance, ohm	Conductivity simens
Ilmenite	58.87% Fe_2O_3 , 35.17% TiO_2	$3 \cdot 10^4$	
Magnetite	N/A	$4 \cdot 10^4$	
LR Rutile	18.7% Fe_2O_3 , 75.5% TiO_2 ,	$1 \cdot 10^{10}$	$0.10 \cdot 10^{-9}$
Hematite	86.36% Fe_2O_3 , 8.58% SiO_2	$2 \cdot 10^{10}$	$0.05 \cdot 10^{-9}$
Rutile	93% TiO_2	$3.3 \cdot 10^{10}$	$0.03 \cdot 10^{-9}$
LR Zircon	65.1% ZrO_2 , 35.5% SiO_2	$1 \cdot 10^{11}$	$0.01 \cdot 10^{-9}$

8.8 Summary

1. With the addition of NaOH or Na₂SiO₃, mechanical attrition at 80°C could remove as much bitumen as naphtha wash did. The key factors in the attrition of SB40 heavy products were: pulp temperature, stirring intensity, pulp pH, and attrition time. Since it avoided the use of naphtha, and produced no CO₂ emission as in the case of roasting, it was expected to be the most promising bitumen removal method.
2. Gravity concentration of mechanically scrubbed SB40 heavy product was effective. A concentrate containing 8% ZrO₂ and 29% TiO₂ with recoveries of above 90% for both titanium and zirconium minerals was obtained.
3. Compared with shaking table, flotation was much less effective in the upgrading of mechanically scrubbed SB40 heavy product.
4. Due to the presence of trace residual bitumen, flotation separation of zircon from titanium minerals was more difficult for mechanically scrubbed SB40 heavy product than for roasted SB40 heavy product. Similar results have been reported by Oxenford et al (2003).
5. Flotation removal of pyrite from the mechanically scrubbed SB40 heavy product was possible, however, due to the association of some of the pyrite particle with quartz and the trace residual bitumen, the separation efficiency was not satisfactory.
6. Electrostatic and magnetic separation suggested that it was possible to separate pyrite from titanium and zirconium minerals by using electrostatic separation plus magnetic separation. However, it was difficult to separate zircon from the low iron-bearing weak-magnetic titanium minerals by electrostatic separation.
7. Mineral electric conductivity measurement suggested that the conductivity difference between zircon and high TiO₂ titanium minerals was very small, electrostatic separation of those minerals would be difficult. More effective electrostatic separators, such as high-tension separator, or screen/plate separator, should be tested.

9 CONCLUSIONS

1. The high concentration of bitumen and small variations in the MCR contents of the residual bitumen in the froth treatment tailings indicated that the residual bitumen should be worth recovering. Bitumen seems to be mainly associated with fine particles since the bitumen content in solids increases linearly with the -400 mesh (passing 38 μm) size materials. The froth treatment tailings contain high concentration of titanium and zirconium which are also worth recovering. Sample No.2 assayed 13.71% TiO_2 and 4.13% ZrO_2 , while sample No.4 assayed 7.33% TiO_2 and 1.49% ZrO_2 . In sample No.2, the titanium and zirconium distributions in -38 μm fraction are 11.33% and 12.36%, respectively, while in sample No.4, the titanium and zirconium distributions in -38 μm fraction are 16.68% and 19.71%, respectively. Recovery of the bitumen will probably result in loss of titanium minerals and zircon in these fine fractions. But this loss is justified since the fine titanium and zirconium minerals are potential liabilities. Froth treatment tailings consist of mineral grains ranging in size from about 20 – 200 μm . The dominant constituents are quartz and accessory minerals include a variety of other silicate minerals, carbonates, zircon, and pyrite, and rutile or anatase. Overall liberation of all constituents in this sample is of a high order. The liberation of zircon mineral is very high, while the liberation of titanium minerals are relatively low (about 80%).
2. The Falcon Centrifugal Concentrator seems to be a better choice than flotation for the first-step processing of the oilsands tailings because it could give an almost clear-cut separation between the heavy minerals and the residual bitumen. Although flotation can give a high concentration ratio for heavy minerals, it gave no separation between heavy minerals and bitumen. For the flotation process, pulp temperature was found to be the key parameter in the flotation of oil sands froth treatment tailings: the flotation recoveries of heavy minerals and bitumen at 85°C were much higher than that at 50°C. The flotation recoveries for sample No. 5 were between 40% and 70% for bitumen, up to 80% for titanium minerals and up to 88% for zircon mineral when the flotation was performed at 50°C; while the recoveries for heavy minerals and bitumen were increased to above 94% for the same sample No.2 at 85°C. Similarly, at 50°C

the flotation recoveries from sample No. 2 were 59.7% for bitumen, 81.2 % for titanium mineral and 84.9% for zircon. After adding NaOH, the recoveries were increased significantly. Combined use of NaOH with MIBC, and/or sodium oleate, and/or kerosene, resulted in bitumen recoveries that were comparable with the tests at a pulp temperature of 85°C. The bitumen content in the SB40 heavy product was low and more or less fixed, and the variation in the bitumen content in the froth treatment tailings only affected the bitumen content in the SB40 slime product. For sample No.5, the Falcon Concentrator produced a heavy product that recovered over 85% of the heavy minerals and 10% of the bitumen, and a light product that recovered about 15% of the heavy minerals (probably all fine heavy mineral particles) and about 90% of the bitumen. While for sample No.2, the heavy product recovered 93.73% of the TiO₂, 91.6% of the ZrO₂ and 54.69% of the bitumen; overall, 4.6% of TiO₂ were lost in the light product (63.8% of them were in the -38µm fraction); 5.2% of the ZrO₂ were lost in the light product (35.1% of them were in the -38µm fraction). For sample No.4, the Falcon concentrator produced a heavy product that recovered 88.8% of TiO₂, 86.7% of the ZrO₂ and 28.7% of the bitumen; overall, 8.7% of TiO₂ were lost in the light product (87.4% of them were in the -38µm fraction); 7.9% of the ZrO₂ were lost in the light product (56.4% of them were in the -38 µm fraction). The light products generated from the Falcon concentrator tests contained primarily particles that were smaller than about 38 µm (over 92% of the materials were -38 µm). Generally, 4% to 10% of the TiO₂ and ZrO₂ were lost into the light products. But since they were of very fine sizes and would not be useful in the final Ti and Zr products, their rejection at this stage may be justified. The heavy products from the centrifugal concentrator were coarser than the flotation concentrate. It is likely that the lost heavy not be desirable in the final heavy mineral concentrate anyway.

3. In the process of bitumen removal by roasting, 400°C seems to be the highest temperature at which the pyrite was not oxidized. While above 450°C the pyrite was obviously oxidized. It needs about 48 hours to remove all the bitumen at 350°C while it needs about 4 hours to remove almost all the bitumen at 400°C. Oxidation roasting could increase the magnetic susceptibility of ilmenite within the temperature range of 500~1000°C. Below 500°C, the magnetic susceptibility was not affected by the

roasting, whereas above 1000°C, the roasting caused sharp reduction in its magnetic susceptibility. Within the temperature range of 500~1000°C, the magnetic susceptibility of ilmenite usually increased with the progress of oxidation roasting, reaching a maximum, which was followed by a sharp drop in the magnetic susceptibility. The time period to reach the maximum depended on the temperature, and was shorter at higher temperatures. X-ray diffraction analyses showed that hematite ($\alpha\text{-Fe}_2\text{O}_3$) was the new phase formed during the oxidation roasting. The highest susceptibility was obtained when the peak intensity ratio between hematite and ilmenite was between 1.5 and 3.5. Reduction roasting of the ilmenite with charcoal as a reducing agent at 800°C increased its magnetic susceptibility significantly, and the magnitude of the increase was higher than oxidation roasting. X-ray diffraction analyses show that some of ilmenite phases have been changed into strongly magnetic maghemite ($\gamma\text{-Fe}_2\text{O}_3$). The reduction roasting of the LR Rutile resulted in an increase in its magnetic susceptibility, and the increase was mainly due to leucoxene, a dominant component in LR Rutile. Upgrading of the LR Rutile was possible by using magnetic separation. With a low intensity magnetic separator (field intensity below 6700 Gauss), a reduction roasting of the sample improved the separation. However, when a high intensity magnetic separator was used, the separation could be achieved without the need for a reduction roasting. The separation seemed only depended on the magnetic field intensity or the magnetic susceptibility, and liberation was not a limiting factor. Roasting the SB40 heavy product to remove the residual bitumen for 60 minutes at over 600°C have resulted in an increase in its magnetic susceptibility. It is likely that the residual bitumen has acted as a reducing agent that converted some of the ferric iron in the leucoxene into ferrous iron. Alternatively, the oxidation of pyrite at this temperature may convert it to hematite which has a higher magnetic susceptibility. Roasting time had little effect on the magnetic susceptibility of the Falcon heavy product, but roasting temperature had a significant effect on the magnetic susceptibility. However, at temperatures above 800°C, incipient fusion of quartz with Fe-bearing minerals occur which would affect subsequent separation. The removal of bitumen by roasting should be conducted at relatively low (about 500°C) temperature in order to produce a high TiO_2 content

product. Compared with shaking table concentration, flotation concentration is less effective in the upgrading of roasted SB40 heavy product. Flotation separation of titanium minerals from zircon is possible but needs to be optimized.

4. Three stages of naphtha washing could reduce the bitumen content of SB40 heavy product from 2.6% to 0.8%. After bitumen removal by solvent washing, mineral surface adjustment such as sulfuric acid attrition is required in order to carry out further mineral separations. Gravity concentration of bitumen-removed SB40 heavy product using a shaking table was effective: a concentrate containing 9% ZrO_2 and 28% TiO_2 with recoveries of above 90% for both titanium and zirconium minerals was obtained. Flotation removal of pyrite from the solvent-washed SB40 heavy product was possible; however, due to the association of some of the pyrite particles with quartz, the separation efficiency was low.
5. With the addition of NaOH or Na_2SiO_3 , attrition at 80°C could remove as much bitumen as the naphtha did. The key factors in the attrition of SB40 heavy products are: pulp temperature, stirring intensity, pulp pH, and attrition time. Since it avoids the using of solvent naphtha, and produces no CO_2 emission as in the case of roasting, it is expected to be the most promising bitumen removal method. Compared with shaking table concentration, flotation concentration is less effective in the upgrading of mechanically scrubbed SB40 heavy product. Flotation removal of pyrite from the bitumen-removed SB40 heavy product is possible, however, but due to the association of some the pyrite particle with quartz, the separation efficiency is not satisfactory. Due to the presence of trace residual bitumen, flotation separation of zircon from titanium minerals is difficult for mechanically scrubbed SB40 heavy product.
6. High intensity magnetic separation is effective in separating the non-magnetic zircon and low iron-bearing weak magnetic titanium minerals from high iron-bearing magnetic titanium minerals; however, electrostatic separation is ineffective in the separation of non-magnetic zircon from the low iron-bearing weak-magnetic titanium minerals. Mineral electric conductivity measurement suggested that the conductivity difference between zircon and high TiO_2 titanium minerals is very small, electrostatic

separation of those minerals would be difficult. More effective electrostatic separators, such as high-tension separator, or screen/plate separator, should be tested.

10 RECOMMENDATIONS

1. Since the Falcon Centrifugal Concentrator can give an almost clear-cut separation between the heavy minerals and the residual bitumen. It seems to be a better choice than flotation for the first-step processing of the oilsands tailings. Due to the small variations in the MCR contents of the residual bitumen in the froth treatment tailings, as well as those in different SB40 products, the residual bitumen after the SB40 centrifugal concentration should be worth recovering. The recovery of residual bitumen in the slime product of Falcon Centrifugal concentration is worth further study. It may be achieved by hydrophobic agglomeration or by solvent dilution and sedimentation. The successful recovery of residual bitumen in the slime product of Falcon Centrifugal concentration would make the recovery of heavy minerals from the froth treatment tailings both economically and environmentally sound.
2. Bitumen removal of SB40 heavy product by mechanical attrition with the addition of NaOH or Na_2SiO_3 , attrition at 80°C could remove as much bitumen as the naphtha did. And since it avoids the using of solvent naphtha, and produces no CO_2 emission as in the case of roasting, it is expected to be the most promising bitumen removal method. But the NaOH dosage of 10kg/T is a little too high, further study is worth conducting to reduce both the reagent dosage and residual bitumen content in the heavy minerals.
3. Electrostatic separation is ineffective in the separation of non-magnetic zircon from the low iron-bearing weak-magnetic titanium minerals. Mineral electric conductivity measurement suggested that the conductivity difference between zircon and high TiO_2 titanium minerals is very small, electrostatic separation of those minerals would be quite difficult. On the other hand, high-tension separation is more efficient and might be effective in the separation of heavy minerals, further study is worth carrying out to use high-tension separation to treat the mechanical scrubbed SB40 heavy product.

11 REFERENCES

1. Albian Sands Energy Inc. www.albiansands.com.
2. Alberta Chamber of Resources, 1996. The Future of the Oil Sands Heavy Mineral Production, Executive Summary, Mineral Developments Agreement, Co-products Study.
3. Balderson, G F, 1982. Test work on scroll centrifuge tailings from Syncrude Canada Ltd., Mineral Deposits Limited Report No. 46.123.1/1. March (cited from Oxenford et al., 2001).
4. Banford, Johnathan, Maud, Geoffrey Elliott, and Demosthenous, Maria Leonida, July 28, 1998. U.S. Patent 5,785,748, Titanium Dioxide Pigments.
5. Blair, S. M, 1950. The Alberta bituminous sands. Government of the Province of Alberta Report, p.12-13.
6. Bulatovic, S, 1999. The recovery of zircon and titanium from Athabasca heavy mineral sand, Report of Investigation, LR5338 and LR5569 (cited from Oxenford et al., 2001).
7. Bulatovic, S, 2000. An Investigation of the recovery of zirconium and titanium from Athabasca oil sand samples, Lakefield Research Final Report. LR5569. June (cited from Oxenford et al., 2001).
8. Burt, Richard O., 1984. Gravity Concentration Technology.
9. Carrigy, M.A., 1963. Criteria for differentiating the McMurray and Clearwater formations in the Athabasca oil sands: Research Council of Alberta Bulletin 14, p. 32

-
10. Carrigy, M.A., 1966. Lithology of the Athabasca oil sands: Research Council of Alberta Bulletin 18, p. 48.
 11. Chao, Tze, and Senkler, George H. Jr., February 4, 1992. U.S. Patent 5,085,837, E.I. Du Pont de Nemours and Company.
 12. CRL, www.consrutile.com.au, 2002.
 13. Deura, Tetsushi N., Wakino, M., Matsunaga, T., Suzuki, Ryosuke O. and Ono, K. Dec. 1998. Titanium Powder Production by $TiCl_4$ Gas Injection into Magnesium Through Molten Salts, Metallurgical and Materials Transactions B, Vol. 29B, p. 1167-1174.
 14. El-Tawil, S.Z., Morsi, I.M., Yehia, A. and Francis, A.A., 1996. Alkali reductive roasting of ilmenite ore. Canadian metallurgical Quarterly, 35(1), p. 31-37.
 15. Falcon Concentrators Inc., 1996.
 16. Gambogi, Joseph, January 2002. U.S. Geological Survey, Mineral Commodity Summaries: Titanium Mineral Concentrates.
 17. Garnar, T. E. and Stanaway, K. J., 1994. Titanium Minerals, in Industrial Minerals and Rocks, 6th Ed., Edited by D.D. Carr. Society of Mining Engineers, Inc., AIME, New York, p. 1071-1090.
 18. Gerdemann, S.J., Oden, L.L., and White, J.C., 1997. Continuous Production of Titanium Powder, Titanium Extraction and Processing, Edited by Mishra, B. and Kipouros, G.J., p. 49-54.

-
19. Helper, L.G. and His, C., 1989. AOSTRA technical handbook on oil sands, bitumen and heavy oils. AOSTRA Technical Publication Series#6, Alberta Oil Sands Technology and Research Authority, Edmonton, AB.
 20. Gurav, Abhijit S., Kodas, Toivo T., and Anderson, Bruce M., Nov. 10, 1998. U.S. Patent 5,833,892, Formation of TiO_2 Pigment by Spray Calcination.
 21. Hedrick, B. James, January 2002. U.S. Geological Survey, Mineral Commodity Summaries: Zirconium and Hafnium.
 22. Helper, L.G. and His, C., 1989. AOSTRA technical handbook on oil sands, bitumen and heavy oils. AOSTRA Technical Publication Series#6, Alberta Oil Sands Technology and Research Authority, Edmonton, AB.
 23. Hiew, Michael and Chegwidan, Philip, Jan. 29, 2002. U.S. Patent 6,342,099, Coated Titanium Dioxide Pigments and Processes for Production and Use.
 24. Hoffman, E.R., 1985. Unpublished data, Shell Canada Ltd., Calgary, Alberta (cited from 'A review of analytical methods for bitumens and heavy oils'. 1988, AOSTRA Technical Publication series #5. Editor, Dean Wallace, Alberta Research Council. 101-120).
 25. Hollitt, Michael John March 23, 1999. U.S. Patent 5,885,536, Process for Alkaline Leaching a Titaniferous Material.
 26. Ityokumbul, M.T., Bulani, W., and Kosaric, N., 1987. Economic and environmental benefits from froth flotation recovery of titanium, zirconium, iron and rare earth minerals from oilsand tailings. *Wat. Sci. Tech.* Vol. 19, Rio, p. 323-331.

-
27. Ityokumbul, M.T., Kosaric, N., Bulani, W., and Cairns, W.L., 1985. Froth flotation for the beneficiation of heavy minerals from oil sand tailings. *AOSTRA Journal of Research*, Vol. 2, No. 1, p. 59-66.
 28. Iwasaki, I. And Prasad, M. S., 1989. Processing techniques for difficult-to-treat ores by combining chemical metallurgy and mineral processing. *Mineral Processing and Extractive Metallurgy Review*, 4, p. 241-276.
 29. Kasperski, K.L., 1985. A review of properties and treatment of oil sands tailings. *AOSTRA J. Research*, 2, p. 21-35.
 30. Kramers, J. and Brown, R.A.S., 1976. Survey of heavy minerals in the surface mineable area of the Athabasca oil sand deposit. *CIM Bulletin*, Vol.69, No.776, p. 92-99.
 31. Lloyd, R.R., 1956. Production of Titanium Metal at Henderson, Nevada, Rocky Mountain Minerals Conference, Salt Lake City, Utah, Sept. 28.
 32. Majid, Abdul and Ripmeester, John A., 1986. Characterization of unextractable organic matter associated with heavy minerals from oil sand, *Fuel*, Vol. 65, p. 1714-1727.
 33. Mao, M., Fornasiero, D., Ralston, J., and Sobieraj, S., 1999. Use of Depressants in the Separation of Zircon from Rutile and Ilmenite, Ian Wark Research Institute, University of South Australia. 38th Annual Conference of Metallurgists of CIM.
 34. McAndrew, J., 1957. Calibration of a Frantz Isodynamic Separator and its application to mineral separation. *Proceedings of the Australian Institute of Mining and Metallurgy*, No.181, p. 59-73.

-
35. McCosh, R, 1996. Geology Executive Summary from Mineral Development Agreement. Final Report, Alberta, Alberta Chamber of Resources. September.
 36. Mellon, G.B., and Wall, J. H., 1956. Geology of the McMurray formation, part 2, Heavy minerals of the McMurray formation: Research Council of Alberta Report 72, p.30-43.
 37. Mineral Sands, www.minerals.org.au, 1999. Minerals Council of Australia and Australian Geological Survey Organization.
 38. Mishra, Brajendra and Kipouros, Georges J., 1996. Titanium: extraction and processing: proceedings of the symposium sponsored by the Reactive Metals Committee of the Light Metals Division of the Minerals, Metals & Materials Society, 1997 Materials Week in Indianapolis, Indiana, September 14-18, 1997 / sponsored by the Reactive Metals Committee, Light Metals Division, TMS: Minerals, Metals & Materials Society.
 39. Moskva, Ugletekhizdat, 1957. Electric-corona Separation of Coal Fines and Certain Minerals.
 40. National Energy Board, October 2000. Canada's Oil Sands: A Supply and Market Outlook to 2015. Cat. No. NE23-89/2000E.
 41. Orth-Gerber, Jurgen, Elfenthal, Lothar and Blumel, Siegfried, Jan. 22, 2002. U.S. Patent 6,340,387, Organically Post-Treated Pigments and Methods for their Production.
 42. Owen, M., 1996. Mineral Development Agreement, Final Report, Alberta Chamber of Resources.

-
43. Owen, M. and Tipman, R., 1999. Co-production of heavy minerals from oil sand tailings. CIM Bulletin, Vol. 92, May, p. 65-73.
 44. Oxenford, J., Coward, J. and Bulatovic, S., 2001. Heavy minerals from Alberta's oil sands. CIM AGM, Quebec City, April 30 –May 2, 2001.
 45. Oxenford, J., Coward, J., Bulatovic, S., and Liu, Q., 2003. Heavy Minerals from Alberta's Oil Sands- Setting New Standards? Second International Heavy Minerals Conference Oct. 8, 2003.
 46. Padmanabhan, N.P.H., Sreenivas, T., and Rao, N.K., 1990. "Processing of Ores of Titanium, Zirconium, Hafnium, Niobium, Tantalum, Molybdenum, Rhenium, and Tungsten: International Trends and the Indian Scene." High Temperature Materials and Processes, Vol. 9, Nos 2-4, p. 217-247.
 47. QIT, www.qit.com, Fer et Titane, 2001.
 48. Scotland, W A and Benthin, H, 1952-1954. Exploration of the Alberta Bituminous Sands. Unpublished report of the Alberta Department of Energy.
 49. Stanley, J. Lefond, 1983. Industrial minerals and rocks (nonmetallics other than fuels), Vol.2, Fifth Edition, New York, p. 1348-1349.
 50. Suncor Energy Inc., www.suncor.ca, 2002.
 51. Syncrude Canada Ltd., www.syncrude.ca, 2001.
 52. Temple, A.K., 1966. Alteration of Ilmenite, Economic Geology, Vol. 61, No. 4, June-July, p. 695-714.

-
53. Trawinski, H. 1976. Theory, Applications, and Practical Operation of Hydrocyclones, Eng. & Min. J., Sept. p. 115-127.
 54. Trevoy, L.W., 1979. Heavy minerals potential of the Athabasca tar sands. Future Heavy Crude and Tar Sands, Int. Conf., 1st, p. 698-702.
 55. Trevoy, L.W. and Schutte, R., 1981. A new source of heavy minerals from Canadian oil sands mining operation. Preprint No.81-20, AIME Annual Meeting, February.
 56. Trevoy, L.W., Schutte, R, Goforth, R. R., 1978. Development of the heavy minerals potential of the Athabasca tar sands. CIM bulletin, March, p. 175-180.
 57. Walpole, E. A., 1997. *Process for separating ilmenite*, US Patent, 5,595,347.
 58. Wills, Barry A., Mineral Processing Technology, 5th Edition, Butterworth-Heinemann, Oxford, 1992.
 59. Wills, Barry A., Mineral Processing Technology, 6th Edition, Butterworth-Heinemann, Oxford, 1997.
 60. Yang, Fenglin and Hlavacek, Vladimir Dec. 1998. Carbochlorination Kinetics of Titanium Dioxide with Carbon and Carbon Monoxide as Reductant, Metallurgical and Materials Transactions B, Vol. 29B, 12971307.